Underwater Inspection of Bridge Substructures Using Imaging

Course No: S12-001

Credit: 12 PDH

Gilbert Gedeon, P.E.



Continuing Education and Development, Inc. 22 Stonewall Court Woodcliff Lake, NJ 07677

P: (877) 322-5800

info@cedengineering.com

Underwater Inspection of Bridge Substructures Using Imaging Technology

June 14, 2018



FOREWORD

With the growth in the range and capabilities of sonar technology, many states are investigating its use for underwater bridge substructure inspection. FHWA provides overall guidance for these inspections and recognized the need for a comprehensive evaluation of the capabilities of sonar technologies for this important activity. In this study, a range of sonar technologies were evaluated in a variety of underwater conditions to evaluate how these technologies can be effectively used in conjunction with or independently of divers. It will be useful for bridge personnel responsible for inspecting bridge foundations. The study described in this report was conducted at the Federal Highway Administration (FHWA) Turner-Fairbank Highway Research Center (TFHRC) J. Sterling Jones Hydraulics Laboratory. The state transportation departments that contributed funding for this study were California, Missouri, North Dakota, South Carolina, Texas, and Wisconsin.

Cheryl Allen Richter, P.E., Ph.D. Director, Office of Infrastructure Research and Development

Notice

This document is disseminated under the sponsorship of the U.S. Department of Transportation in the interest of information exchange. The U.S. Government assumes no liability for the use of the information contained in this document. This report does not constitute a standard, specification, or regulation.

The U.S. Government does not endorse products or manufacturers. Trademarks or manufacturers' names appear in this report only because they are considered essential to the objective of the document. They are included for informational purposes only and are not intended to reflect a preference, approval, or endorsement of any one product or entity.

Quality Assurance Statement

The Federal Highway Administration (FHWA) provides high-quality information to serve Government, industry, and the public in a manner that promotes public understanding. Standards and policies are used to ensure and maximize the quality, objectivity, utility, and integrity of its information. FHWA periodically reviews quality issues and adjusts its programs and processes to ensure continuous quality improvement.

TECHNICAL DOCUMENTATION PAGE

1. Report No.	2. Government Accession No.	3. Recipient's Catalog No.
FHWA-HIF-18-049		
4. Title and Subtitle		5. Report Date
Underwater Inspection of Bridge Sub	structures Using Imaging Technology	June 14, 2018
		6. Performing Organization Code
7. Author(s)		8. Performing Organization Report No.
Jerry Shen, Roy Forsyth, and Roger l	Kilgore	
9. Performing Organization Name and	d Address	10. Work Unit No. (TRAIS)
GENEX SYSTEMS, LLC		
2 Eaton Street, Suite 603		11. Contract or Grant No.
Hampton, VA 23669		DTFH61-11-D00010-T-5009
12. Sponsoring Agency Name and Ad	ldress	13. Type of Report and Period Covered
Office of Infrastructure Research and	Development	Pooled Fund Study Report
Federal Highway Administration		October 2011 – July 2016
6300 Georgetown Pike		14. Sponsoring Agency Code
McLean, VA 22101-2296		

15. Supplementary Notes

The Contracting Officer's Technical Representative (COR) was Kornel Kerenyi (HRDI-50). Thomas Everett, Ian Friedland, Sheila Duwadi, and Gary Moss reviewed interim project documents. Dr. Bret Webb (University of South Alabama) provided technical review of the document.

16. Abstract

As sonar technologies improve, interest in applying these tools for underwater bridge inspection is increasing. While the capabilities, standards, and processes are well-established for bathymetric surveying, sonar use for identifying important characteristics relevant for underwater bridge inspection is evolving. FHWA, working with several states, developed and implemented a series of field tests to evaluate the capabilities of sonar in underwater bridge inspection. This report provides an overview of sonar basics, the types of 2D and 3D sonar technologies available, and factors affecting the reliability of sonar data. The report also describes the field testing and results. The field testing evaluation focused on: 1) identification of relevant underwater features, 2) performance in adverse environments, 3) data collection/reporting time, 4) equipment costs, and 5) personnel requirements.

Findings demonstrated that sonar technology is capable of identifying larger scale characteristics of interest such as scour holes, debris, and moderate to large size voids and protrusions. It is more limited in identifying small scale cracks or features hidden by marine growth. The results showed that sonar is particularly effective in adverse conditions where limitations on diver bottom time exist, such as deep water, and conditions where diver safety or mobility is of particular concern including swift currents or turbid water. In all environments, including those with adverse conditions, sonar technology is useful for identifying macro features quickly. These technologies can be used to inspect underwater structural elements where divers cannot work effectively, to guide divers for a closer look, or to provide independent inspection insights. Sonar can also be effective in covering large areas quickly.

The study led to two broad conclusions. First, sonar inspections have not demonstrated the ability to identify some smaller scale elements of substructure condition that may be important in assessing the bridge and recommending maintenance. Second, sonar technologies offer significant opportunities for improving underwater bridge inspections, especially in adverse environments or to inspect extensive areas.

The study provided recommendations that support the expansion of sonar technologies for bridge inspections:

1) develop guidance or benchmarking information for the use of sonar technologies in underwater bridge inspection,

2) develop a program of training for bridge inspectors in the use of acoustic technologies, and 3) encourage the use of sonar technologies to improve underwater bridge inspection.

17. Key Words		18. Distribution Statement		
acoustic imaging, bridge inspection, condit	No restrictions.			
assessment, defect documentation, deterioration				
evaluation, diving, scour, sonar, underwater imaging,				
underwater inspection				
19. Security Classif. (of this report)	20. Security C	Classif. (of this page)	21. No. of Pages	22. Price
Unclassified	Unclassified		153	

		RN METRIC) CONVER		
Symbol	When You Know	Multiply By	To Find	Symbol
		LENGTH		
in:	inches	25.4	millimeters	mm
n	feet	0.305	meters	m
yd	vards	0.914	melers	m
mi	miles	1.61	kilometers	km
440	Hines	7 7 7 7 7 7 7 7 7 7 7 7 7 7 7 7 7 7 7 7	KIKHIPOIGIS	PART
. 4	and the beautiful	AREA	Name and Add and Hills and Add Lot	7
m ²	square inches	645.2	square millimeters	mm
ft ²	square feet	0.093	square meters	m²
ya,	square yard.	0.836	square meters	m ²
ac	acres	0.405	hectures	ha
m²	square miles	2.59	square kilometers	km
		VOLUME	The second second	
floz	fluid punces	29.57	militers	mL
	gallons	3 785	liters	L.
gal nº	cubic feet	0.028	cubic melars	m
yd ⁴	cubic yards	0.765	cubic melers	m
14	NO.	E volumes greater than 1000 L shall be	e shown in m ³	316
	NO	and the second s	200 (A) 11 III	
		MASS	According to the second	160
OZ.	ounces	28.35	grams	g.
b ·	pounds	0.454	kilograms	kg
Ţ	short tons (2000 (b)	0.907	megagrams (or "metric ton")	Mg (0/ 'T')
		TEMPERATURE (exact deg	rees)	
°F	Fahrenheit	5 (F-32)/9	Calsius	rtc
	T. M.D. WHITTON	or (F-32)/1.8	The same of	
		ILLUMINATION		
	Actividades.		No.	No
fc.	foot-candles	10.76	lux	lx.
n	foot-Lamberts	3.426	candela/m*	cd/m²
		FORCE and PRESSURE or ST	TRESS	
lbt -	poundforce	4.45	newlons	N
fbf/in ²	poundforce per square	inch 6.89	kitopascals	kPa
	APPRO	XIMATE CONVERSIONS F	ROM SI UNITS	
Symbol	When You Know	Multiply By	To Find	Symbol
- Jimbo	THEO TOLL MINER	LENGTH	10,11114	- J.,,,,,,,
mm	millimeters	0.039	inches	in
		3.28	feet	
m	meters	1.09		140
in.	meters		vards	ya
km.	kilometers	0.621	miles	mi
		AREA		
mm²	square millimeters	0.0016	square inches	m²
m ²	square malers	10 764	square feet	117
m ²	square meters	1 195	square yards	yd ^z
tin .	hectares	2.47	acres	ac
km ^T	square kilometers	0.366	square miles	·mi ²
	- Annual Control of the Control of t	VOLUME		
	militare		Build numers	Ban
tent.	milliliters	0.034	fluid ounces	fl.oz
mt.		0.264	gallons	gal ft ²
D)	liters			10
L m*	liters cubic meters	35.314	cubic feet	Aug Chi
L m*	liters	35.314 1.307	cubic yards	Ad ₁
L m*	liters cubic meters	35.314		Vit.
L m³ m²	liters cubic meters	35.314 1.307		oz oz
m ³ m ⁴	liters cubic meters cubic meters grams	35.314 1.307 MASS 0.035	cubic yards ounces	oz oz
L m ³ m ⁴ a kg	liters cubic meters cubic meters grams kilograms	35.314 1.307 MASS 0.035 2.202	ounces pounds	Agr
L m ³ m ⁴ a kg	liters cubic meters cubic meters grams	35,314 1,307 MASS 0,035 2,202 1,103	ounces pounds short tons (2000 tb)	oz ib
L m ¹ m ² a kg Mg (or 'T')	liters cubic meters cubic meters grams kilograms megagrams (or 'metric	35,314 1,307 MASS 9,035 2,202 1,103 TEMPERATURE (exact degi	ounces pounds short tons (2000 lb)	va* oz ib T
L m ¹ m ² a kg Mg (or 'T')	liters cubic meters cubic meters grams kilograms	35,314 1,307 MASS 0,035 2,202 1,103 TEMPERATURE (exact degi	ounces pounds short tons (2000 tb)	oz b
L m ¹ m ² a kg Mg (or 'T')	liters cubic meters cubic meters grams kilograms megagrams (or 'metric	35,314 1,307 MASS 9,035 2,202 1,103 TEMPERATURE (exact degi	ounces pounds short tons (2000 lb)	vd* oz ib T
L m ¹ a kg Mg (ar "T") "C	liters cubic meters cubic meters grams kilograms megagrams (or 'metric	35,314 1,307 MASS 0,035 2,202 1,103 TEMPERATURE (exact degi	ounces pounds short tons (2000 lb)	va* oz ib T
L m ¹ a kg Mg (ar "T") "C	inters cubic meters cubic meters grams kilograms megagrams (or metric	35,374 1,307 MASS 0,035 2,202 1,103 TEMPERATURE (exact degi 1,8C+32 ILLUMINATION	ounces pounds short tons (2000 lb) rees) Fahrenheil	vd* oz ib T
m" m" kg Mg (or "T")	inters cubic meters cubic meters grams kilograms megagrams (or metric	35,374 1,307 MASS 0,035 2,202 1,103 TEMPERATURE (exact degi 1,805-32 ILLUMINATION 0,0929 0,2919	ounces pounds short (ons (2000 lb) rees) Fahrenheit foot-candles foot-Lamberts	vd* oz ib T **F
L m ³ g kg Mg (or "T") ⁼ C lx cd/m ²	inters cubic meters cubic meters grams kilograms megagrams (or metric Celsius lux candelaim ²	35,314 1,307 MASS 0,035 2,202 ton") 1,103 TEMPERATURE (exact degi 1,80-32 ILLUMINATION 0,0929 0,2919 FORCE and PRESSURE or ST	ounces pounds short (ons (2000 tb) rees) Fahrenheit foot-candles foot-Lamberts	vd* oz ib T TE fc
L m [*] o kg Mg (or "T") "C	inters cubic meters cubic meters grams kilograms megagrams (or metric	35,374 1,307 MASS 0,035 2,202 1,103 TEMPERATURE (exact degi 1,805-32 ILLUMINATION 0,0929 0,2919	ounces pounds short (ons (2000 lb) rees) Fahrenheit foot-candles foot-Lamberts	vd* oz ib T **F

[&]quot;SI is the symbol for the international System of Units: Appropriate munding should be made to comply with Section 4 of ASTM E380 (Revised March 2003)

TABLE OF CONTENTS

Chapter 1. Background and Objectives	
Guidance Development for Underwater Bridge Inspection	
Diver Qualifications and Certification	
Underwater Imaging	4
Chapter 2. Sonar Basics	7
How Sonar Works	7
Sound Speed and Angle	9
Return Echoes	10
Georeferencing	13
Chapter 3. Sonar Technologies	15
Three-Dimensional Sonar Systems	
Fathometers/Echosounders (Single-Beam)	
Geophysical Sub-Bottom Profilers	
Multibeam Swath and Mechanical Scanning Sonar	18
Real-Time Multibeam Sonar	
Two-Dimensional Imaging Sonar	20
Side-Scan Sonar	20
Sector-Scanning Sonar	24
Lens-Based Multibeam Sonar	25
Chapter 4. Sonar Reliability	27
Variations in the Speed of Sound	27
Transducer Head Movement	
Interference and Noise	28
Acoustic Multipath	29
Transverse and Range Resolution	29
Acoustic Shadows	30
Slant-Range Distortion	31
GPS Accuracy	32
Chapter 5. Field Program	35
Technology Selection	
3D Real-Time Multibeam	
2D Multibeam and 3D Mechanical Multibeam	
2D Sector-scanning and 3D Profiler	38
Dive Equipment	
Underwater Bridge Inspection Environment	
Construction Materials and Defects	40
Concrete	40
Steel	40
Unreinforced Masonry	40
Timber	
Composite Materials	
Geometric Configuration	41

Environmental Influences	42
Chapter 6. Phase I Field Testing	43
Overview of Bridge Sites and Logistics	43
Georgiana Slough Bridge	
3D Real-Time Multibeam (Inspection Team A)	
2D Multibeam and 3D Mechanical Multibeam (Inspection Team B)	
2D Sector-scanning and 3D Profiler (Inspection Team C)	
Dive Inspection	
James E. Roberts Bridge	54
3D Real-Time Multibeam (Inspection Team A)	55
2D Multibeam and 3D Mechanical Multibeam (Inspection Team B)	
2D Sector-scanning and 3D Profiler (Inspection Team C)	58
Divers	61
Carquinez Bridge (1958)	63
3D Real-Time Multibeam (Inspection Team A)	63
2D Sector-scanning and 3D Mechanical Multibeam (Inspection Team C)	66
Carquinez Bridge (2003)	68
3D Real-Time Multibeam (Inspection Team A)	70
2D Multibeam and 3D Mechanical Multibeam (Inspection Team B)	71
Divers	73
Evaluation of Phase I Findings	74
Identification of Features	
Performance in Adverse Environments	
Data Collection/Reporting Time	76
Onsite Mobilization and Data Collection	
Post-Processing	
Equipment and Personnel Costs	78
Personnel Requirements	79
Summary	79
Chapter 7. Phase II Field Testing	81
Background and Approach	
Inspection Conditions	
Dive Inspection	
Sonar Inspection Teams and Reporting	
Sonar Technologies	
3D Real-Time Multibeam	
2D Multibeam and 3D Mechanical Multibeam	
2D Sector-scanning and 3D Profiler	
San Francisco-Oakland Bay Bridge	
Inspection Findings at Pier W2	
Inspection Findings at Pier W6	
Post-Inspection Review	
Third Street Bridge	
Inspection Findings at the Third Street Bridge	
Post-Inspection Review	
Evaluation of Phase II Findings	

Identification of Features	117
Performance in Adverse Environments	118
Chapter 8. Summary, Conclusions, and Recommendations	119
Summary	119
Conclusions	
Recommendations	122
Appendix A – Recent Research	125
U.S. Army Corps of Engineers (2006, 2007)	
Massachusetts DOT (2008)	
University of Delaware (2008)	125
Wisconsin DOT (2008, 2010)	
Queens University (2009, 2010)	
Idaho DOT (2011)	126
Appendix B – Sonar Applications	129
Rapid Condition Assessment	
Scour Detection and Documentation	130
Underwater Construction Inspection	131
Security Threat Assessment	132
Visual Representation of the Underwater Structure	132
Enhancing Diver Safety and Efficiency	133
References	135
Acknowledgments	139

LIST OF FIGURES

Figure 1. Graph. Examples of low and high frequency sound waves	8
Figure 2. Graphic. Sonar cone angle and side lobes.	
Figure 3. Graphic. Direction of sound waves through varying water layers	11
Figure 4. Graphic. Incidence angle.	
Figure 5. Graphic. Effect of target shape on return echo.	12
Figure 6. Photo/graphic. Typical single-beam hydrographic survey of a bridge site	
Figure 7. Graphic. Example of a false sonar echo return near a bridge pier	
Figure 8. Graphic. Multibeam swath sonar beam pattern.	18
Figure 9. Graphic. Real-time multibeam sonar pattern	
Figure 10. Graphic. Orientation of fan beam to produce a plan view image	21
Figure 11. Graphic. Orientation of fan beam to produce a section cut image	21
Figure 12. Graphic. Orientation of fan beam to produce an elevation view image	
Figure 13. Graphic. Side-scan sonar beam shape and step pattern	
Figure 14. Graphic. Side-scan sonar mounting positions for structural imaging (right) and bo	
scanning (left).	
Figure 15. Graphic. Sector-scanning sonar beam shape and step pattern	
Figure 16. Graphic. Lens-based multibeam sonar beam pattern.	
Figure 17. Graphic. Depictions of roll, pitch, yaw, and heave.	
Figure 18. Image. Sector-scanning sonar image with shadows on the face of a concrete pier	
Figure 19. Schematic. Fixed scour monitor system mounted on bridge foundation	
Figure 20. Graphic. Echoed range versus plotted distance of a sector-scanning sonar	
Figure 21. Photo. 3D real-time multibeam sonar mounted on the boat	
Figure 22. Photo. Boat mount methods.	
Figure 23. Photo. Stationary mounting methods.	
Figure 24. Photo. The Georgiana Slough Bridge.	
Figure 25. Drawing. As-built drawing of the Georgiana Slough Bridge	
Figure 26. Image. Piles from back side of the fender (Georgiana Slough)	
Figure 27. Image. Curved pile alignment in plan view (Georgiana Slough)	
Figure 28. Image. Coordinates from which length of a pile is estimated (Georgiana Slough).	
Figure 29. Image. 2D image from a single ping at Georgiana Slough (plan view)	
Figure 30. Image. 3D scan locations (Georgiana Slough).	
Figure 31. Image. 3D image (Georgiana Slough)	
Figure 32. Image. Indications of scouring from 3D image (Georgiana Slough)	
Figure 33. Image. Bottom drop locations (Georgiana Slough)	
Figure 34. Image. Mosaic of bottom drop images.	
Figure 35. Image. Merged point cloud data at Georgiana Slough Bridge.	
Figure 36. Photo. Steel pile showing marine growth and a level II cleaned area	
Figure 37. Photo. Above water view of steel cables.	
Figure 38. Photo. Northwest face of bent 4.	
Figure 39. Drawing. As-built drawing of bent 4 of the James E. Roberts Bridge	
Figure 40. Image. Bent 4 with boat location showing sonar range	
Figure 41. Image. Data mosaic viewed from the west	
Figure 42. Image. Bent 4 mud line side image.	
Figure 43. Image. Bent 4 face naming convention.	
0	

Figure 44. Image. Sonar wing at the bottom of face 3	58
Figure 45. Sketch. Drop and face location key for team B.	
Figure 46. Image. Mosaic bed image of the James E. Roberts Bridge	
Figure 47. Image. Face 6 of the James E. Roberts Bridge	
Figure 48. Photo. Marine growth on concrete 15 ft (4.6 m) below the waterline	
Figure 49. Photo. Typical concrete condition with level II cleaning (15 ft (4.6 m) below the	
waterline).	62
Figure 50. Photo. Typical cold joint after cleaning.	
Figure 51. Photo. Pier 3 of the 1958 Carquinez Bridge (2003 bridge in background)	
Figure 52. Photo. Aerial view of pier 3 (1958 bridge on the right)	
Figure 53. Drawing. As-built drawing for the 1958 Carquinez Bridge.	
Figure 54. Image. Pier 3 plan view.	
Figure 55. Image. Pier 3 viewed from the north.	
Figure 56. Image. Pier 3 viewed from the south	
Figure 57. Sketch. Area of 3D scanning and 2D pass alignments	
Figure 58. Image. 2D sonar image.	
Figure 59. Image. 3D view of base of pier 3.	
Figure 60. Photo. Aerial view of tower 3 (2003 bridge on the left).	
Figure 61. Photo. Tower 3 pile cap.	
Figure 62. Photo. Tower 3 pile cap close-up.	70
Figure 63. Drawing. As-built drawing for the 2003 Carquinez Bridge.	70
Figure 64. Image. Tower 3 plan view.	
Figure 65. Image. View of tower 3 from the north	71
Figure 66. Image. View of tower 3 from the south	72
Figure 67. Image. 2D image from an eastward scanning pass	
Figure 68. Image. 3D image viewed from the west side of the pier foundation	73
Figure 69. Photos. Wave and current condition during the diving operation	
Figure 70. Photo. SF-OBB viewed from the south.	81
Figure 71. Photo. Third Street Bridge	82
Figure 72. Photo. Target number 1: plastic coated cable	84
Figure 73. Photo. Target number 2: a chain	
Figure 74. Photo. Target number 3: chrome bar and accordion hose	85
Figure 75. Photo. Target number 4: a steel pin with handle	85
Figure 76. Photo. Pier W2 viewed from the east.	89
Figure 77. Photo. Pier W6 viewed from the west.	90
Figure 78. Drawing. Plan view schematic of pier W2	
Figure 79. Image. Pier W2 viewed from the east.	94
Figure 80. Image. Pier W2 3D data viewed from west	95
Figure 81. Image. Detail at bed near pier W2	95
Figure 82. Image. Southeast corner of pier W2.	96
Figure 83. Drawing. Plan view schematic of pier W6	
Figure 84. Image. Pier W6 viewed from the west.	.100
Figure 85. Image. South face of pier W6 in a 2D sonar image	
Figure 86. Image. West face of pier W6.	
Figure 87. Image. Page from the 1995 diver inspection report on SF-OBB pier W2	
Figure 88. Image. 2D multibeam point cloud data of the east face of the W2 pier	

Figure 89. Image. Close-up view of the east face of pier W2.	104
Figure 90. Image. South face of pier W6	105
Figure 91. Photo. Third Street Bridge in San Francisco.	106
Figure 92. Drawing. Plan view of the Third Street Bridge	106
Figure 93. Image. North and south piers of the Third Street Bridge.	112
Figure 94. Image. Close-up of the south channel pier (Third Street Bridge)	112
Figure 95. Image. Detail of east support for the north channel pier.	113
Figure 96. Image. South channel pier viewed from the northeast	113
Figure 97. Image. Detail of south face of west support of the north channel pier	114
Figure 98. Image. Raw image of north channel pier, east support, south face	115
Figure 99. Image. Raw image of north channel pier, west support south face	116

LIST OF TABLES

Table 1. Effects of temperature and salinity at 5 ft (1.5 m)	9
Table 2. Effects of temperature and salinity at 200 ft (61 m)	10
Table 3. Approximate footprint with transducer cone angle and depth	16
Table 4. Summary comparison of acoustic imaging technology qualities	35
Table 5. Selected imaging sonar products and specifications	37
Table 6. Phase I bridge characteristics and site conditions	
Table 7. Phase I field test schedule.	44
Table 8. Summary of time requirements	77
Table 9. Cost summary for phase I field work	78
Table 10. Phase II site information.	82
Table 11. Phase II sonar field test schedule.	86
Table 12. SF-OBB pier W2 inspection comparison summary.	92
Table 13. SF-OBB pier W6 inspection comparison summary.	
Table 14. Third Street bridge inspection comparison summary	108

GLOSSARY OF ACRONYMS

2D Two-Dimensional3D Three-Dimensional

ADCI Association of Dive Contractors International

ASCE American Society of Civil Engineers

ASTM American Society for Testing and Materials

AUV Autonomous Underwater Vehicle

DGPS Differential Global Positioning System

DHS Department of Homeland Security

DOT Department of Transportation

FAA Federal Aviation Administration

EM Engineering Manual (Published by USACE)

FBI Federal Bureau of Investigation

FHWA Federal Highway Administration

GPR Ground Penetrating Radar
GPS Global Positioning System

NAUI National Association of Underwater Instructors

NBI National Bridge Inventory

NBIS National Bridge inspection Standards

NOAA National Oceanic and Atmospheric Association

NHI National Highway Institute

OSHA Occupational Safety and Health Administration

PADI Professional Association of Diving Instructors

PDIC Professional Diving Instructors Corporation

ROV Remotely Operated Vehicle

RTK Real Time Kinematic

SAR Synthetic Aperture Radar

SSA Surface Supplied Air

SSI Scuba Schools International

TA Technical Advisory

TDI Technical Diving International

TFHRC Turner-Fairbank Highway Research Center

TPF Transportation Pooled Fund

USACE United States Army Corps of Engineers

USCG United States Coast Guard

USGS United States Geological Survey

WAAS Wide Area Augmentation System

CHAPTER 1. BACKGROUND AND OBJECTIVES

According to the 2011 National Bridge Inventory (NBI) data, there are approximately 500,000 bridges in the United States that span waterways. Additionally, state highway agencies oversee approximately 31,000 bridges with submerged substructures that require underwater bridge inspection. Approximately 7,600 of these bridges are designated as scour critical. Furthermore, there are numerous additional bridges requiring underwater inspections under the jurisdiction of various federal agencies including Federal Highway Administration (FHWA), Department of Defense, Bureau of Reclamation, Bureau of Indian Affairs, Forest Service, and others. Several security-related and science agencies including the Department of Homeland Security (DHS), the United States Geological Survey (USGS), the Federal Bureau of Investigation (FBI), and the National Oceanic and Atmospheric Administration (NOAA) also have an interest in underwater inspection of infrastructure.

The requirements for underwater bridge inspection procedures using divers are well documented within the U.S. However, some bridge inspectors and owners have increasingly been supplementing dive inspections with acoustic imaging technology to enhance inspection quality, increase safety, increase efficiency, and improve documentation of findings. This trend has accelerated, in part, because of advancements in sonar technology. The trend has also accelerated because site conditions adverse to dive inspections—such as limited underwater visibility, high velocity currents, submerged debris, and extreme water depths—exist at many bridge sites. Because these adverse conditions can limit a diver's ability to inspect a bridge below water, acoustic imaging technology has supplemented dive inspectors to improve inspections.

Acoustic imaging has many potential applications for underwater inspection of bridges. These include:

- Rapid condition assessment (e.g., post-seismic events, vessel impact inspection).
- Scour detection and documentation (e.g., channel bottom and foundation exposure information).
- Underwater construction inspection (e.g., quality control, progress payments, pre/post site conditions).
- Security threat assessment (e.g., detection of submerged explosives, intruder detection).
- Visual documentation of an underwater structure (e.g., as-built plans, large scale defects).
- Diver safety and improved efficiency at challenging dive sites (e.g., fast current, heavy debris, extreme depth, polluted water, and dangerous wildlife).

FHWA initiated this Transportation Pooled Fund Research Study (TPF-5 (131)) to support development of guidance for the use of acoustic imaging for underwater inspection of bridges. The objectives of this research study are to: 1) describe the quality of data that commercially-available acoustic imaging devices produce, especially in swift currents, deep waters, and low visibility situations and 2) demonstrate how these data compare with inspection findings documented by a qualified underwater inspection diver.

GUIDANCE DEVELOPMENT FOR UNDERWATER BRIDGE INSPECTION

The collapse of the Silver Bridge in 1967 prompted Congress to prepare the Federal-Aid Highways Act of 1968 that required establishment of a national bridge inspection standard and a program to train bridge inspectors. By 1981, only 15 state transportation agencies routinely conducted underwater bridge inspections. In April 1985, the US 43 bridge over Chickasawbogue Creek in Alabama collapsed, causing officials to reinforce the requirement for each state to have an underwater bridge inspection program.

Following the tragic collapse of the Schoharie Creek Bridge in New York in 1987, the Federal Government implemented revisions to the National Bridge Inspection Standards (NBIS) that, among other things, mandated underwater bridge inspection. In addition, FHWA issued Technical Advisory (TA) 5140.21 "Revisions to the NBIS" on September 16, 1988 to provide guidance on underwater bridge inspection.

Recognizing the potential for technological advancement, the TA provided flexibility by stating that "inspections in deep water will generally require diving or other appropriate techniques to determine underwater conditions" and that "the underwater inspection requirements of Title 23 Code of Federal Regulations Section 650.303 pertain to inspections that require diving or other special methods of equipment." (3) As a result of the 1988 revisions to the NBIS, all state transportation agencies now require underwater inspections of their submerged bridge substructures and oversee underwater bridge inspection programs at the local level. The TA describes three levels of effort for routine underwater bridge inspections:

- Level I A "swim-by" overview, with minimal cleaning to remove marine growth, which should be performed on 100 percent of the underwater portion of the structure.
- Level II Limited measurements of damaged or deteriorated members, which should be conducted on 10 percent of underwater units and requires removal of marine growth for closer examination.
- Level III Highly detailed inspection utilizing nondestructive tests such as ultrasound or minimally destructive tests such coring of wood or concrete. Level III effort is performed on an as needed basis if Level I and Level II efforts are inconclusive.

Although the NBIS and TA 5140.21 do not specifically require FHWA approval on of the use of "appropriate techniques" for underwater inspection, seeking FHWA concurrence has been common practice to achieve the "required level of certainty" mandated in the TA as part of FHWA oversight of the highway agency inspection program. (3) For example, Washington Department of Transportation (DOT) and Colorado DOT obtained approval from their FHWA Division Offices to use camera-mounted remotely operated vehicles (ROVs) to supplement divers for underwater inspections in water depths exceeding 120 ft (37 m).

To support TA 5140.21, FHWA produced a guidance manual in 1989 titled "*Underwater Inspection of Bridges*" and sponsored nationwide bridge inspection demonstration training sessions (FHWA Demonstration Project 80 – *Bridge Inspection Techniques and Equipment*). In the 1990's, FHWA Training Demonstration Project 98 - *Underwater Evaluation and Repair of Bridge Components* was offered nationwide.⁽⁴⁾

In 2001, the American Society of Civil Engineers (ASCE) published *Standard Practice Manual* 101 – Underwater Investigations. ⁽⁵⁾ Additional revisions were made to the NBIS in 2004 (effective 2005). To provide training on the underwater inspection components of the NBIS, the National Highway Institute (NHI) developed the Underwater Bridge Inspection Course 130091.

In 2010, FHWA completed development of a comprehensive state-of-the-art reference manual to replace the 1989 FHWA Underwater Bridge Inspection Manual. This manual thoroughly documented underwater bridge inspections using divers, but only provided introductory information on the use of underwater acoustic imaging for bridge inspections. ⁽⁶⁾ FHWA also updated NHI course 130091 with the new information from the updated manual. ⁽⁷⁾

Several highway agencies have explored the application underwater acoustic imaging and have requested further guidance from the FHWA on the use of this technology. FHWA recognized the need for additional guidance as acoustic imaging technology improved and was committed to further research. In 2009, the FHWA's Technical Resource Center advised bridge owners that sonar technology could only be used to supplement bridge inspection diving operations (that is, to document findings in conjunction with their Level I and Level II efforts) and in situations where underwater inspections could not be safely performed by divers. (8) Sonar results alone were not allowed as a substitute for data obtained by a qualified diving inspector, as outlined by FHWA guidelines.

DIVER QUALIFICATIONS AND CERTIFICATION

The NBIS include specific sections related to application of standards (23 CFR 650.303), inspection procedures (23 CFR 650.313), frequency of inspections (23 CFR 650.311), qualifications of personnel (23 CFR 650.309), and inventory (23 CFR 650.315), as well as expectations for inspection reports. While there are state by state variations, each agency has implemented policies to comply with the requirements of the NBIS regarding underwater inspections. (9)

Qualification standards define the necessary inspection and diving skills required to conduct an underwater bridge inspection. Underwater inspection divers are generally categorized as either engineer-divers or construction-divers. Engineer-divers have college-level degrees in engineering (generally civil or structural), and construction-divers have skilled-trade training in activities like welding, concrete placement, pipework, etc. In order to be qualified to inspect a bridge in accordance with the NBIS, a diver is required to complete a comprehensive bridge inspection training course such as FHWA-NHI-130055 "Safety Inspection of In-Service Bridges" (or an approved equal) or the FHWA-NHI-130091 "Underwater Bridge Inspection" course. Furthermore, an inspection team leader must complete a comprehensive bridge inspection training course and meet the educational and experience requirements outlined in the NBIS.

In addition to federal requirements, many states have more stringent requirements for an underwater inspection diver and for an inspection team leader. For example, some state highway agencies require all divers to complete the NHI Underwater Bridge Inspection Course 130091 and require that the team leader physically dive a minimum percentage of the bridge. A number

of state highway agencies (including Minnesota and Oregon) take the additional step of certifying bridge inspectors through competency exams.

Occupational Safety and Health Administration (OSHA) 29 CFR 1910 Commercial Diving Regulations require underwater diving operations to be performed by personnel trained in the specific tasks assigned. (10) OSHA allows both commercial scuba and surface supplied air (SSA) diving for underwater operations. The Association of Diving Contractors International (ADCI) publishes Consensus Standards on best practices that include provisions for both scuba and SSA diving for underwater operations.

OSHA Directive CPL 02-00-151 titled 29 CFR Part 1910, Subpart T – Commercial Diving Operations was published on June 13, 2011 to clarify acceptable dive training and regulations. (10) Currently, both scuba and SSA dive modes are frequently used by public-sector and private-sector dive teams.

While recreational sport divers, scientific divers, and many government agency divers, such as emergency fire/rescue/police, may be outside the jurisdiction of the federal OSHA regulations, they are not exempt from OSHA regulations when performing underwater bridge inspections since that technical work is not related to their exempted primary nature of activities. (6)

UNDERWATER IMAGING

Underwater imaging is a field that encompasses a wide variety of technologies that can produce two-dimensional (2D) and three-dimensional (3D) images depending on the type of technology. Optical technologies, such as underwater photography and underwater videography, are the most commonly used underwater imaging methods. Water clarity greatly affects the quality of the images obtained by optical means. Furthermore, camera range and lighting for underwater photography and videography often prohibit large panoramic views and only provide 2D perspectives.

Non-optical technologies include sonar, laser, and radar. Laser scanning (often referred to as Light Detection and Ranging (LiDAR) in above-water applications) can produce extremely accurate underwater images, but is limited in range when water clarity is poor. Laser scanning is more widely used for offshore ocean structures than for inland waterway bridges.

Radar technologies, such as ground penetrating radar (GPR), can produce underwater images primarily of internal concrete defects or subsurface channel-bottom geotechnical strata layers. Synthetic aperture radar (SAR) has been used to obtain large-area perspective underwater imaging of channel-bottom topography. (11)

Of the non-optical underwater imaging technologies, sonar has demonstrated the most potential for—and is the most widely used—for bridge inspection applications. Even in the most turbid waters with zero visibility, sonar can provide water depth data and high-quality images. Sonar employs sound waves and is, therefore, considered an acoustic imaging technology. Sonar images vary in quality, resolution, and dimensional perspective (2D or 3D) depending on the particular sonar device. This research concentrates primarily on sonar technologies, although other related technologies are briefly mentioned.

There are no specific required qualifications or certification processes for the use of acoustic imaging devices. There are related standards for sonar use in the hydrographic surveying industry, but these are not directly applicable to the underwater inspection of bridges. In particular, the U.S. Army Corps of Engineers (USACE) has established sonar procedures in EM 1110-2-1003 *Hydrographic Surveying* and the American Congress on Surveying and Mapping (ACSM) administers exams for Certified Hydrographers, but these organizations exclude underwater acoustic imaging. The American Society for Testing and Materials (ASTM) International Committee E57 does set standards for 3D imaging, but the criteria to-date have only been focused on above water laser scanning and LiDAR.

CHAPTER 2. SONAR BASICS

Bridge inspection program managers and bridge inspectors should understand the principles governing underwater acoustics to effectively evaluate and apply underwater acoustic imaging to bridge inspection. To explain the basic principles of acoustics, water depth measurements using sonar are frequently used as examples in this chapter. Basic water depth measurements and high definition sonar images of bridge substructures are both governed by the same acoustic theory.

HOW SONAR WORKS

The word "sonar" originated as an acronym for "SOund NAvigation and Ranging." In the simplest sense, sonar works by emitting an acoustic pulse (sound) into the water column and measuring the amount of time that the sound wave takes to bounce off of a target and return to the source. In most applications of sonar in science and industry, a transducer is used to both emit and receive the acoustic pulse. As an emitter or projector, the transducer converts electrical energy into sound waves. A sonar "ping" is generated from an oscillating electric signal with frequency characteristics that can be uniquely distinguished. The oscillating electric signals are converted into mechanical vibrations that are transmitted into the water as an oscillating pressure or a sound wave. When the sound wave returns as an echo from the sea floor, the sound pulse is received and converted back into electrical signals by the transducer acting as a hydrophone. (12)

Sound travels through water in a series of pressure waves known as compression waves. Figure 1 illustrates pressure waves with two different wave lengths. These pressure waves propagate at a constant speed through a uniform water environment. The distance between pressure waves is referred to as the wave length. The number of pressure fronts that pass a stationary point in the water per second is the frequency measured in Hz or kHz. (12)

When a sonar transducer emits an acoustic pulse, the sound travels through the water in an inverted dome pattern in all directions as shown in figure 2. The pulse is strongest directly below the transducer and weakens as the angle from the central axis increases. A transducer cone angle is a measure of the acoustic beam central focus defined as the distance from the central axis to the point of half power. This characteristic can be related in non-acoustic terms to a flashlight and a laser pointer each being pointed at a wall. The flashlight (wide cone angle) illuminates a large area while the laser pointer (small cone angle) focuses on a point.

The smallest available cone angle is usually preferred when performing hydrographic surveys or gathering bridge sounding depth data because readings directly below the transducer are desired. Conversely, if a sonar operator was interested in identifying the shallowest point in an area or an obstruction in a channel, a wider cone angle would be more appropriate to view a larger area. Transducer cone angles can also take on elliptical or even fan shapes.

Another aspect of sonar beam shape is an attribute known as side lobes. Side lobes exist in all sonar beams and consist of weaker misdirected energy that is projected to the sides of the main lobe. Side lobes can cause return echoes that may be misinterpreted especially when working near vertical surfaces. (12)

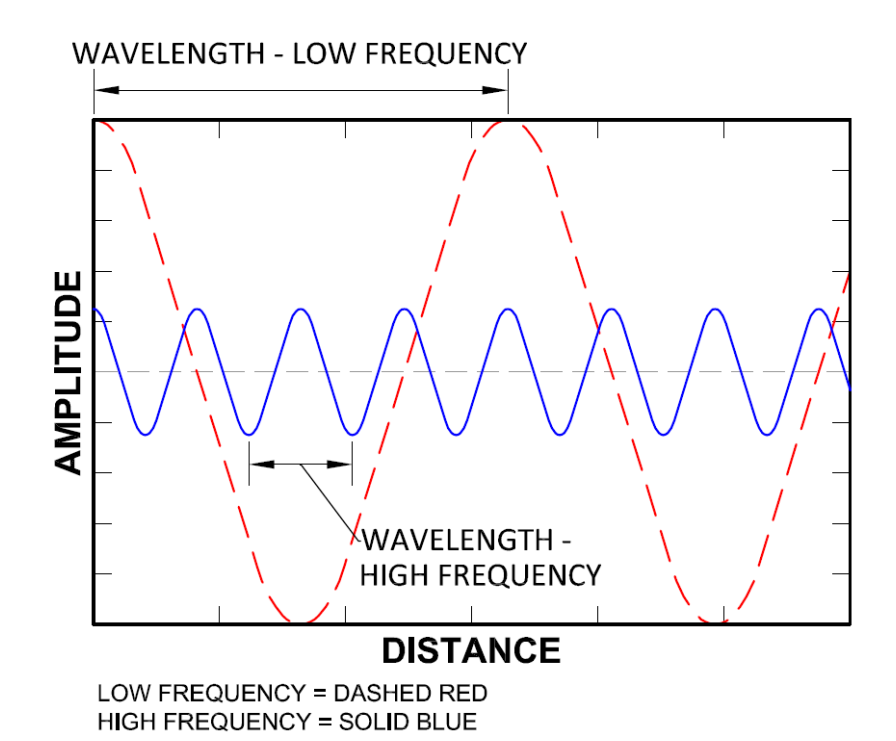


Figure 1. Graph. Examples of low and high frequency sound waves.

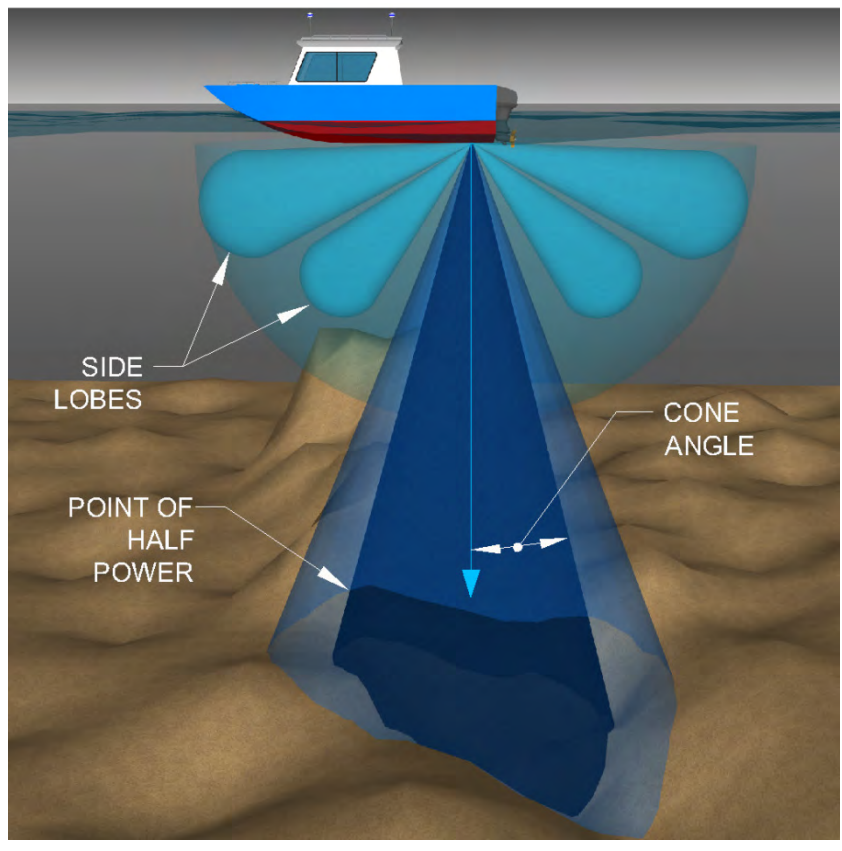


Figure 2. Graphic. Sonar cone angle and side lobes.

SOUND SPEED AND ANGLE

The most basic sonar systems assume that the water environment is homogeneous and the speed of sound does not change throughout the environment. However, changes in water density, which changes with depth, temperature, and salinity, affects the speed of sound. When the speed of sound changes from one environment to another, the wave length changes proportionally, but the frequency remains constant. The speed of sound in water changes as follows:

- 1.7 ft/s per 100 ft change in depth (1.7 m/s per 100 m).
- 6.4 ft/s per 1 °F change in temperature (3.5 m/s per 1 °C).
- 4.6 ft/s per 1ppt change in salinity (1.4 m/s per 1 ppt).

Table 1 summarizes a comparison of sound speeds at a water depth of 5 ft (1.5 m) with different combinations of temperature and salinity. At a temperature of 35 °F (1.7 °C) and a salinity of 0.5 ppt (fresh water), the speed of sound is 4627 ft/s (1410 m/s). If water temperature increases (environment 2), salinity increases (environment 3), or both (environment 4), the speed of sound changes. If these changes are not accounted for, the last column in the table shows the error in depth measurement. Assuming environment 1 when the true environment is 4 results in a depth measurement error of 0.5 ft (0.15 m) or approximately 10 percent of the total depth.

Table 1. Effects of temperature and salinity at 5 ft (1.5 m).

	Temp- erature	Temp- erature	Salinity	Speed of sound	Speed of sound	Error from environ. 1	Error from environ. 1
Environment	(°F)	(°C)	(ppt)	(ft/s)	(m/s)	(ft)	(m)
1. Fresh Water	35	1.7	0.5	4627	1410	0.0	0.00
2. Fresh Water	85	29.4	0.5	4947	1508	0.3	0.09
3. Ocean Water	35	1.7	35	4779	1457	0.2	0.06
4. Ocean Water	85	29.4	35	5067	1544	0.5	0.15

Table 2 provides a similar summary at a water depth of 200 ft (61 m). At a temperature of 35 °F (1.7 °C) and a salinity of 0.5 ppt (fresh water), the speed of sound is 4637 ft/s (1413 m/s) for this environment, which is slightly higher than for the same temperature and salinity conditions at a depth of 5 ft (1.5 m). The depth error of assuming environment 5 when the true environment is 8 is 19 ft (5.8 m), which is approximately 10 percent of the total depth. The percentage error is close to that from table 1 because the speed of sound does not vary significantly with depth alone. However, the absolute error is much greater at a greater depth because the error in velocity acts over a greater time as the sound wave travels down and back.

Most bridge substructure elements exist at depths less than 200 ft (61 m). Because the difference in speed of sound at a depth of 5 ft (1.5 m) versus 200 ft (61 m) is only 10 ft/s (3.05 m/s) changes in the speed of sound based on depth variation is relatively small for underwater bridge inspection.

Table 2. Effects of temperature and salinity at 200 ft (61 m).

	Temp- erature	Temp- erature	Salinity	Speed of sound	Speed of sound	Error from environ. 5	Error from environ. 5
Environment	(°F)	(°C)	(ppt)	(ft/s)	(m/s)	(ft)	(m)
5. Fresh Water	35	1.7	0.5	4637	1413	0.0	0.0
6. Fresh Water	85	29.4	0.5	4958	1511	13.9	4.2
7. Ocean Water	35	1.7	35	4789	1460	6.6	2.0
8. Ocean Water	85	29.4	35	5077	1547	19.0	5.8

However, temperature and salinity variations could result in unacceptable errors if not properly considered. If a thermocline exists at a bridge or if the incorrect temperature is assumed, significant error is possible.

Salinity is typically uniform around a bridge site. Exceptions occur at bridges located in brackish water, near tidal currents, or near large discharge pipes. If a halocline (separation of water layers with differing salinity levels) exists within the water column, a moderate change in sound velocity can be expected between the water layers.

In addition to sound velocity changing as it progresses through the water column, the angle of a sound wave also changes as it crosses between environments of different density. This phenomenon is known as refraction. The result is that an acoustic pulse that is sent downward from a boat may actually hit the channel bottom or other target at a location that is not directly along the same line as when it was emitted from the transducer. When a sound wave enters a region of lower sound velocity, the wave bends toward the vertical axis. When a sound wave enters a region of higher sound velocity, the wave bends away from the vertical axis. This process affects both the emitted pulse and the return echo. If not properly accounted for, the resulting interpretation can lead to inaccuracy in both depth and position measurements. Figure 3 illustrates the path sound takes as it travels through water layers with varying properties.

RETURN ECHOES

Sonar works by emitting an acoustic pulse into the water column and measuring the amount of time that sound takes to bounce off of a target and return to the instrument. Sound loses energy as it travels through the water (a process known as attenuation). Losses occur from the sound wave spherically spreading and thinning over distance.

In general, sound loses energy faster in salt water than in fresh water. The ability of sound to maintain energy as it travels is primarily a function of frequency with high frequency sound generally losing energy faster than low frequency sound. For this reason, sonar uses lower frequencies, especially when it is desirable to penetrate layers of sediment, extremely turbid water, or for long distance communication. Conversely, higher frequencies are typically more desirable for high definition imaging applications because higher frequencies have smaller more defined sound waves. (12)

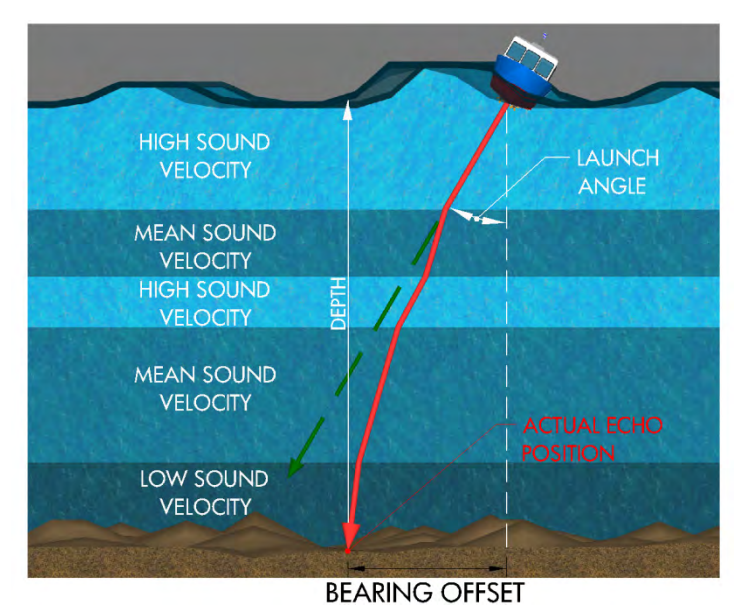


Figure 3. Graphic. Direction of sound waves through varying water layers.

Some of the sound energy is absorbed by the target and the rest reflects off of the target. The amount of sound energy absorbed depends on the acoustic reflectivity of the object. Acoustic reflectivity depends on the frequency of the sonar being used, pulse duration, incident angle, acoustic roughness, and composition of the target, as well as the size, thickness, and shape of the target. The sound absorption coefficient indicates the amount of the sound that is absorbed into the material and is expressed as the ratio of the absorbed sound energy to the incident energy. It varies with the frequency of the sound. An absorption coefficient equal to 1.0 implies full absorption and a coefficient of 0.0 implies full reflection. (13)

In general, bridge construction materials have an internal speed of sound much different than water and tend to be good reflectors. For this reason, sonar imaging of concrete, masonry, or steel bridge substructures can generally be expected to produce strong returns. On the other hand, saturated timber formwork, old timber piles, and some types of rubber fender material have much higher sound absorption coefficients and reflect very little acoustic energy. In some cases, these materials may actually produce an image resembling a void. Marine growth on the material will also affect the sound absorption. Similarly, rock or gravel channel bottoms have a lower sound absorption coefficient than sand or silt, therefore, solid/large aggregates are better sound reflectors. (13)

The amount of the sound that reflects back in the direction of the sonar receiver also depends on the angle at which the pulse hits the target. The reflection depends on the angle of incidence, as shown in figure 4, which is defined as the angle between a line perpendicular to the face of the target and a line from the transducer to the target. (12)

The shape of the target object also influences the reflectance back to the transmitter. As shown in figure 5, the majority of the sound energy is reflected back if the angle of incidence to a flat surface is 0 degrees. Conversely, a round target tends to scatter most of the sound. However, a round target is also the only shape that guarantees a portion of the surface to have an incident angle of 0 degrees relative to the transducer. When a target has a round surface, the ability to detect the outside limits of the target becomes less as the angle of incidence increases because more energy is

reflected away from the transducer in undesirable directions. This is the primary reason that round bridge piles are more difficult to image with sonar than large rectangular pier shafts. Additionally, heavy surface texture of the target can cause the energy to scatter in unpredictable directions. (13) Examples of heavy surface texture include stone masonry, scaled concrete, or an architectural form-liner produced concrete surface finish.

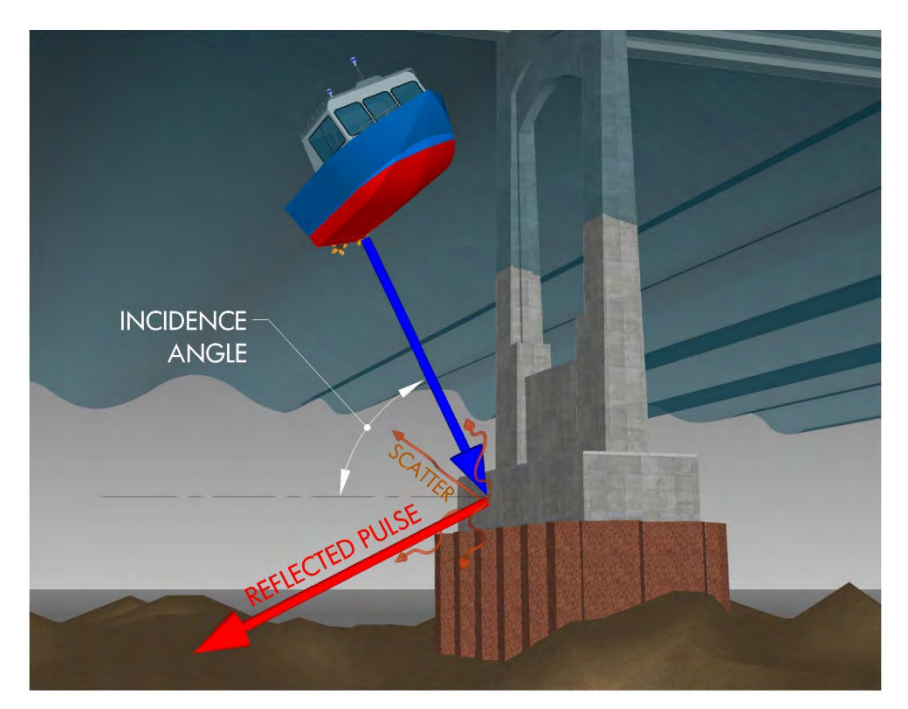


Figure 4. Graphic. Incidence angle.

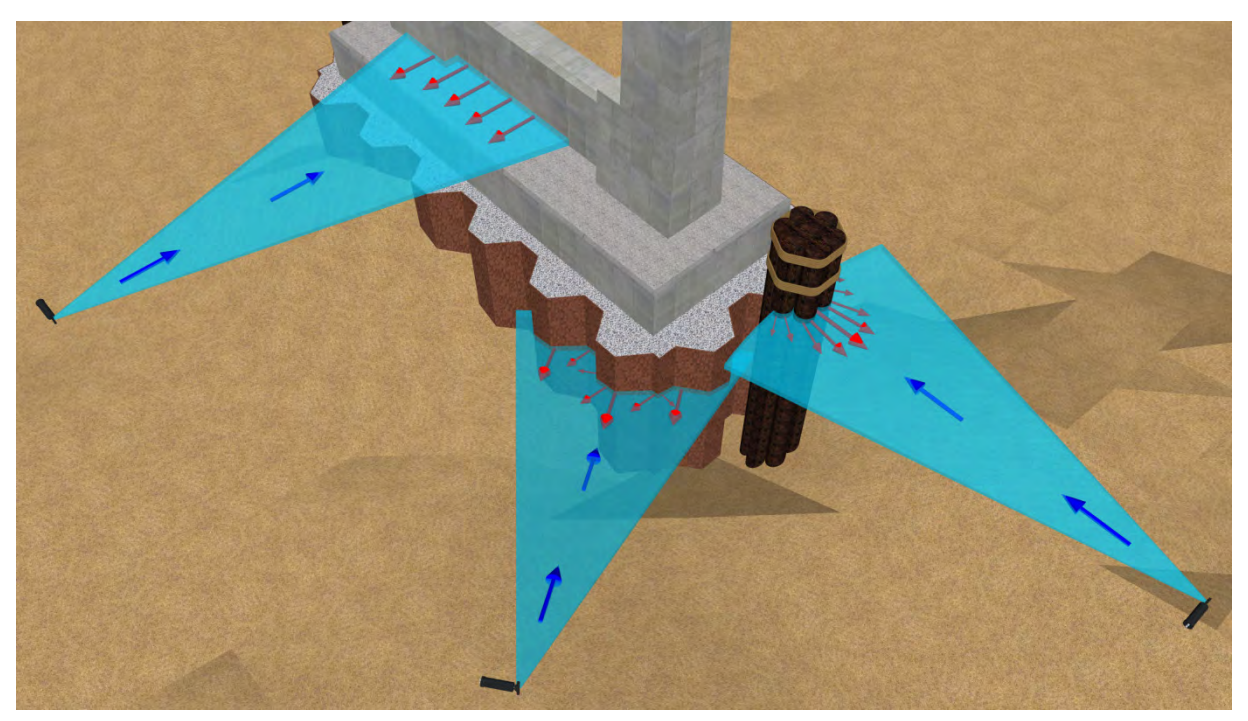


Figure 5. Graphic. Effect of target shape on return echo.

GEOREFERENCING

Acoustic data are collected in a moving reference frame that is a function of both space and time. The measurements obtained are relative to the acoustic sensor itself. For example, a simple vertical beam echosounder returns, at a minimum, the distance from the sensor to the bottom and a corresponding time stamp. If the position of the sensor is known as a function of time, then the corresponding location of each depth measurement can be determined with reasonable accuracy. This is generally referred to as georeferencing. Georeferencing describes the process of representing collected data in a known coordinate reference system and, possibly, in a vertical reference system (vertical datum). This process of georeferencing data is necessary if multiple acoustic surveys are being conducted for the purpose of comparison.

There are many ways in which data can be georeferenced. The most basic type requires using the survey vessel's GPS data (time, location, heading, course over ground, speed over ground, etc.) to georeference the sensor data using simple time interpolation between the GPS and acoustic sensor data. These fairly simple adjustments can be applied following data collection. However, these adjustments only provide the horizontal position of each measurement and do not account for vessel motion. Most modern acoustic surveys make use of proprietary software packages, either offered by the instrument manufacturer or a separate company, that integrate the input from an acoustic sensor, positioning system (e.g., vessel GPS, external GPS, etc.), and gyrocompass to more completely describe the position/location of each measurement in space and time. The gyrocompass is a device that accounts for vessel motion: heave, pitch, and roll (described in Chapter 4).

Referencing measurements to a known vertical datum can be done using one of two methods. First, if the vessel's GPS is linked to an absolute Real Time Kinematic (RTK) system, then the acoustic measurements can be referenced to the vertical datum specified by the user when setting up the RTK GPS system. Otherwise, acoustic measurements must be referenced to the tidal elevation at the time of the survey using a nearby tide gage. Those elevations may be relative to a desired tidal datum or an orthometric survey datum (e.g., NAVD88) if the relationship between the two is known. When a local tide gage is not available, it may be necessary to deploy a temporary tide gage or install a temporary tide staff at the field site for the duration of the survey.

When acoustic data are acquired from a source other than a vessel, like a portable diver-operated unit, then other methods of georeferencing must be used. In such cases, a common method would be to deploy targets in the survey area that have known horizontal and vertical positions. Post-processing software packages can then be used to georeference each measurement based on its position relative to that of the known targets.

CHAPTER 3. SONAR TECHNOLOGIES

Sonar technologies can be classified into two broad categories based on the type of data that they produce: 2D versus 3D. 2D sonar systems take a 3D space and plot it on a 2D screen. 2D sonar produces the best definition when the angle of incidence is very high. 3D data consists of many data points each with unique x, y, and z coordinates. These data require interpolation to create a rendered sonar image. 3D sonar works best when the angle of incidence is very low.

THREE-DIMENSIONAL SONAR SYSTEMS

The detail generated by 3D sonar systems depends on: 1) how small of an area on which the beam is focused to obtain a point reading and 2) the number of points obtained. The number of data points obtained in an area is referred to as data density. If a sonar system has more beams, or a faster ping rate, the ability to obtain more dense data coverage becomes possible in less time. 3D sonar systems include fathometers/echosounders, geophysical sub-bottom profilers, multibeam swath sonar, and real-time multibeam sonar.

Fathometers/Echosounders (Single-Beam)

Modern fathometers and echosounders are single-beam sonar systems that gather 3D data when connected to a GPS or other geographical coordinate collection system. Fathometer frequencies typically range between 24 kHz and 340 kHz, with higher frequencies yielding higher resolution, but little or no channel-bottom penetration. Because channel-bottom penetration is typically not desired when performing a fathometer survey, a higher frequency of 200 kHz is commonly used. Figure 6 illustrates the result of a bridge site survey using single-beam sonar revealing scour around the piers.

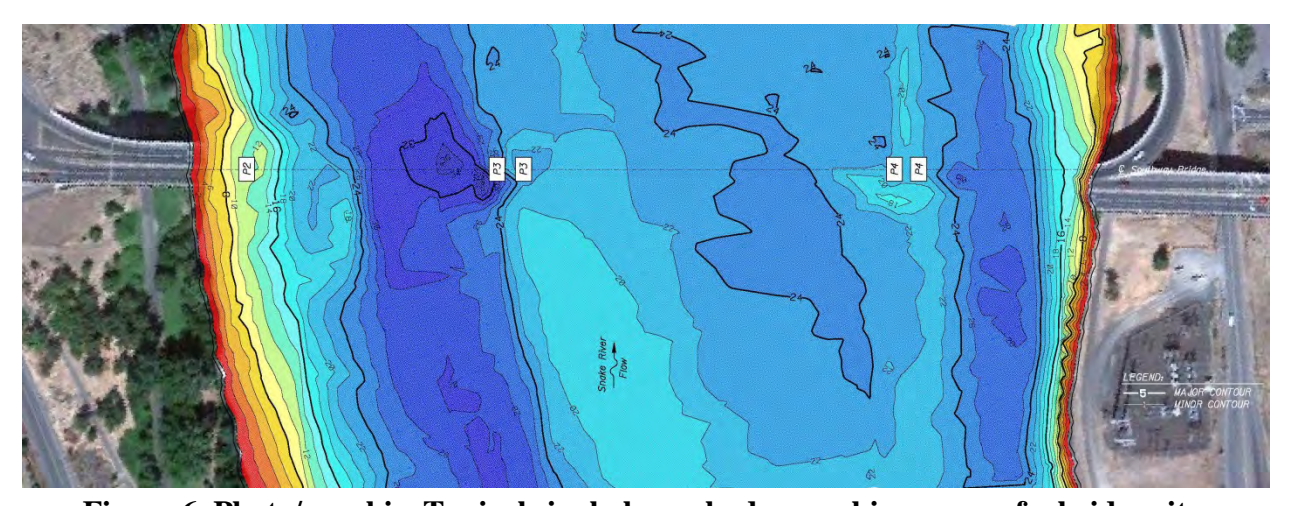


Figure 6. Photo/graphic. Typical single-beam hydrographic survey of a bridge site.

Table 3 provides examples of the size of the footprint on the bed as it varies with transducer cone angle and depth. (15) Larger cone angles and deeper depths result in larger footprints. Within the footprint, the strongest echo is usually returned to the unit and recorded as the depth. However,

variations in the channel bottom configuration may not always result in the strongest echo returning from the center of the sonar cone resulting in some distortion in the readings.

Projected depth (ft)	Projected depth (m)	0.75 deg (ft ²)	0.75 deg (m ²)	1.5 deg (ft ²)	1.5 deg (m ²)	4 deg (ft²)	4 deg (m²)	10 deg (ft²)	10 deg (m ²)
10	3.0	< 1	< 0.09	< 1	< 0.09	< 2	< 0.19	10	0.93
25	7.6	< 1	< 0.09	< 2	< 0.19	10	0.93	60	5.6
50	15.2	< 2	< 0.19	5	0.46	40	3.72	250	23.2
75	22.9	3	0.28	10	0.93	90	8.36	550	51.1

Because sonar footprints with single-beam sonar can become quite large at depth and the exact location of the return echo is not always known, the sonar operator must be careful not to confuse an exposed bridge footing or other submerged obstruction as the channel bottom. Figure 7 illustrates an example where a false return echo near a bridge pier is coming from the pier foundation rather than the channel bottom.

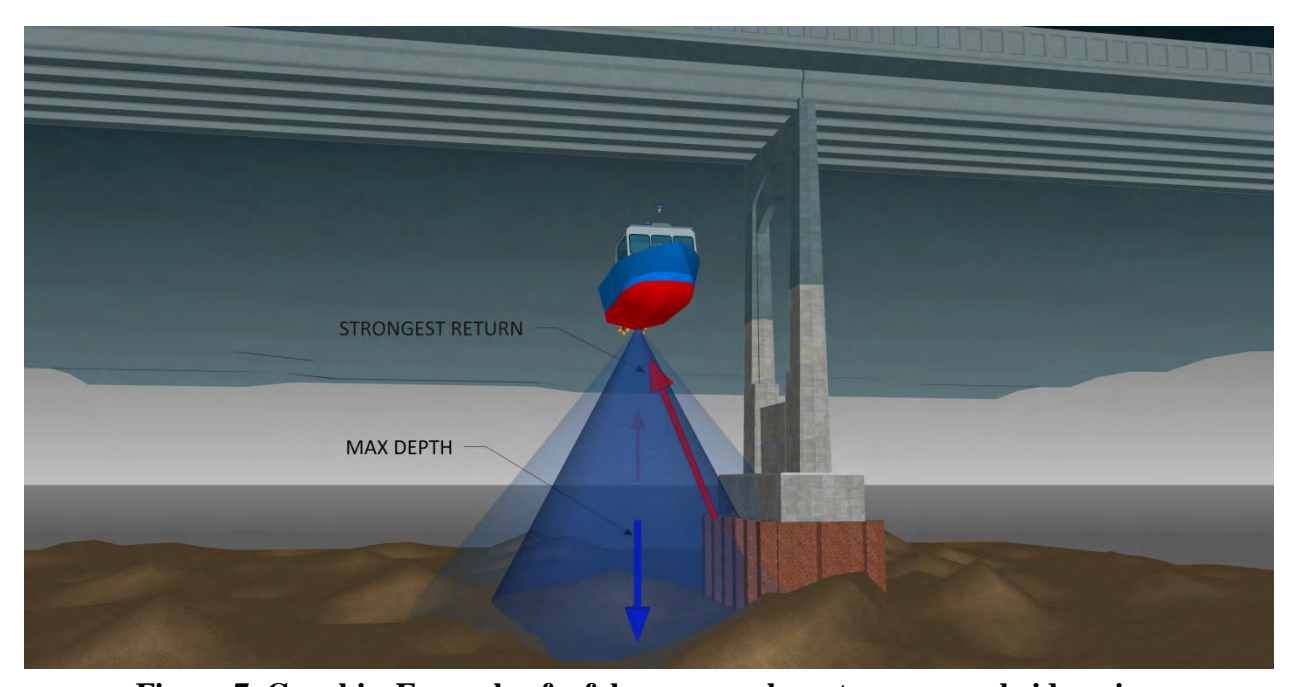


Figure 7. Graphic. Example of a false sonar echo return near a bridge pier.

More sophisticated fathometer systems are compatible with GPS receivers or robotic total stations that allow geographic coordinates to be associated with each depth reading. With such tools, water depths can be post-processed and referenced to a state plane or other horizontal coordinate system. This allows for accurate channel-bottom surveys that can be easily compared to previous and future surveys if they are also georeferenced. When water conditions allow, a boat-mounted transducer allows efficient data collection. Transducers mounted on poles, floats, or articulated arms have also been used when maneuvering a boat is not feasible. (14)

Data density is typically low in comparison to data obtained by multibeam sonar collection methods. A single-beam fathometer survey will typically cover only 5 to 10 percent of the total channel-bottom area. (16) This limits detection of channel-bottom irregularities or scour holes unless the vessel passes directly over the top of the interested area with a narrow beam. Contour maps created from single-beam sonar rely heavily on interpolation between data points. For channel bottoms that are relatively flat, or that have a gentle slope, this method works well. However, the presence of steep or irregular surfaces can result in an inaccurate representation of actual conditions.

The primary benefit of a fathometer is the ability to obtain georeferenced channel-bottom profiles. The profiles can be used to locate and quantify apparent scour depressions, areas of infilling, and channel-bottom objects such as exposed pier footings or debris accumulation. Overlaying and comparing channel-bottom profiles from successive underwater bridge inspections can alert engineers to possible channel-related problems. Bridge foundation information from as-built plans can be superimposed onto the channel cross-sections and profiles for reference purposes. (17)

The primary limitation of fathometers is the inability to collect data outside the path of the vessel transporting the transducer. For this reason, the functionality of fathometers is limited to obtaining channel-bottom depth information only and imaging of vertical structure faces is not practical. Likewise, fathometers will not provide information about the channel-bottom elevation located directly below a footing and cannot provide undermining dimensions. (14)

Geophysical Sub-Bottom Profilers

Sub-bottom profilers were first introduced in the mid-1960s and have been successfully used for defining sediment stratification and detecting bedrock for many years. The surface component of the system generates images of the sediment stratifications, bedrock, and objects embedded in the channel bottom using either a digital or paper recording device. Geophysical profiling systems can either be acoustic or electromagnetic radar. Electromagnetic radar systems are referred to as Ground Penetrating Radar (GPR).

Sub-bottom profilers can be used to locate the position and depth of buried submarine cables below movable bridges prior to repair work or channel dredging operations. They can also be used to identify scour holes that have refilled masking the threat of scour to bridge foundations. Because the redeposited sediment will typically consist of a different material or have a different density than the undisturbed channel-bottom sediment, sub-bottom profilers can depict the location of the previously undisturbed channel bottom and, therefore, the extent of a refilled scour hole.

The primary benefit of sub-bottom profilers is the ability to locate sediment stratification, bedrock, and objects embedded in the channel bottom. As a result, sub-bottom profilers are frequently used prior to marine structure construction or as part of a scour evaluation to detect infilling of depressions. With regard to underwater bridge inspection, sub-bottom profilers can be used to measure the true depth of scour depressions and locate unknown elevations of embedded pier footings. (17)

A primary limitation of sub-bottom profilers is acoustic interference that results in sub-bottom images that are difficult to interpret. Acoustic interferences include sonar bouncing off of multiple objects prior to returning (multipath) when operating in shallow water. Additionally, because sub-bottom profilers use significantly lower operating frequencies than fathometers, the cone angles are typically much wider. As a result of these wider cone angles, collecting good quality sub-bottom images close to in-water structures is challenging. Side-lobe interference can occur when the acoustic pulses encounter vertical objects, such as a bridge pier. (17)

There are also several important limitations specifically for GPR used in waterways. GPR cannot currently be used in saline waters or at depths that are greater than approximately 30 ft (9.1 m). (18)

Multibeam Swath and Mechanical Scanning Sonar

Multibeam swath sonar, first developed in the mid 1960's for the U.S. Navy, is also referred to as swath echo sounding. They function similarly to single-beam echo sounders except they simultaneously project a fanned array of sonar beams covering a "swath width" as shown in figure 8. Multibeam swath sonar allows for much more dense data coverage in a shorter period of time. A typical multibeam survey may have a fanned array that is capable of a swath width of seven times the water depth. Therefore, if the water depth is 100 ft (30.5 m), bathymetric data can be obtained for a swath width of 700 ft (210 m).

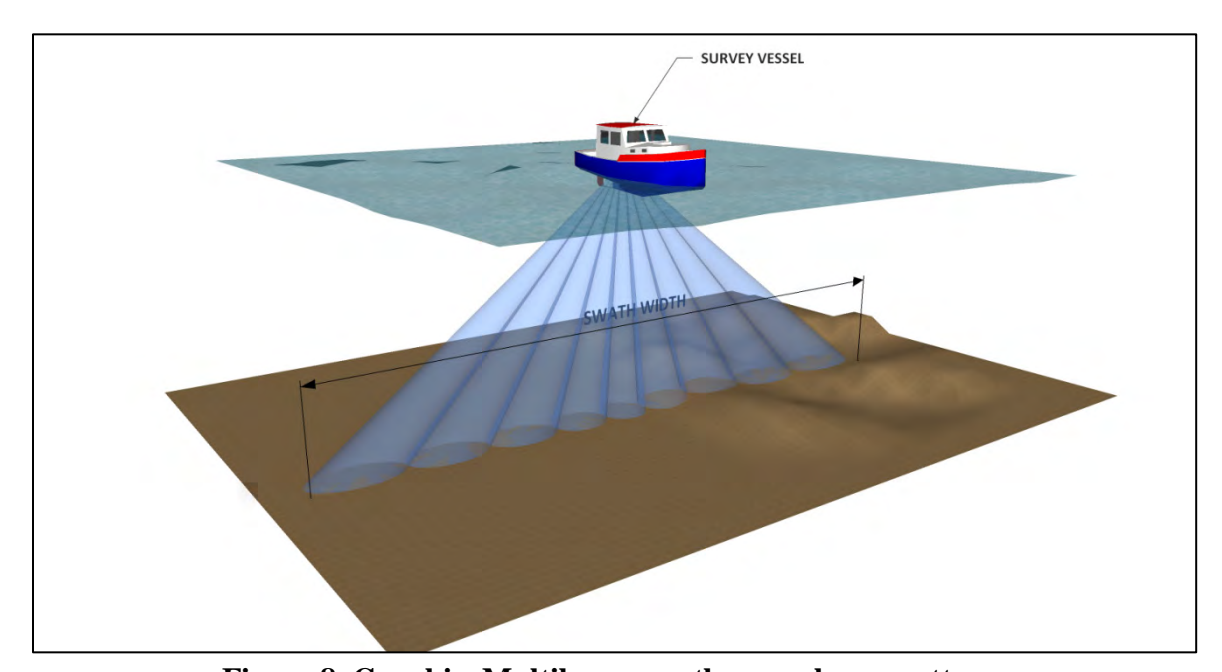


Figure 8. Graphic. Multibeam swath sonar beam pattern.

The beam arrangement allows detailed mapping of a very thin transverse section with each sonar pulse. Most systems are boat mounted and require forward progress of the boat to advance the position of the send/receive signal. Operating frequencies usually range between 0.7 MHz and 1.8 MHz. Multibeam swath systems for sub-bottom profiling applications use extremely low frequencies. The section of the send of the

Another form of multibeam sonar is 3D mechanical scanning sonar, which is essentially a multibeam sonar unit fitted with a mechanical stepping motor. This type of sonar unit remains stationary while performing scans.

The primary benefit of multibeam swath sonar is the ability to quickly obtain large quantities of 3D data. Multibeam swath sonar produces a 3D still image that is often referred to as a point cloud. By using multiple or overlapping passes, the sonar operator is able to obtain greater data density and 100 percent bottom coverage of an area. (14)

A primary limitation of multibeam swath sonar is that the vast quantities of data produced can be cumbersome and time consuming to post process. Because of the additional sensors required and the complexity of the relationship between these sensors, a temporary multibeam installation is significantly more complex and time consuming than a comparable single-beam installation. Both field operation and data post processing require significant training and skill to master. Additionally, multibeam sonar systems are considerably more expensive than other types of sonar technologies.

For bridge inspection applications, the multibeam swath sonar 3D data might allow an inspector to document and assess the depth of spalling, scaling, or, possibly, foundation undermining. However, a limitation of multibeam sonar for bridge inspection is the difficulty of smoothly transitioning from acquiring data from the channel bed to the vertical face of a bridge support when the sonar is in a downward looking configuration. This is a challenge because multibeam systems are finely tuned through power and gain adjustments to detect the channel bottom and, therefore, do not always accurately record returns from dissimilar materials and locations. Additionally, these data often require significant manual post processing to filter out acoustic noise. In the hands of a skilled technician multibeam swath sonar can yield high quality surveys.

Real-Time Multibeam Sonar

Real-time multibeam sonar is a volumetric sonar system. Rather than a single line of narrow beams, it contains many rows and columns of narrow beams that ensonify a volume as illustrated in figure 9. The matrix of narrow beams allows for more dense data coverage creating thousands of data points with a single ping compared with hundreds of pings for multibeam swath systems. These systems create three-dimensional images that are updated in real time, similar to watching a video. They can be mounted on a fixed installation or mounted on a vessel, ROV, or autonomous underwater vehicle (AUV).

Real-time multibeam sonar provides the benefits of 3D data. Compared with multibeam swath sonar, some technologies can be more rapidly deployed, require less special operator skills and training, and reduce post processing effort. Because of the large number of beams and high data density, large and complex structures can be covered quickly without the need for multiple passes. The end result is greatly increased productivity. (19)

Because a single georeferenced point on an object is continuously ensonified from different angles as the platform moves, multipath error can be reduced by software algorithms that track whether objects remain stationary between consecutive pings. This produces datasets with less acoustic noise. Another advantage to continuously scanning each object from multiple angles is

that the dataset produced has fewer acoustic shadows resulting in fewer unknowns from the dataset. (20)

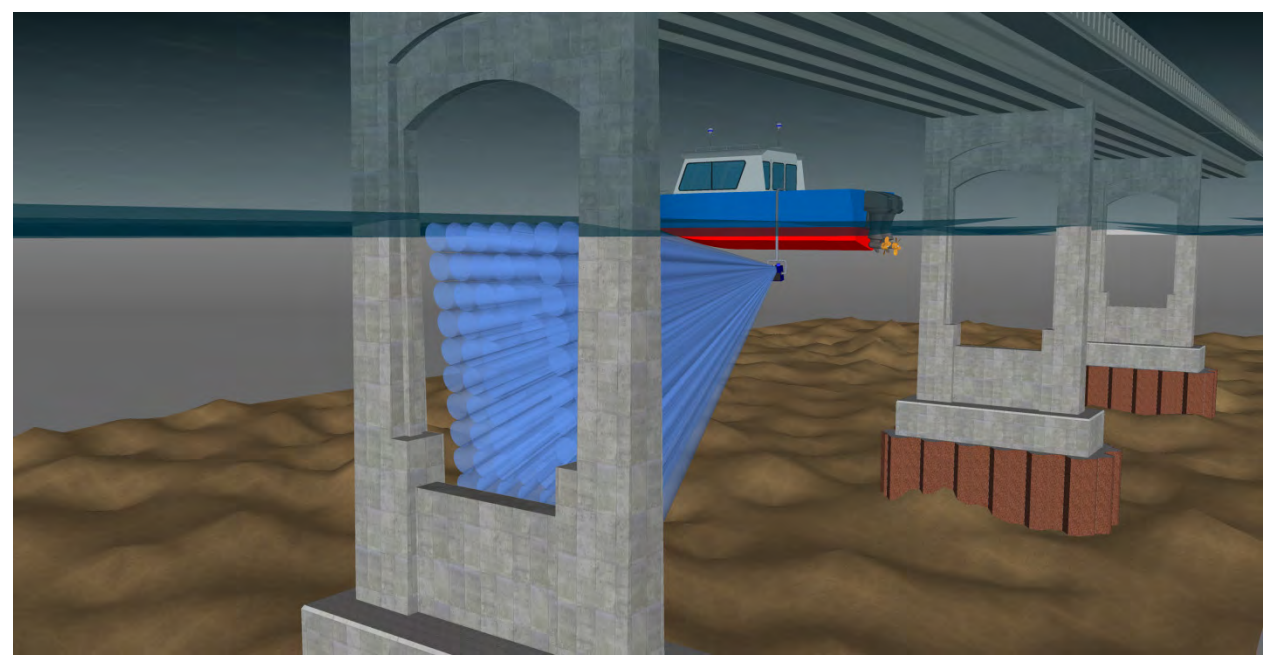


Figure 9. Graphic. Real-time multibeam sonar pattern.

A limitation of real-time multibeam sonar is that the vast quantities of data produced can be cumbersome and time consuming to post process. Another limitation is that although real-time multibeam sonar systems can be used as a "stand alone" unit, they still need to be fully georeferenced using GPS and motion compensating devices for best results. This adds an extra level of cost to already expensive systems. Such systems may also require more equipment to maintain.

TWO-DIMENSIONAL IMAGING SONAR

2D imaging sonar systems have oblong, fan-shaped beams. They record the full range of returns from the wide dimension of the cone angle and plot them on a 2D drawing. The sonar unit cannot distinguish which portion of the wide cone angle a return came from but it can determine if an echo returns from more than one distance.

Figure 10 illustrates the orientation of a fan beam to produce a plan view image of a pier foundation. Figure 11 and figure 12 show the orientation for producing a section cut image and an elevation view, respectively. The same beam orientations are used to produce 2D images with the side-scan, sector-scan, and lens-based multibeam sonar systems.

Side-Scan Sonar

Side-scan sonar was first introduced in the early 1960s and has been successfully used for documenting underwater findings for many years. Side-scan sonar emits fan-shaped acoustic pulses through the water column at operating frequencies usually between 83 kHz and 800 kHz. The beam is narrow in one plane (typically less than 1 degree) and wide in the other plane

(typically between 35 and 60 degrees). Figure 13 shows the shape of a typical side-scan sonar beam.

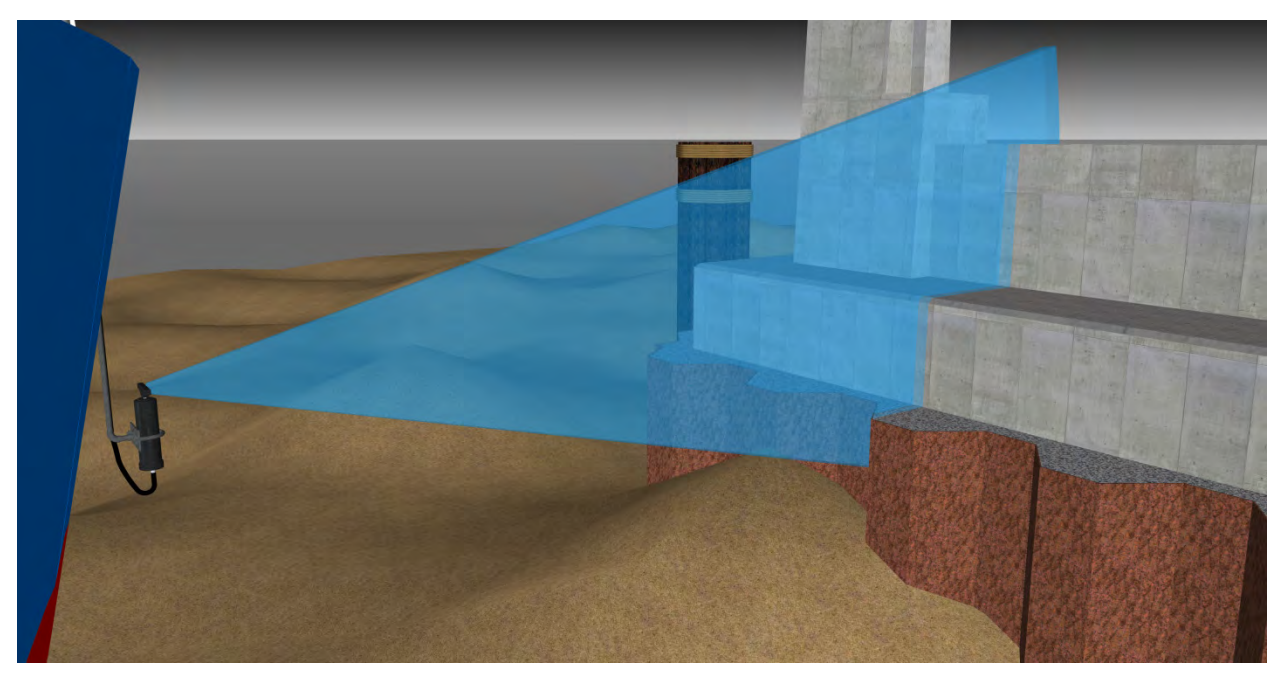


Figure 10. Graphic. Orientation of fan beam to produce a plan view image.

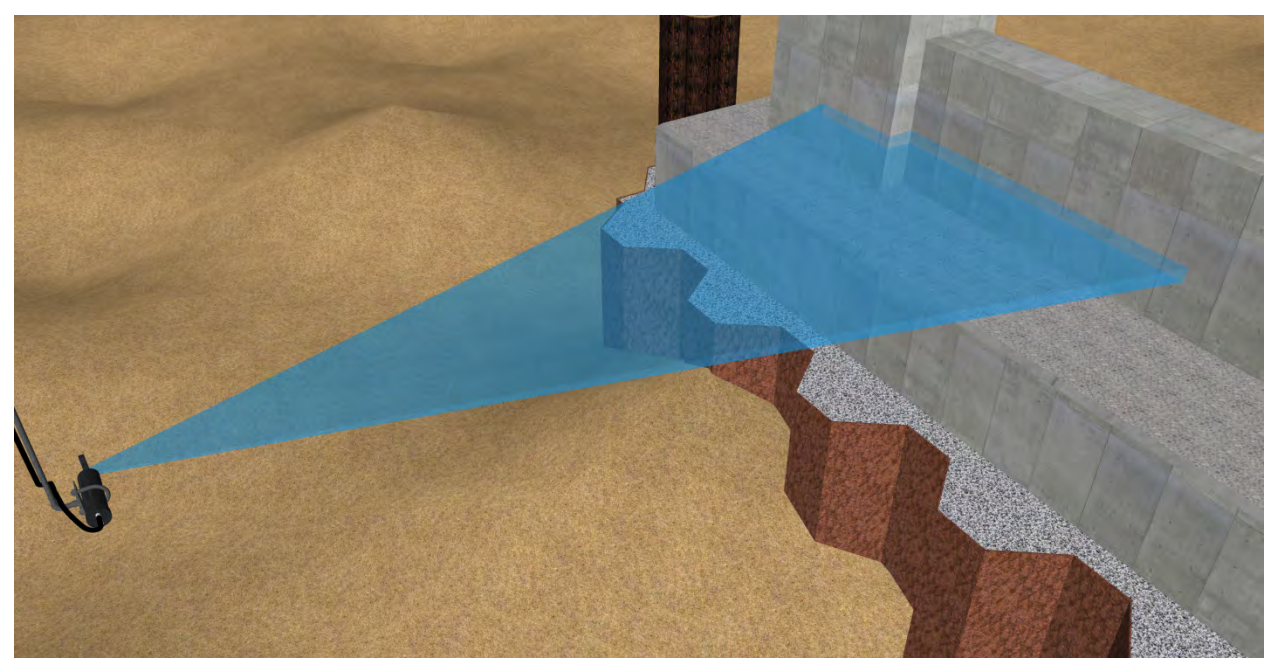


Figure 11. Graphic. Orientation of fan beam to produce a section cut image.

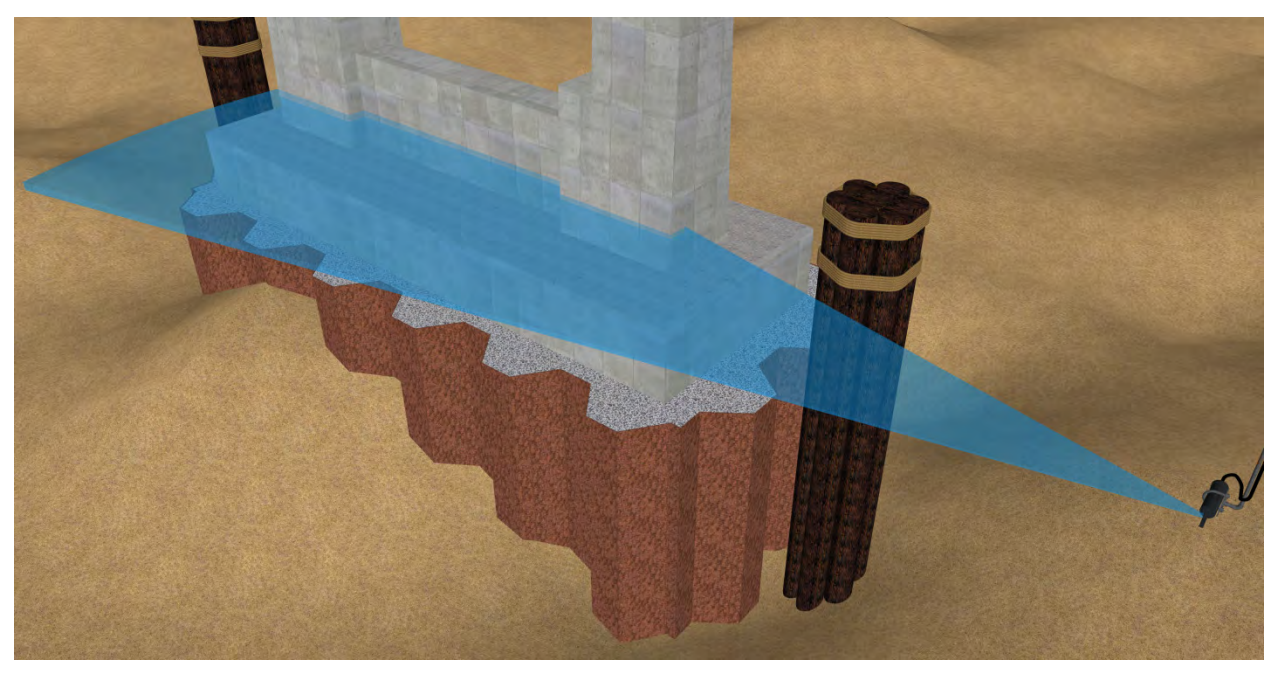


Figure 12. Graphic. Orientation of fan beam to produce an elevation view image.

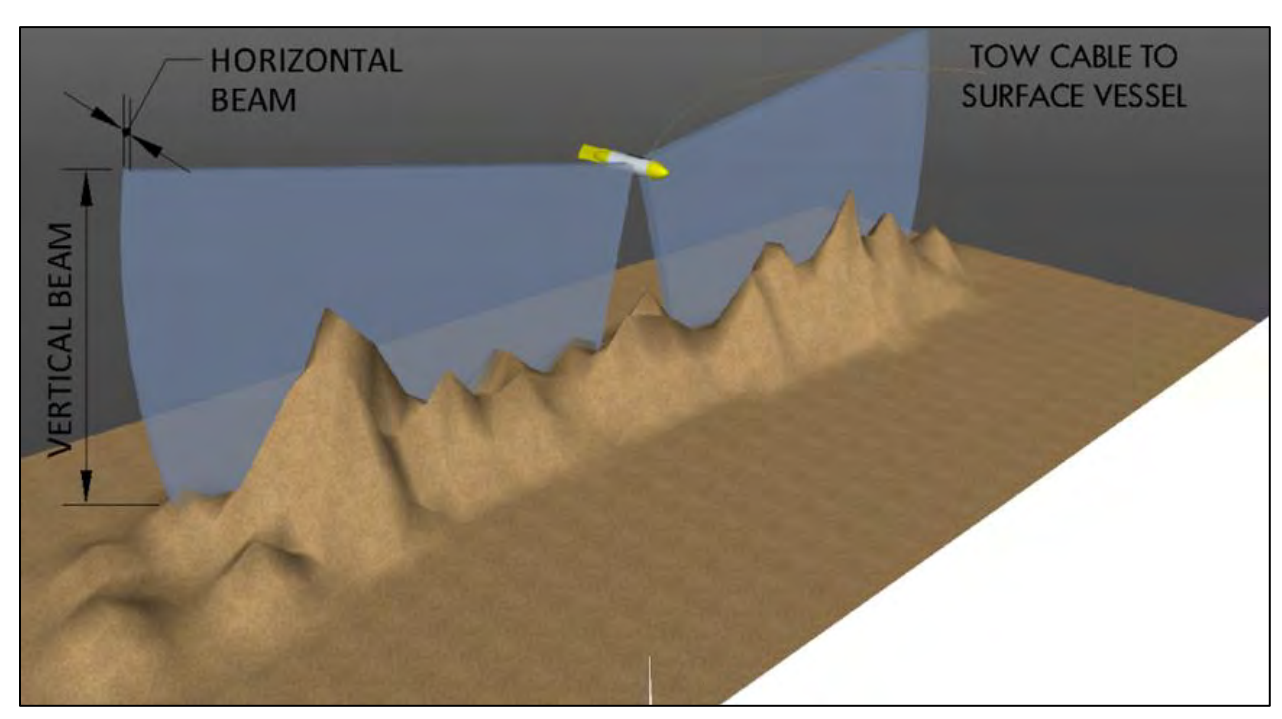


Figure 13. Graphic. Side-scan sonar beam shape and step pattern.

The transducer is either towed behind a boat (a towfish) or mounted on the transom or hull of the vessel. Side-scan sonar requires the boat to move forward so that each successive sonar ping will be positioned slightly in front of the previous ping. Processing of the echoed (backscattered) target intensity within the geometric coverage of the beam results in images of the channel bottom and objects located on the bottom or in the water column. When the images are stitched

together along the direction of travel, they form a continuous image of the bottom and objects located on the bottom or in the water column. (17)

The primary benefit of side-scan sonar is the ability to quickly and efficiently generate images of large areas of the channel bottom. For this reason, side-scan sonar is considered the tool of choice for large-scale search operations. Side-scan sonar can be used for many purposes including delineation of exposed sediment and geologic formations, detection of underwater debris or objects that may be hazardous to marine operations and searching for shipwrecks. In addition, the general location and configuration of submerged structures, pipelines, and cables can be investigated using side-scan sonar. (13)

The primary limitation of side-scan sonar is the difficulty generating images of the vertical components of submerged structures. It is possible to image vertical components of bridge substructures if the transducers are rotated 90 degrees and pole-mounted. The quality of the image that results is largely dependent on operator ability to maintain a close and constant distance to the pier face and maintain a constant speed past the bridge pier. ⁽¹³⁾ Figure 14 demonstrates the beam pattern that a side-scan sonar produces when being utilized for bottom scanning and when rotated 90 degrees for imaging vertical surfaces.

Challenges with side-scan sonar include detecting narrow linear targets that are parallel to the beams and maintaining a consistent line at a constant speed. For towed systems it is important to maintain the towfish at a constant location behind the vessel and at a constant elevation in the water column. For hull-mounted applications, vessel pitch and roll must be considered. (14)

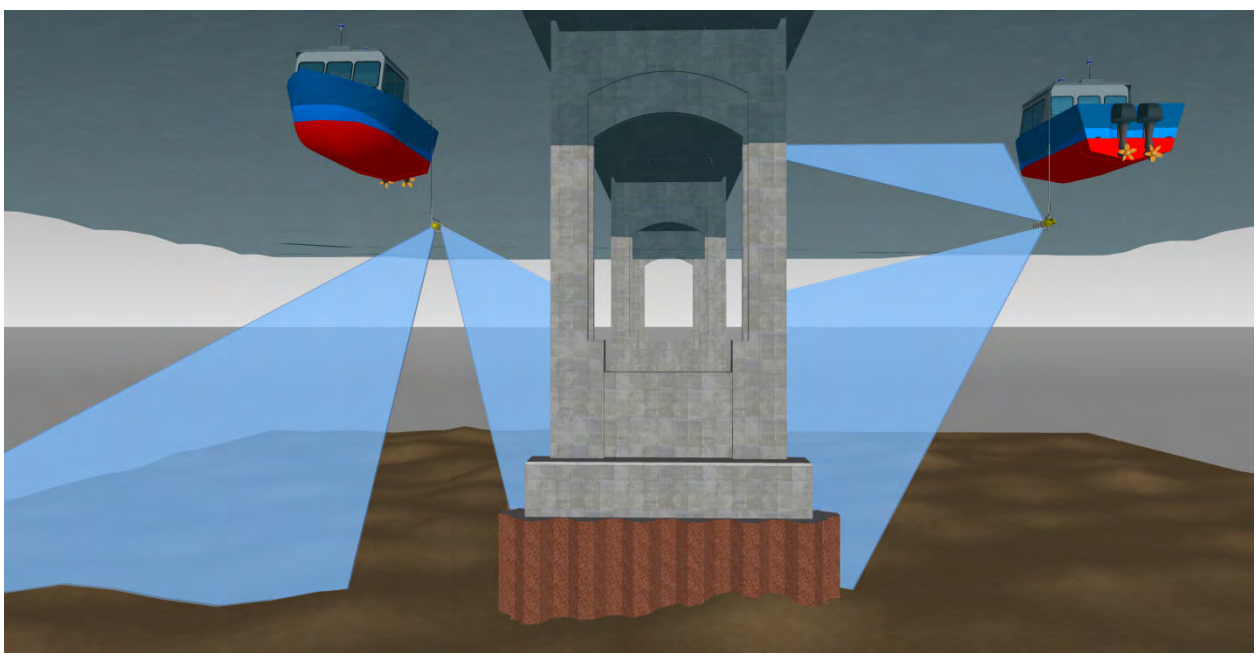


Figure 14. Graphic. Side-scan sonar mounting positions for structural imaging (right) and bottom scanning (left).

Sector-Scanning Sonar

The first known use of sector-scanning sonar for bridge assessment was to investigate the location and resting position of a sunken pontoon bridge deck for the Washington DOT in 1990. Since 2000, the underwater conditions at numerous bridges have been documented using sector-scanning sonar. (14)

Sector-scanning sonar emits fan-shaped acoustic pulses through the water. However, unlike side-scan sonar, which requires vessel movement to develop an image, sector-scanning sonar works best if the transducer remains stationary while the head is mechanically rotating. The acoustic images are recorded in a series of "slices" generated by a ping after each rotation of the transducer. Sector-scanning sonar operating frequencies usually range between 330 kHz and 2.25 MHz, with a common frequency used for channel bottom and structural imaging of 675 kHz. (14) Figure 15 shows the fan-shaped beam and scanning pattern produced by typical sector-scanning sonar.

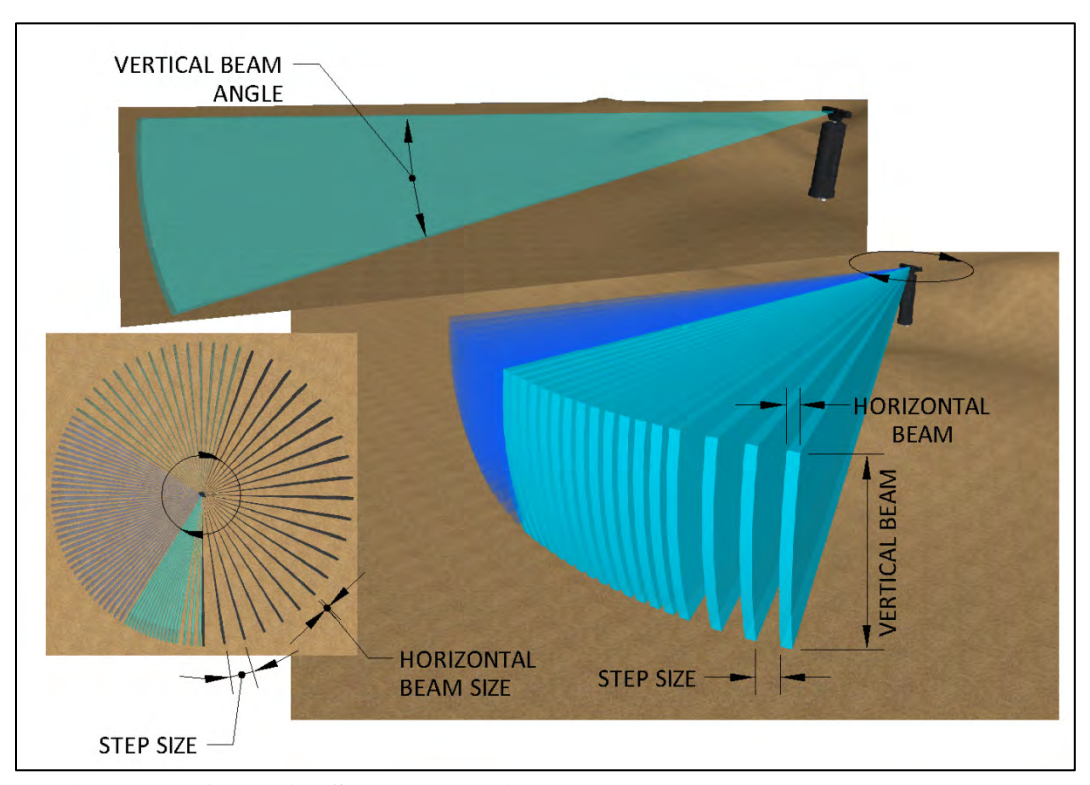


Figure 15. Graphic. Sector-scanning sonar beam shape and step pattern.

The primary benefit of sector-scanning sonar is the ability to produce detailed images of the channel bottom and vertical components of submerged structures that extend from the channel bottom to the water surface. Scanning sonar can also be used prior to and during diving operations to direct the underwater inspector to potential deficiencies, as well as direct the inspector around potential below-water hazards. Sector scanning of vertical structure surfaces typically does not require georeferencing thus simplifying the process.

Because of the limited range and the need for the sonar head to be located in a stable mounting position, the primary limitation of sector-scanning sonar is that stationary setups require greater

time to obtain. Additionally, developing highly detailed images using sector-scanning sonar is heavily dependent on sonar positioning and stability. (14)

Lens-Based Multibeam Sonar

In the late 1990s, the U.S. Navy funded the development of lens-based multibeam sonar at the University of Washington Applied Physics Laboratory to identify swimmer intruders. Around 2004, the offshore oil and gas industry began using lens-based multibeam sonar for structural inspection and for navigation with ROVs. (14)

Lens-based multibeam sonar is essentially sector-scanning sonar that does not rotate. Where sector-scanning sonar consists of one beam that mechanically moves each transmit/receive cycle to create an image line by line, lens-based multibeam sonar consists of numerous elliptical beams placed side by side to create an image in one transmit/receive cycle as shown in figure 16. Operating frequencies typically range between 0.7 MHz and 1.8 MHz.⁽¹⁴⁾

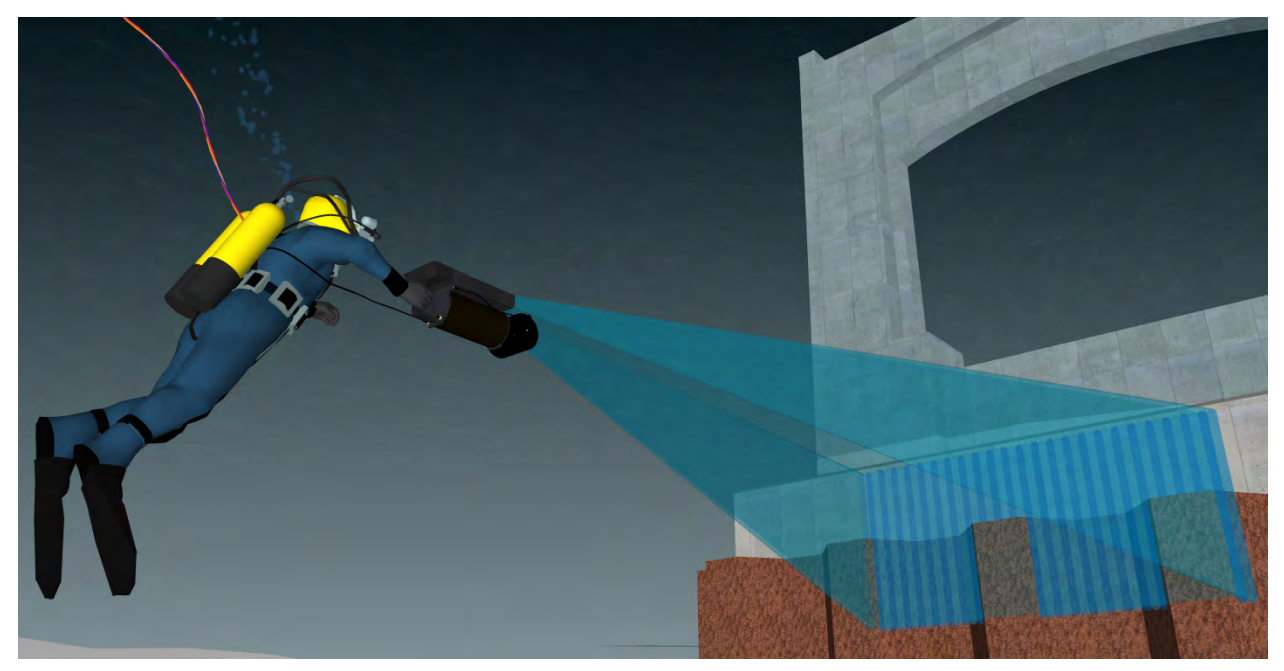


Figure 16. Graphic. Lens-based multibeam sonar beam pattern.

The primary benefit of lens-based multibeam sonar is that it provides real-time images similar to a video. In addition, battery operated units with a mask-mounted display can be carried by an underwater inspector. Using a diver carried unit, an underwater inspector can navigate to potential deficiencies as well as around potential below-water hazards. Because lens-based multibeam sonar displays images in real time, they show promise for use in tracking or directing a dive inspector and are not as sensitive to movement of the transducer head.

The primary limitation of lens-based multibeam sonar units is the difficulty obtaining complete images of vertical surfaces. Additionally, because the image produced is two-dimensional, obtaining depth of scaling or undermining penetration information is not possible. (14)

CHAPTER 4. SONAR RELIABILITY

FHWA TA 5140.21 states that "underwater members must be inspected to the extent necessary to determine structural safety with certainty." However, the reliability of underwater data collection is subject to a number of factors including inspector skill, equipment limitations, and environmental conditions.

Sonar reliability for determining bathymetry is well-established. Dredging projects use sonar data for environmental planning, accurate progress measurement, and final contractor payment of work completed. The inherent errors and correction methods associated with single-beam and multibeam sonar data have been well documented in the hydrographic survey industry. This chapter addresses reliability of collection and interpretation of sonar data for inspection of underwater structures.

For underwater bridge inspection, the demands on sonar data collection expand from a focus on the horizontal to additional emphasis on the vertical as well as on the transition between the two. There is very little literature available on acoustic imaging of submerged vertical surfaces. Fortunately, the principles related to sonar data collection and interpretation in the vertical and horizontal share common features. The following sections discuss aspects of sonar technology that challenge sonar reliability, but are manageable with an understanding of the issues.

VARIATIONS IN THE SPEED OF SOUND

Because the speed at which sound travels through water is not constant throughout a typical water column, calibration of sonar equipment to local conditions is necessary for accurate data recording. The two primary methods for measuring and correcting for variances in sound velocity through the water column are the bar check and the sound velocity probe (profiler). (15)

The bar check is a procedure that measures the distance to an object set at a known depth and adjusts for the actual speed of sound to correct identified inaccuracies. This effort is usually completed by lowering a metal disk suspended by a chain into the water. This method corrects the depth readings based on an assumed average velocity. The bar check does not correct the sound velocity along the full depth of the water column, nor does it generate the necessary information to make corrections for sound refraction as it passes through layers of water with varying properties.⁽¹⁵⁾

Alternatively, a sound velocity probe (profiler) may be lowered through the water column. This technique uses an instrument that measures sound velocity at each point throughout the full height of a water column. With the input of this data, software will either apply an average velocity over the entire column, or velocities will be continuously corrected at each depth throughout the water column. (15)

TRANSDUCER HEAD MOVEMENT

Production of high quality sonar data requires that the exact position and orientation of the transducer head be known at all times. If a transducer head is fixed (i.e., set in a tri-pod on the channel bottom), this criterion is met. If the transducer head is attached to a boat, the effects of

waves, current, and other boat movements will affect the resulting sonar data unless accurate correction factors are applied. (15)

Movements of a typical boat-mounted transducer can be classified into the categories of roll, pitch, yaw, and heave as illustrated in figure 17. Roll is defined as rocking of the boat from side to side. Pitch is defined as rocking of the boat from front to back. Yaw is defined as the change of compass orientation of the vessel. Finally, heave is defined as the up and down movement of a boat, usually produced by waves. Since the direction and angle of the beams can change with the heave, pitch, and roll of the survey vessel, it is necessary to have motion compensators and a gyrocompass that account (in real time) for the motion and relay correction factors back to the on-board processor. (15)

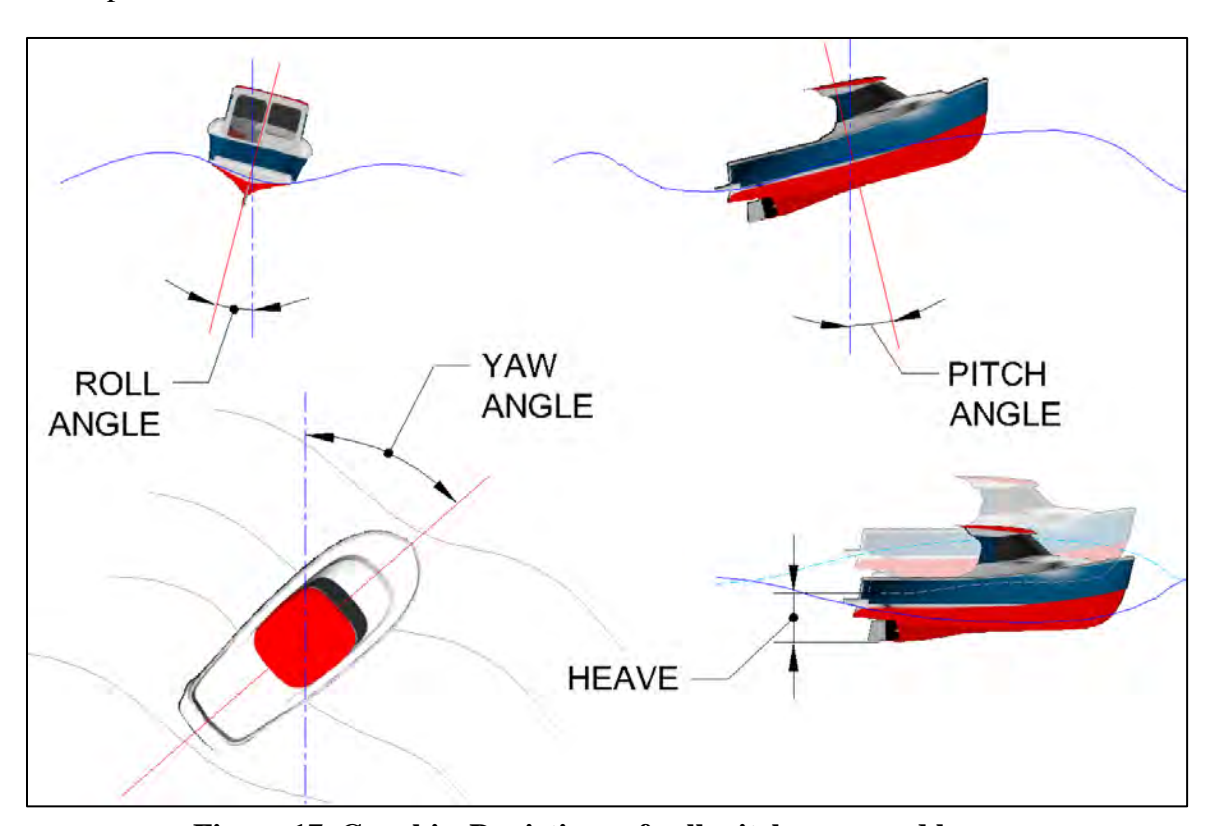


Figure 17. Graphic. Depictions of roll, pitch, yaw, and heave.

INTERFERENCE AND NOISE

The duration of each transducer ping is called the pulse length. The bandwidth is a term that refers to the range of frequencies that a sonar receiver can recognize in the return echo. The bandwidth is typically set to accept a range of frequencies from slightly above to slightly below the frequency transmitted by the transducer. Optimum high-resolution imaging conditions require a short pulse length and a wide receiver bandwidth. However, if the bandwidth is set too high, the system becomes susceptible to background noise from outside sources such as ship motors, other sonar systems in the area, rain, waves, whales or other mammals, pile driving, and vibrations from traffic passing over a bridge deck. Ideally, sonar system software should allow the user to turn off the transmit cycle to the system and allow the operator to identify any noise in the area. (13)

Some imaging sonar systems are equipped with a variable bandwidth setting. The combination of these two functions allow a sonar operator to listen to and map local background noise, then select an operating frequency and bandwidth that will produce the highest resolution images with the least interference.⁽¹³⁾

ACOUSTIC MULTIPATH

Acoustic multipath refers to a sonar echo event bouncing off of multiple objects prior to returning to the transducer. This phenomenon can occur when scatter from the return echo bounces off the water surface, thermocline, or other object before returning to the transducer. The sonar receiver is not able to distinguish that the sound did not take a direct route to the target and back and, therefore, it is typically displayed as multiple targets at incremental distances from the transducer when only one target exists. Acoustic multipath becomes an increasingly common problem when working in relatively shallow water depths. Such depths do occur at bridge sites.⁽¹³⁾

Acoustic multipath can usually be eliminated by (13):

- Selecting a shorter operating range.
- Changing the transducer height in the water column.
- Tilting the transducer away from the water surface.
- Using a transducer with a narrow beam.

TRANSVERSE AND RANGE RESOLUTION

Resolution of a sonar system refers to its ability to accurately display small objects. The resolution is dependent on many factors including frequency, bandwidth, pulse length, target reflectivity, and monitor pixel size. Resolution differs in the transverse and longitudinal directions and both resolutions are commonly reported by manufacturers.

Transverse resolution refers to a sonar system's ability to resolve small target images in the direction perpendicular to the sonar beam. It is primarily dependent upon the sonar cone angle and the distance from the transducer to the target being imaged. When viewing a sonar image, if two targets fall within the footprint of the sonar cone, the sonar will not be capable of distinguishing between them.

Transverse resolution can also be affected by step size. For scanning sonar, step size refers to the distance that the sonar head is rotated with each mechanical advancement. For side-scan or multibeam sonar, this is typically dependent upon the speed at which the boat is moving. For practical purposes, if the step size exceeds the footprint of the sonar beam, full coverage of the surface being imaged will not be obtained. This reliability issue relating to resolution can typically be avoided by scanning at slow speeds. (13)

Range (longitudinal) resolution refers to the ability of a sonar system to resolve small target images in the direction parallel to the sonar beam. It is primarily dependent upon the sonar pulse length and the speed of sound through the water. When viewing a sonar image, if two targets fall

within this distance to each other, the sonar will not be capable of distinguishing between them. (13)

Most sonar systems automatically set a sonar pulse length based on a selected range without allowing the user to manually adjust. If pulse length is manually set, it is important to note that simply selecting a longer range will decrease resolution regardless of the distance to the target. If a sonar system allows manual selection of pulse length, the operator can select a shorter pulse length to achieve better resolution or a longer pulse length to achieve longer range. (13)

An understanding of resolution is critical to understanding the limitations of images produced by sonar. The resolution value can be thought of as the image pixel size that the sonar is capable of defining. A smaller resolution value provides higher resolution images because the pixel size is smaller allowing more pixels for a given area.

ACOUSTIC SHADOWS

Another characteristic of some sonar images is the formation of acoustic shadows. Shadows appear as dark areas on an image and are formed when a target blocks sound from reflecting off of that area of the surface. Shadows can look very similar in appearance to areas with extremely low reflectivity with the only revealing factor often being whether or not a target is shown at the leading edge. Depending on the angle of incidence, a sonar operator can often tell more about a target by its shadow than the actual sonar return. (13)

Shadows can easily be misinterpreted as defects in a bridge substructure. For example, an inverted T-shape is apparent on the face of the concrete pier in figure 18. An inspector unfamiliar with sonar may misinterpret this image as concrete deterioration or cracking. However, as shown in the bridge plans for this location in figure 19, the shape is actually a steel frame designed to mount a fixed scour monitoring device to the pier. The acoustic shadow connects to the target that formed it at the location where the steel frame is connected to the pier face.

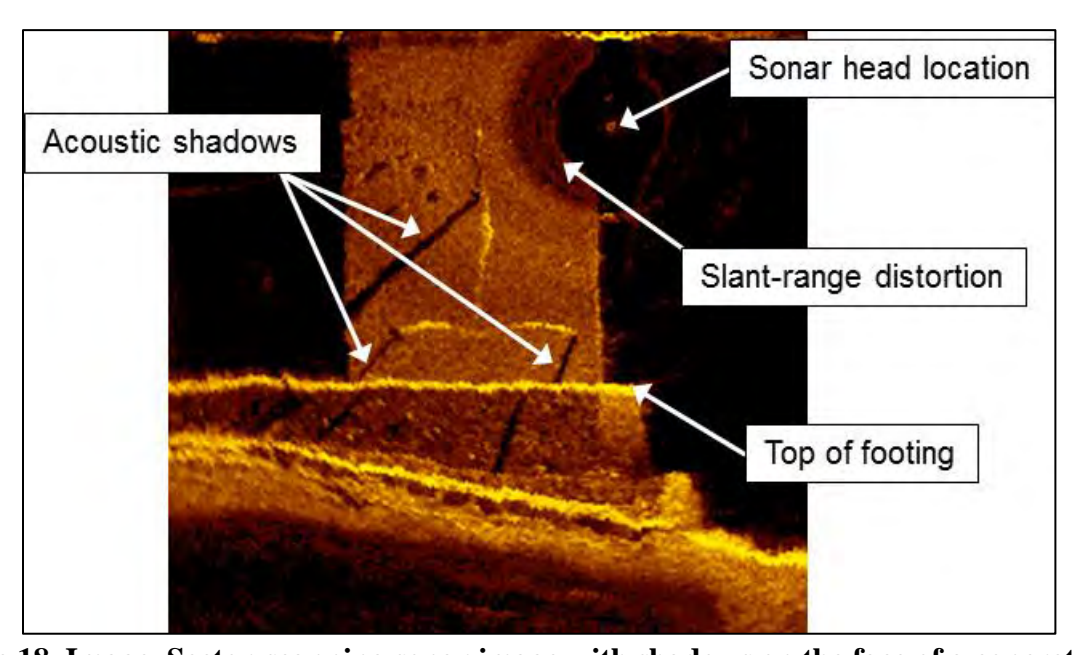


Figure 18. Image. Sector-scanning sonar image with shadows on the face of a concrete pier.

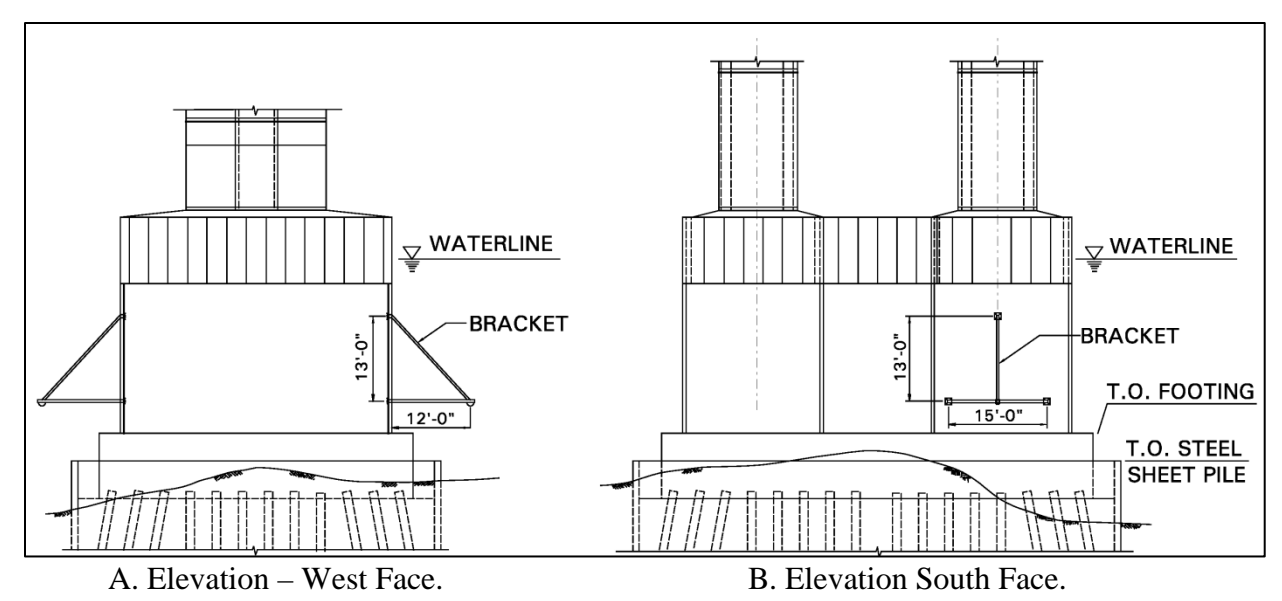


Figure 19. Schematic. Fixed scour monitor system mounted on bridge foundation.

SLANT-RANGE DISTORTION

Most two-dimensional imaging sonar systems such as side-scan sonar, sector-scanning sonar, and lens-based multibeam sonar have oblong, fan-shaped beams. They essentially work by recording the full range of returns from the wide dimension of the cone angle and plotting them on a two-dimensional drawing. Because the sonar unit can't distinguish which portion of the wide cone angle a return came from, a distortion error (referred to as slant-range distortion) is produced. Targets at the centerline of the beam are resolved at the correct distance but targets near either edge of the beam are plotted with respect to their echoed range as illustrated in figure 20. Slant-range distortion is visually depicted by a concave or curved surface and is most pronounced near the sonar head. (13)

While slant-range distortion does continue throughout the full range of the beam, it is most pronounced near the sonar head and can be compounded by the effects of side lobes providing false readings. Slant-range distortion can be calculated based on the difference between the lateral and diagonal distance to a point on the structure being imaged. Thus, the distance at which the sonar head is held from the surface being imaged also effects slant range by increasing the angle to the target surface. Therefore, it is useful to document the imaging stand-off distance used at a bridge site.

To reduce the effects of slant-range distortion, the sonar head should be positioned a sufficient distance away from a target to reduce the effects. Another method of visually minimizing the effects of slant-range distortion is to remove heavily affected areas during image mosaic post processing. Additionally, some scanning sonar software has a built-in function that attempts to correct slant-range distortions. (13)

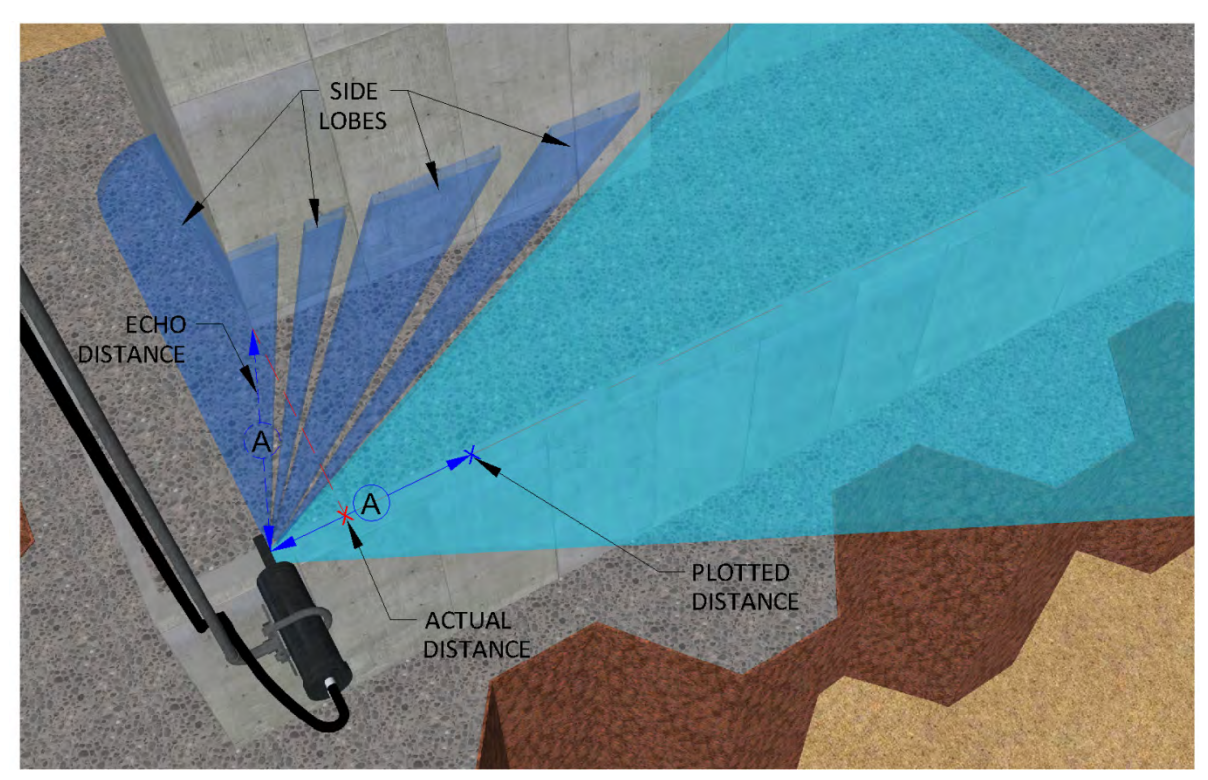


Figure 20. Graphic. Echoed range versus plotted distance of a sector-scanning sonar.

GPS ACCURACY

Accurate georeferencing of collected sonar points influences data representation. Multibeam point cloud surveys and two-dimensional scanning sonar can both be used with or without Global Positioning Systems (GPS) or motion compensation. However, georeferencing the data ensures repeatability for comparison with past and future inspection if they are also georeferenced. One of the main limitations of typical multibeam bridge surveys, however, is that almost all high-resolution multibeam surveys rely on RTK Differential Global Positioning System (DGPS) data for tracking precise vessel position and elevation during the survey. (16) While extremely accurate, this system relies on having a good "line-of-sight" with the satellite constellation to maintain a position fix. Imaging a bridge may require the boat to frequently pass beneath the bridge into areas where maintaining good satellite reception is difficult. In fact, it is not uncommon for sonar data to be improperly referenced or lost when the survey vessel is positioned under a bridge. The amount of error introduced into the data can vary depending on many factors, including the height of the bridge (i.e. the existing freeboard between the waterline and superstructure), the number/location of satellites, and the location of the survey line relative to the satellites. To mitigate this error, RTK DGPS can be supplemented with other methods of obtaining a position such as use of a total station. (15) There are also devices that use a dedicated vertical beam for the purpose of "bottom tracking." The bottom tracking allows determination of location in geographic coordinates if the GPS signal is lost for a period of time.

Some commercial off-the-shelf single-beam fathometers are also capable of using the Federal Aviation Administration (FAA) and U.S. Department of Transportation (USDOT) Wide Area Augmentation System (WAAS). The WAAS uses ground reference stations positioned

throughout the United States to correct for signal errors caused by ionospheric disturbances, timing, and satellite orbit errors. A surveyor with a WAAS-capable GPS receiver can expect position accuracy up to five times greater than when using conventional GPS alone, but less accuracy compared with RTK DGPS. The same issues of line-of-sight around bridges and trees can cause position error similar to that encountered by RTK DGPS. (15)

CHAPTER 5. FIELD PROGRAM

A field evaluation program was developed to deploy and evaluate sonar technologies for underwater bridge inspection. Design of the field program considered appropriate technology, field test conditions, and site selection. Based on the need for a comparative reference of existing conditions within the same time period, field test sonar imaging results are compared to inspection results obtained by qualified inspection divers.

TECHNOLOGY SELECTION

The technologies described in Chapter 3 were rated by the research team to identify those most applicable for underwater bridge inspection. The criteria are listed in Table 4 along with a rating for each technology. The ratings ranged from 1 representing the lowest (poorest) to 4 representing the highest (best). The assigned ratings were not considered to be definitive, but rather a qualitative tool to identify technologies to be used for the field evaluations in this project. The technologies with the three highest ratings were selected for field evaluation: 1) real-time multibeam (3D), 2) sector-scanning (2D), and 3) multibeam swath (3D).

Table 4. Summary comparison of acoustic imaging technology qualities.

Criteria	Multibeam Swath (3D)	Real-Time Multibeam (3D)	Side-Scan (2D)	Sector- scanning (2D)	Lens-Based (2D)
Perspective (2D, 3D)	4	4	2	2	2
Accuracy	4	4	2	2	2
Object ID/Resolution	4	4	2	2	2
Portability	2	3	4	4	4
Cost	2	1	3	4	3
Ease of Use	1	2	2	3	3
Ability to Image Vertical Surfaces	3	4	2	4	3
Post Processing Time	2	4	2	3	2
Total Score	22	26	19	24	21

Based on the scores from table 4, the real-time multibeam (3D) sonar exhibits the most desirable qualities for underwater bridge inspection. Although the technology has been being used in the offshore energy and security industries for several years, there are few case studies demonstrating performance in conditions often encountered at bridge sites. Real-time multibeam (3D) sonar captures 3D point clouds several times per second that, if georeferenced, can be combined into more comprehensive models of underwater conditions. The technology also produces photo-like images. Because of the speed and accuracy of data acquisition, the Coda Octopus Echoscope® was selected to represent this technology for this study.

The second highest rated class of technology was 2D sector-scanning. 2D sector-scanning technologies work well for capturing features that stand out or are depressed from the main surface. They require relatively stationary mounting for maximum effectiveness. However, when using the traditional method of positioning the acoustic beam near parallel to the surface being imaged this technology does not have the capability to obtain penetration depth data for structural defects and voids. Field research with 2D imaging technologies should focus on obtaining penetration depths of voids and other defects. In addition, the utility of data obtained using 2D sector-scanning sonar with a tilt block head should be compared to data obtained by a similar unit without the tilt block head. Because of the quality of data, ease of use, and history in the industry, the Kongsberg Mesotech 1071/1171 sonar heads with MS1000 processing software were selected to represent this technology category for this study. Selection of deployment method (vessel mounted or tripod) may be site specific with extra attention being paid to minimization of sonar head movement.

The third rated technology class, multibeam swath sonar has been used to document submerged structures. Beyond its use in hydrographic surveys, the literature reports few applications for this technology in scanning vertical surfaces for structural defects or foundations for undermining. Based on its accuracy, affordability, and ease of use in comparison to other multibeam swath systems, the BlueView BV5000 was selected to represent this technology class for this study.

Two other technologies were applied in this study that were available from the previously mentioned manufacturers. The BlueView BV3100-900-130A is a 2D multibeam array sonar. This type of sonar is analogous to the sector-scanning technology, but gathers data instantaneously through a specified view angle. It also allows for mounting on a moving boat. It produces 2D videos and, similar to sector-scanning, 2D multibeam technology produces photolike images.

Finally, a Kongsberg Mesotech 3D profiler is a 3D single beam profiler. Similar to other 3D sonar, it also produces 3D point clouds. These operate most effectively with stationary mounting.

Table 5 summarizes the technologies available for this study. The data were compiled from manufacturer-published specification data sheets. The sonar inspection field work for this study was completed by three inspection teams. The details of the technologies used by each inspection team are described in the following sections. Descriptions of the process and results of the field inspections are provided later in this report.

3D Real-Time Multibeam

Sonar inspection team A used a dual frequency 3D real-time multibeam sonar for this study. In addition to the information in table 5, the equipment operated with the following characteristics and supporting software:

• Minimum range: 3 ft (1 m).

• Range resolution: 1.2 in (3 cm).

• Ping rate: Up to 12 Hz.

• Angular coverage: 50 degrees x 50 degrees.

- Beam spacing: 0.39 degrees.
- Motion/position: Coda Octopus F180 Motion Reference/GPS unit (F185+ according to labeling).
- Mount: Universal Sonar Mount (USM) pole mount and vessel of opportunity (VOOP) kit.
- Software: Coda Octopus Underwater Survey Explorer.

Setup and mounting of the equipment is shown in figure 21.

Table 5. Selected imaging sonar products and specifications.

Company	Unit Type	Unit	Cost*	Frequency	Number of Beams	Max Range (ft (m))
Kongsberg Mesotech	2D Sector-scanning	1071/1171 sonar heads with MS1000 processing software	\$20,000 (\$22,000 with tilt block head)	675 kHz	1	430 (131)
Kongsberg Mesotech	3D Single Beam Profiler	MS1000 with dual motor tripod	\$65,000			
Teledyne BlueView	2D Multibeam	BV3100-900-130	\$27,157			
Teledyne BlueView	3D Multibeam Mechanical Scanning	BV-5000 1350	\$113,945	1.35 MHz	256	98 (30)
Coda Octopus	Real-Time Multibeam (3D)	Coda Echoscope® (dual frequency)	\$260,400	375kHz	128 x 128 (16,384)	500 (152)

^{*} Cost does not include operating computer, software, training, custom built transducer mount, or ancillary components. Costs were as reported at the time of the field work and may have changed.

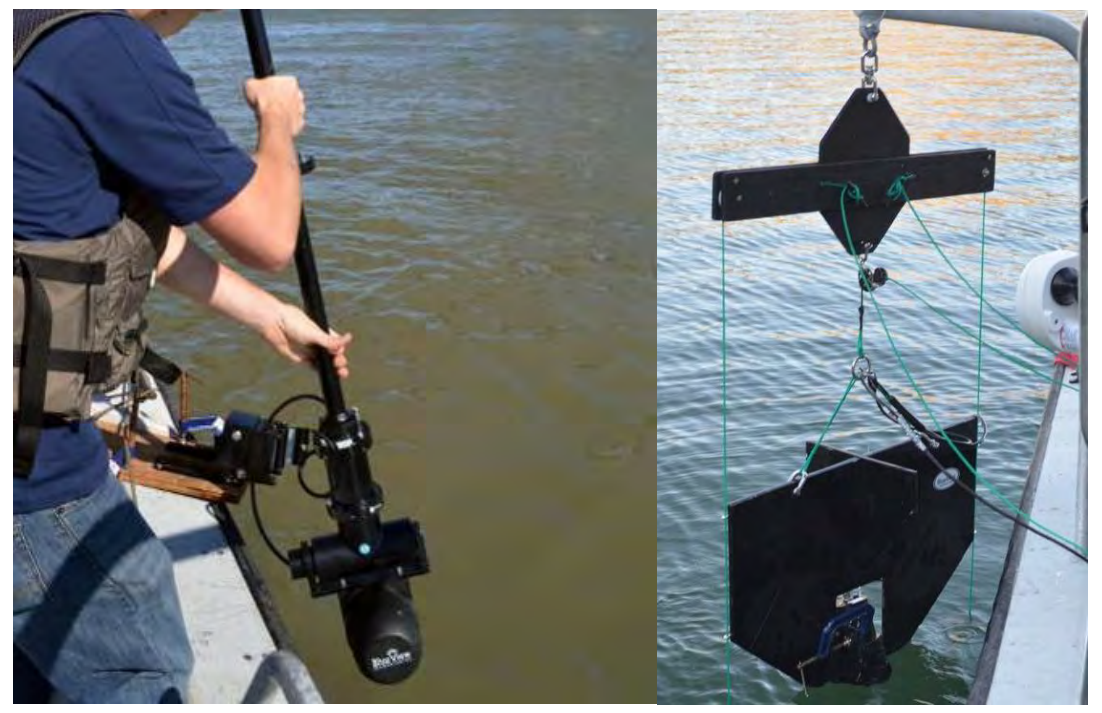


Figure 21. Photo. 3D real-time multibeam sonar mounted on the boat.

2D Multibeam and 3D Mechanical Multibeam

Sonar inspection team B used a 2D multibeam sonar and a 3D mechanical multibeam sonar as described in table 5. The primary sonar used in the field was the 2D multibeam imaging sonar. This sonar unit can be mounted in several ways including on a side pole or attached to a vertical scanning wing as shown in figure 22. The pole-mount requires a special clamping apparatus.

In addition, a 3D mechanical multibeam scanning sonar was used by inspection team B. This unit requires stationary mounting, usually on the water body bed. A tripod and a heavy-plate mounting were both used in this study as shown in figure 23. The 3D mechanical multibeam scanning unit had a beam pattern of 1 degree by 1 degree with a 0.18 degree spacing. The mechanical step size was a minimum of 0.4 degrees.



A. Side pole.

B. Vertical scanning wing.

Figure 22. Photo. Boat mount methods.

2D Sector-scanning and 3D Profiler

Sonar inspection team C used two sonar types: a 2D sector-scanning sonar and a 3D profiler sonar. In addition to the information in table 5, the equipment included the following:

- Sonar head: 1171-series 975-23700000 high resolution head with tunable frequencies from 900kHz-1300kHz.
- Mounting: Pole mounted with an attached rotator/head arrangement and a collocated 3axis sensor.
- Open Source Software: MeshLab and CloudCompare were used to assemble the data.

The 2D sector-scanning equipment had a beam pattern 0.9 degrees by 30 degrees with a minimum step size of 0.225 degrees.

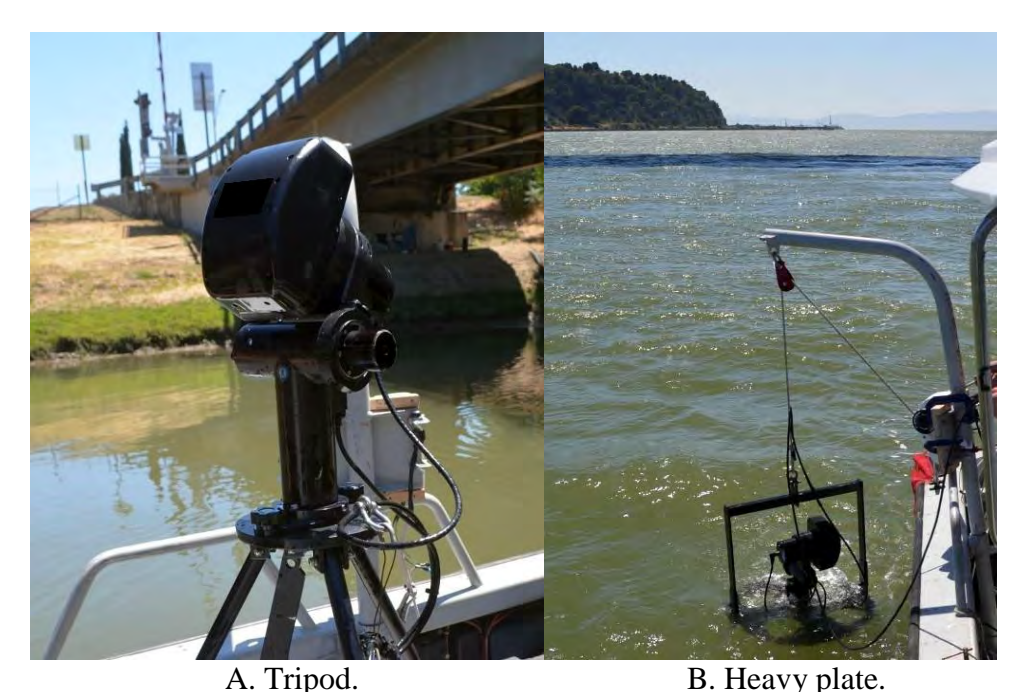


Figure 23. Photo. Stationary mounting methods.

Dive Equipment

Dive inspection teams were also used as part of this study to compare inspection findings with the sonar inspection teams. The dive equipment used included:

- Two 300 ft (91 m) dive umbilicals.
- KM-37 dive helmet.
- Aga dive mask.
- Kirby Morgan KMACS 5 dive console.
- Two 30 ft³ (0.85 m³) bailout bottles.
- Eight 80 ft³ (2.3 m³) dive tanks.
- Diver personal gear.
- Camera with underwater housing.

UNDERWATER BRIDGE INSPECTION ENVIRONMENT

Sonar technology and divers must be able to detect and distinguish certain characteristics of the underwater structure in a range of environmental conditions. The characteristics and conditions expected can be categorized into several categories: construction materials and associated

defects, geometric configuration, and environmental influences. These are described in the following sections.

Construction Materials and Defects

The underwater portions of a structure are generally subject to distress and deterioration. The characteristics of a construction material will influence the types of deterioration that might occur, the quality of an acoustic image, and the ability to detect defects based on surface texture and differing acoustic absorption coefficients. Because acoustic imaging methods do not provide a definitive identification of submerged construction material type, consultation of as-built bridge plans is recommended to aid in the analysis of acoustic imaging results. The most common bridge construction materials and the defects associated with each are discussed in the following sections.

Concrete

Concrete bridge elements generally include unreinforced, reinforced, and/or pre-stressed members. Concrete defects fall into three categories:

- Cracking: Because concrete has little tensile strength, cracks occur due to volume changes as temperatures vary and concrete members contract or expand. Cracks may result from structural and non-structural causes. Cracks may also be an indication of overloading, corrosion of reinforcing steel, or settlement of the structure.
- Scaling: Scaling is a gradual and continuous loss of surface mortar and aggregate from an
 area. This condition is commonly found at the waterline on piers and piles where freezethaw action occurs.
- Spalling: Spalling is a depression in the surface of concrete which exposes reinforcing steel to corrosion. It is primarily the result of internal expansive forces caused by corrosion of the steel.

Steel

Steel is used as a structural material for piling and bracing and as external protective cladding on concrete elements. The primary cause of damage to steel is corrosion. Corrosion is most prevalent in the splash and tidal zones, but can occur both above and below water. Corrosion can be especially severe when a bridge is located in salt water or brackish water. The most important factors influencing and producing corrosion are the presence of oxygen, moisture, chemicals, pollution, stray electrical currents, certain microbes, and water velocity. Heavy marine growth, found in seawater, can sometimes inhibit corrosion, but it can also hide severe distress. Steel coatings are commonly used to prevent corrosion. The underwater inspection of coated steel structural members should assess deterioration of the coating.

Unreinforced Masonry

Masonry is not commonly used in new bridge construction, although it is sometimes used as an ornamental facing. Many older bridges have piers and abutments constructed of masonry. Typical problems in masonry structures include cracking, scaling, and deteriorated grout.

Timber

Deterioration of timber members results from a variety of causes, including decay, marine infestation, bacterial degradation, abrasion, and collision. Varying densities and saturation levels of timber may affect acoustic imaging results.

Composite Materials

Composites, or fiber reinforced polymers (FRP), are a mixture of fibers and resins. Most mechanical defects of composite materials result from impact, abrasion, or construction related events. Composites are susceptible to fire and degradation by ultra-violet rays and are more resistant to marine borers than timber.

Geometric Configuration

For both structural and architectural reasons, there are many geometric variations of bridge substructures. The shape and type of the substructure unit element involved in a field test of this study may limit the coverage of an acoustic image to less than 100 percent by shadowing certain portions. Additionally, long slender members are visually more affected by distortions. This distortion can cause members to appear bent or buckled when they are not. Common substructure configurations that currently exist in the NBI that may affect imaging include:

- Pier shafts: Piers are intermediate supports constructed of concrete, masonry, timber, or steel. A pier consists of three basic elements: a footing, a shaft, and a pier cap. Footings can be founded on driven piles, drilled shafts, caissons, or directly on soil or rock, i.e., on spread footings.
- Abutments: The term "abutment" is usually applied to the substructure units at the ends of bridges. An abutment provides end support for a bridge and retains the approach embankment.
- Pile bents: Pile bents are structural supports consisting of piles and pile caps. Superstructure loads are distributed to the piles by the pile cap. Pile bents, which can be constructed of timber, concrete, steel, composites, or a combination of these, are used both as intermediate supports and as abutments.
- Cofferdams and foundation seals: Bridge piers and abutments are often constructed in the dry using cofferdams and foundation seals. Cofferdams are typically constructed of steel sheet piling. After the foundation construction is completed, the sheeting may be removed or cut off near the channel bottom. It may be separated from the foundation material or the sheeting may be used as a form against which concrete is cast making the sheeting an integral part of the foundation.
- Substructure columns and caissons: A caisson is an enclosure used to build a pier's foundation and carry superstructure and substructure loads through poor soil and water to sound soil or rock. Caissons are constructed of timber, reinforced concrete, steel plates, or a combination of materials. The floating structure is towed to the construction site and sunk. Soil below a caisson is removed through openings in its bottom. Once the caisson is in place, it is filled with concrete and the bridge pier is built on it.

• Fenders and protection devices: Dolphins, fenders, and shear fences are placed around bridge substructure units to protect them from vessel impacts. While protection devices are commonly inspected by divers during routine underwater inspections, the presence of protection devices can hinder access to the substructure for acoustic imaging.

Environmental Influences

Environmental factors that may influence the quality of acoustic imaging of a bridge include water temperature, salinity, and depth. Assuming that the sonar device being used has the appropriate feature, these factors can be accounted for based on calibration of the equipment with regards to the local speed of sound.

Additional environmental factors include:

- Turbidity level: Turbidity may affect results produced at certain sonar frequencies.
- Current: Current may affect the deployment of the sonar head to reduce heave, roll, pitch, and yaw.
- Marine growth: Marine growth may obstruct sound waves from reaching the surface being imaged.
- Turbulence: Turbulence may suspend air bubbles in the water column.
- Depth: Very deep water may result in images with poor resolution and very shallow water may present sonar deployment issues and multipath errors.

CHAPTER 6. PHASE I FIELD TESTING

Bridge sites for the phase I field testing were selected considering a broad range of conditions relevant to comparing underwater inspection techniques: depth, clarity, current, marine growth, and type/material of foundation. Caltrans provided information on the bridge sites and facilitated access for inspections conducted for this study. The goals of the phase I field testing can be summarized as:

- 1. Evaluate the capabilities and limitations of sonar technologies and compare findings referenced to divers under various conditions.
- 2. Identify areas of inspection work where acoustic imaging can provide significant assistance to divers.
- 3. Identify work conditions that may pose significant danger to divers and where acoustic imaging can complete the work with less risk.
- 4. Identify areas of inspection where acoustic imaging may produce significant increase in efficiency and quality.
- 5. Produce quantitative measurements of cost, efficiency, and, if possible, safety.

OVERVIEW OF BRIDGE SITES AND LOGISTICS

Four bridges in California were identified for this phase of the field work. Because a full inspection of the entire bridge was beyond the scope of this study, selected portions of each bridge were targeted. The four bridges are: 1) a bridge over the Georgiana Slough, 2) the James E. Roberts Bridge crossing the Tuolumne River, 3) the Carquinez Bridge (1958) and the Carquinez Bridge (2003). The latter two bridges span the Carquinez straight with one being a newer span than the other.

Table 6 provides a summary of selected bridge characteristics and site conditions. The type of bridge substructure at each location is given as are site conditions such as water depth, visibility, and current.

Table 0. I have I bridge characteristics and site conditions.											
Bridge Name	Bridge #	Water Depth	Visibility	Current	Marine Growth	Conc. Monolith	Concrete Piles	Steel Piles	Timber Piles	Fender System	Pile Cap
Georgiana Slough	24C0039	25 ft (7.6 m)	Low	Slow	Light		X	X	X	X	X
James E Roberts	32 0018	< 200 ft (61 m)	High	None	None		X				
Carquinez (1958)	23- 0015R	< 100 ft (30.5 m)	Low	Swift Tidal	Light	X					
Carquinez (2003)	23- 0352L	< 100 ft (30.5 m)	Low	Swift Tidal	Light		X	Shell			X

Table 6. Phase I bridge characteristics and site conditions.

Three sonar inspection teams and one dive inspection team performed an inspection at each bridge. The phase I field tests were conducted according to the schedule in table 7. Each team conducted its inspection independently of the other teams. Specialized equipment and operators were engaged as required. General equipment and supplies were provided by Collins Engineers. This included a boat (Boston Whaler), generator, life jackets, and typical boating supplies.

Table 7. Phase I field test schedule.

Dates	Team
July 27 – 28, 2012	Sonar inspection team A
July 29 – 30, 2012	Sonar inspection team B
July 31 – Aug. 1, 2012	Sonar inspection team C
Aug. 2 – 3, 2012	Diving inspection team D

After the field work, each team was asked to prepare an inspection report loosely based on the common format presented in the underwater inspection manual. The following information was also requested:

- Team composition.
- Standard/code/specifications (if any) used during and in preparation for the work.
- Test log (file names vs. locations) for the two days.
- Rental and purchase pricing.
- Equipment inventory that shows all equipment that went on the boat and was used in the inspection.
- Documentation of effort (time) used in post processing.

Highlights from the reports prepared by each inspection team are summarized in the next sections for each bridge site. In general, the sonar inspection reports are more graphical than normal bridge inspection reports because of the automated data collection and post-processing methods. The graphical outputs required interpretation by experienced bridge inspectors to identify findings that would be of concern for the preservation and protection of the bridge substructures.

GEORGIANA SLOUGH BRIDGE

The Georgiana Slough Bridge, shown in figure 24, is located on Isleton Road crossing Georgiana Slough near Walnut Grove, California. The main feature is a pivot pier (pier 2) supported on concrete-filled steel piles. It also features a treated timber fender system next to the pier and across the stream. An as-built drawing of the bridge is provided in figure 25. Post-test discussion with Caltrans revealed that previous inspections reported that the main pier has tilted.

Access is possible by boat and from the deck. Bank access is possible, but the pier and fender system are at least approximately 50 ft (15 m) away with water depths beyond those suitable for wading.



A. Looking north behind the timber fender.



B. Looking north from the main channel.

Figure 24. Photo. The Georgiana Slough Bridge.

3D Real-Time Multibeam (Inspection Team A)

Using a real-time multibeam sonar, inspection team A collected data in the field that produced images that captured general pile features. The images in figure 26 and figure 27 reveal the piles supporting the fender in profile and plan view, respectively. In the profile view, it is evident that several piles are not aligned vertically. In the plan view, the curved aligned of the set of piles is clearly seen.

Figure 28 displays a close-up of several piles. With the x,y,z capability, it is possible to estimate feature dimensions such as object length.

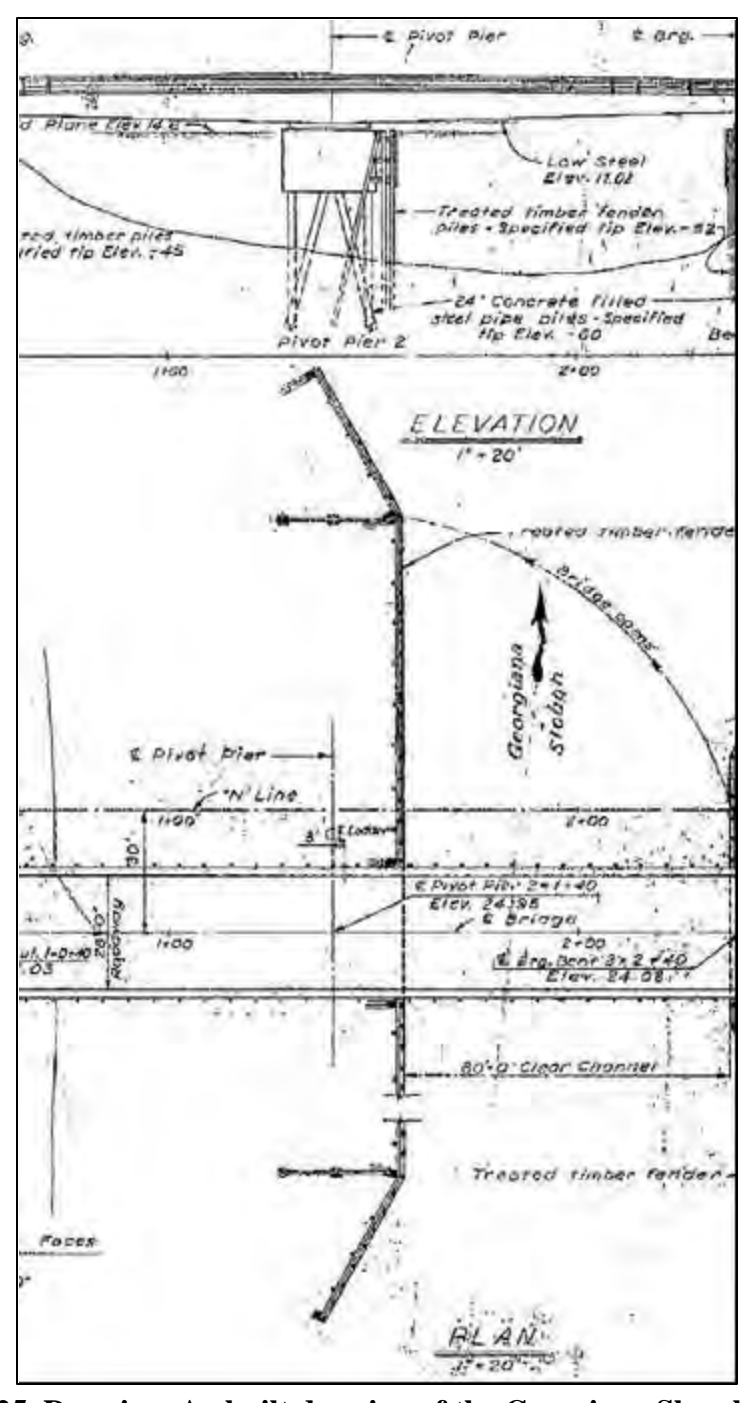


Figure 25. Drawing. As-built drawing of the Georgiana Slough Bridge.

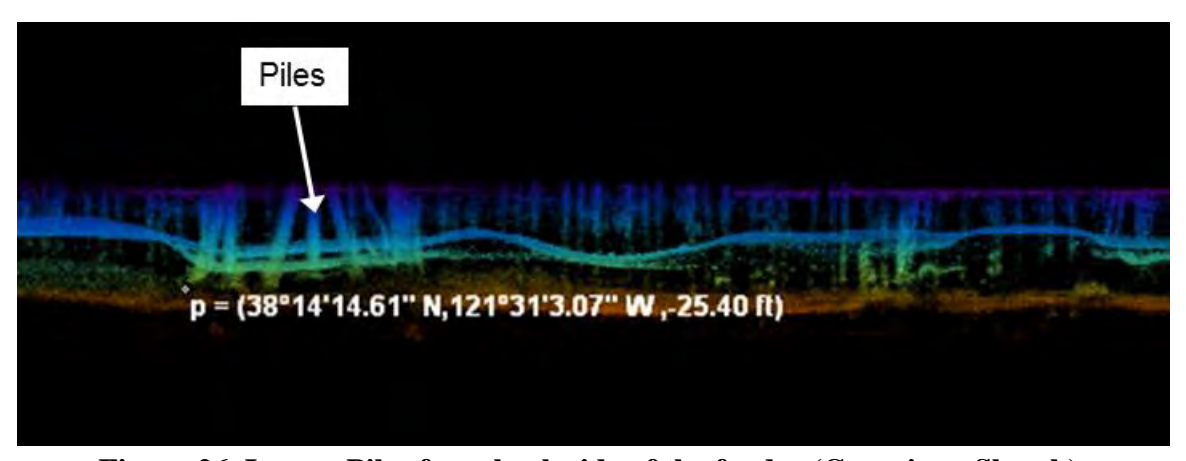


Figure 26. Image. Piles from back side of the fender (Georgiana Slough).



Figure 27. Image. Curved pile alignment in plan view (Georgiana Slough).

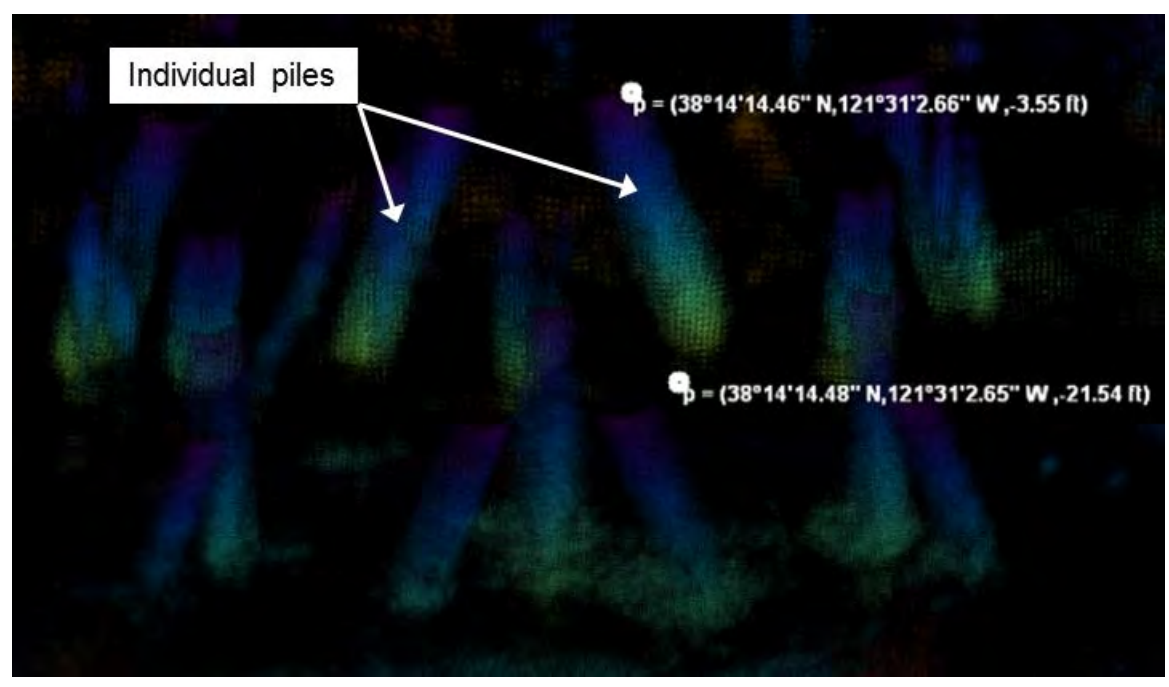


Figure 28. Image. Coordinates from which length of a pile is estimated (Georgiana Slough).

2D Multibeam and 3D Mechanical Multibeam (Inspection Team B)

Inspection team B employed two sonar technologies for the inspection of the Georgiana Slough Bridge. Figure 29 shows an example image from a 2D multibeam sonar along with the inset providing the location of the image at the site. The image resulted from a single ping and was captured from boat-mounted equipment. The piles on either side of the channel are evident as is a cable crossing the channel.

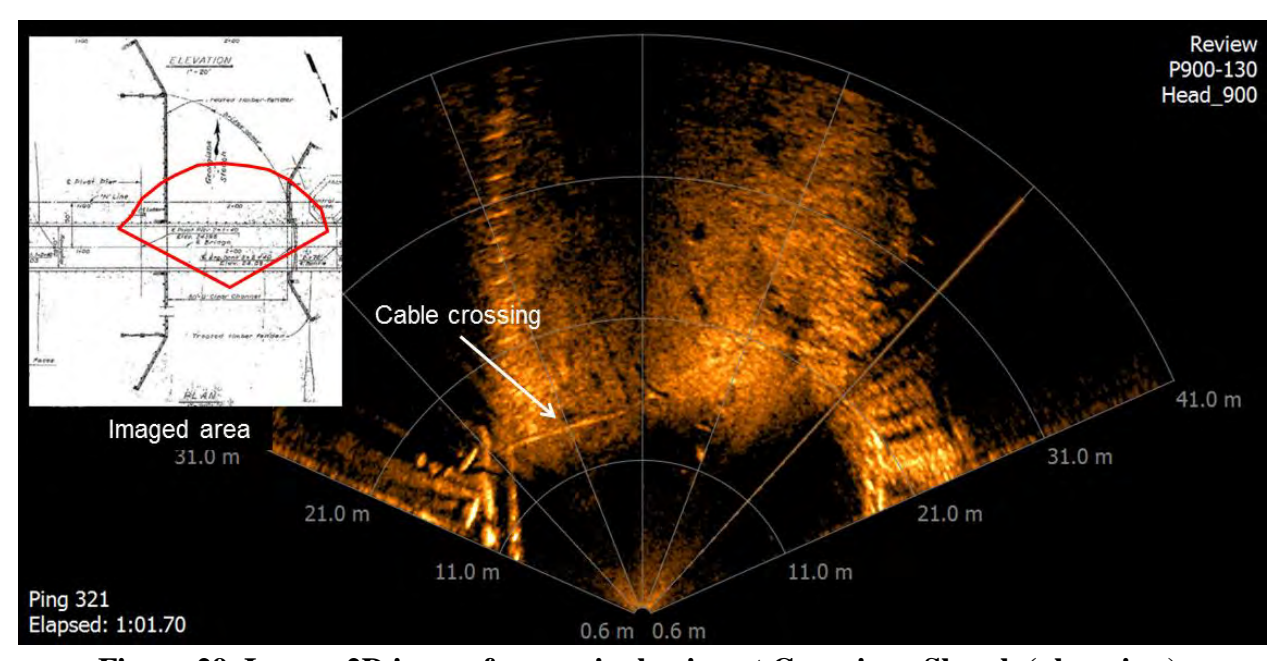
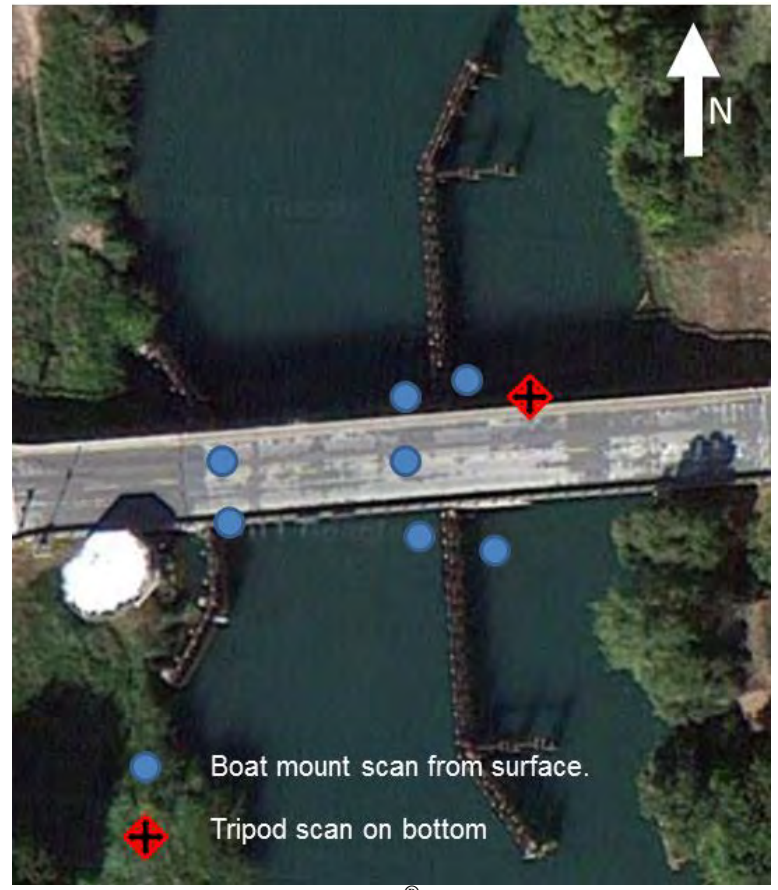


Figure 29. Image. 2D image from a single ping at Georgiana Slough (plan view).

Inspection team B also used a 3D mechanical multibeam sonar. Figure 30 shows a plan view of the scanning locations for generating the image in figure 31. The 3D image clearly shows the piles on both sides of the channel.

Figure 32 provides a sonar image overlain on an aerial photo that highlights darker areas indicative of minor scour around the structures. The image also shows moderate levels of debris, including tree limbs and tires, but no visible damage to the substructure.



Original Photo. © 2012 Google®

Figure 30. Image. 3D scan locations (Georgiana Slough).

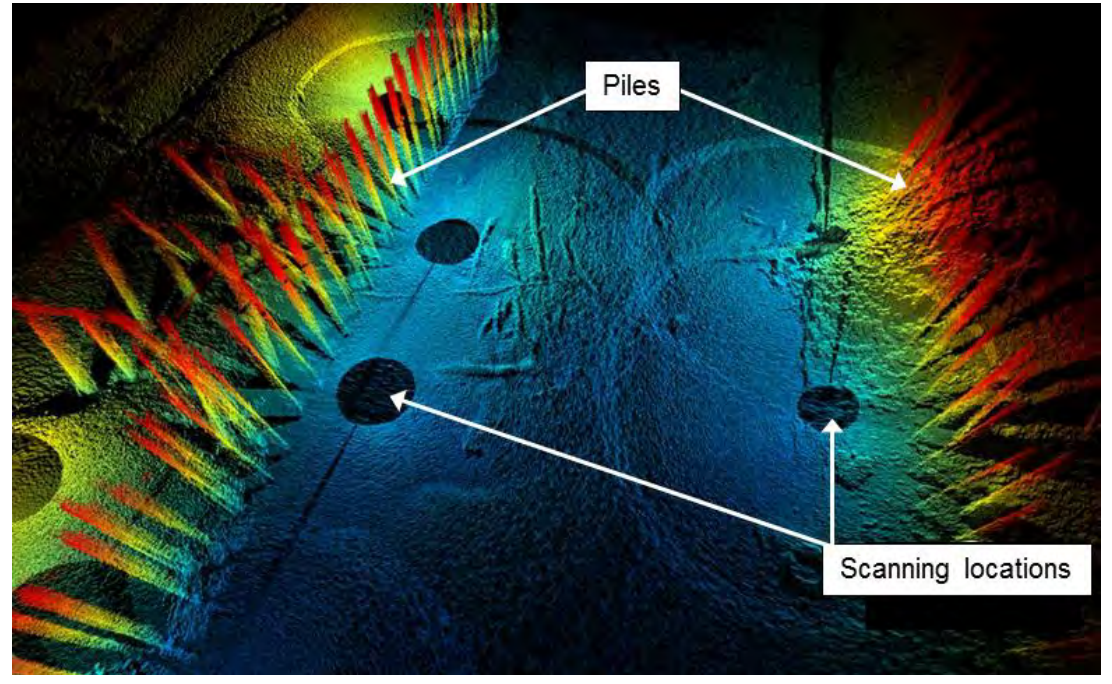
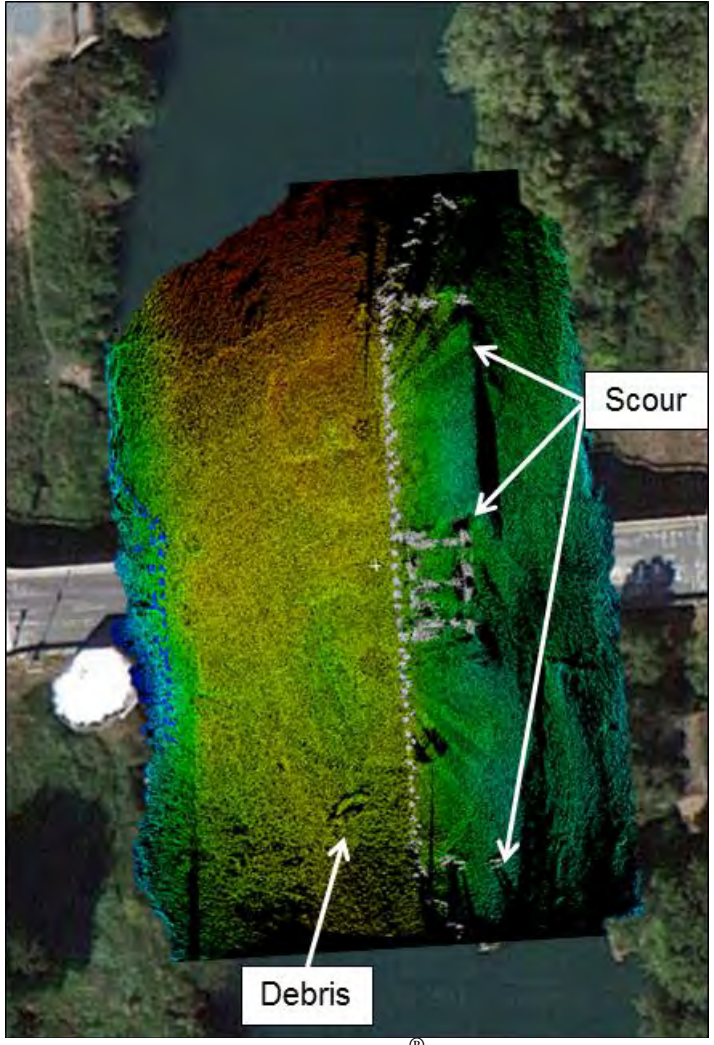


Figure 31. Image. 3D image (Georgiana Slough).



Original Photo. © 2012 Google®

Figure 32. Image. Indications of scouring from 3D image (Georgiana Slough).

2D Sector-scanning and 3D Profiler (Inspection Team C)

Inspection team C used 2D sector-scanning sonar and 3D profiler sonar to collect riverbed and vertical visualization scans of the underwater portion of pier 2 of the Georgiana Slough Bridge. Bottom scans, taken with the sonar head fitted onto a tripod, were collected adjacent to the structure. The bottom scan locations are shown in figure 33 with a resulting mosaic of the drop images shown in figure 34. The bridge pier, piling, bathymetry, and some debris are visible.

After completing the bottom drops, the head was horizontally mounted on a pole and positioned three feet below the surface to vertically scan the fender wall. The data collected from the bottom drops and vertical scans were merged to create 3D representations as shown in figure 35.

The inspection team observed in both the imaging and profiling datasets that although the fender system is there to protect the structure from vessel traffic, it appears to have caused localized scour on the upstream side of the pier. This local scour has induced sediment degradation on the upstream nose and aggregation on the downstream side of the structure. The fender system

appears to be structurally sound with no breaks or splits in the piles. Debris build up was noted on the upstream dogleg. The team reported that the vertical and batter pipe piles appeared to be structurally sound with no visible impact damage or structural deterioration.



Original Photo. © 2012 Google®

Figure 33. Image. Bottom drop locations (Georgiana Slough).

The acoustic imaging and profiling data sets displayed the electrical cable(s) for the swing bridge hanging beneath the structure (confirmed by divers in an earlier survey). The cables appeared to be clear of debris and entanglement.

In the main channel the imaging data showed different stratigraphic units comprised of gravel, or possibly, hardpan clays. The imaging also showed the complexity of the generally stable river bottom. A box-shaped target was observed near the fender piles on the main channel downstream side; this target was confirmed by divers to be an old refrigerator. There are several angular targets in the main channel; their angularity and out of character nature to the natural bottom suggest they are human debris.

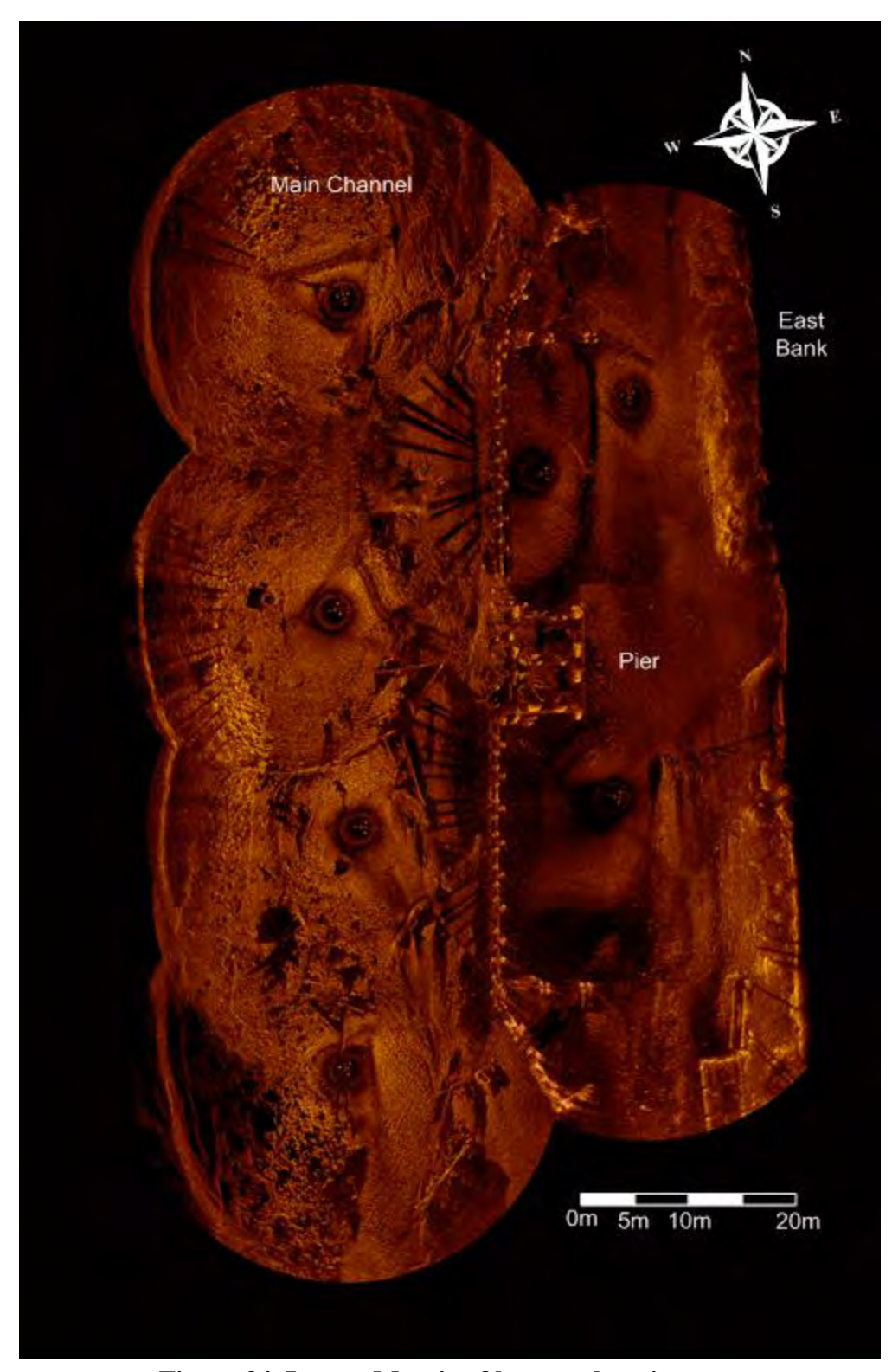


Figure 34. Image. Mosaic of bottom drop images.

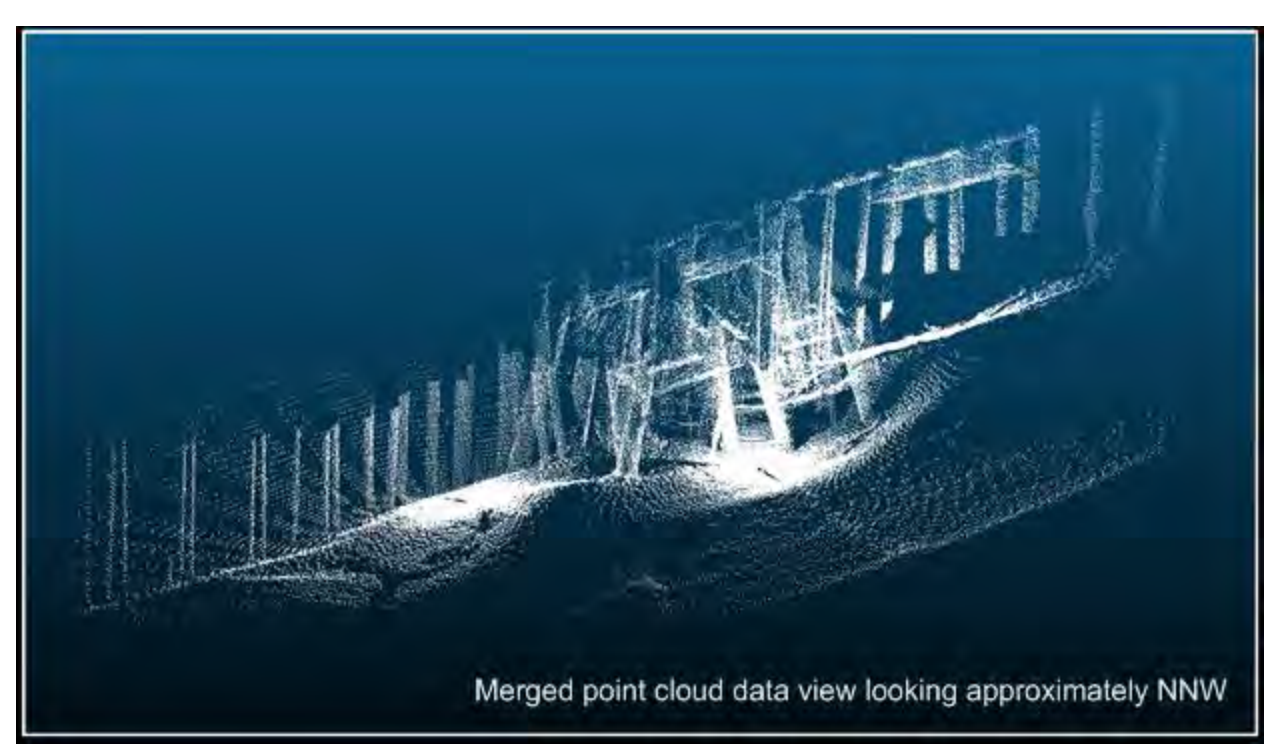


Figure 35. Image. Merged point cloud data at Georgiana Slough Bridge.

Dive Inspection

Qualified divers conducted an inspection of pier 2 of the Georgiana Slough Bridge. At the time of inspection the estimated underwater visibility was 1 ft (0.3 m) and there was no current. The waterline was located 11.8 ft (3.6 m) below the top of concrete cap at pier 2. This corresponded to a waterline elevation of +3.5 ft (1.1 m). Inspection observations included the following:

- The channel bottom consisted of sandy clay with 3-inch (76 mm) maximum penetration.
- Steel pipe piles exhibited surface corrosion and pitting with 1/32-inch (0.8 mm) typical penetration and 1/16-inch (1.6 mm) maximum penetration over generally 100 percent of the surface area.
- Steel and concrete surfaces were covered with a ¼-inch to 1-inch (6 to 25 mm) thick layer of aquatic growth as shown in figure 36 with a level II cleaned area also visible in the figure.
- Concrete was sound without any detected major defects. The concrete surfaces exhibited scaling with 1/16-inch (1.6 mm) typical penetration from 18 inches (460 mm) above to 6 inches (150 mm) below the waterline.
- Two open bays formed by the concrete cap beams were detected. Timber and steel formwork was still in place along the underside of the concrete cap beams.
- Three 4-inch (100 mm) diameter steel cables were observed extending vertically from the northwest quadrant of the south bay to the channel bottom as shown in figure 37.

- Timber fender piles were typically lightly weathered with 1/16-inch (1.6 mm) awl penetration. The full fender system was not inspected.
- A broken timber pile located 3 ft (0.9 m) west of the fender face and 10 ft (3 m) north of the south fender corner was observed protruding 6 ft (1.8 m) from the channel bottom.

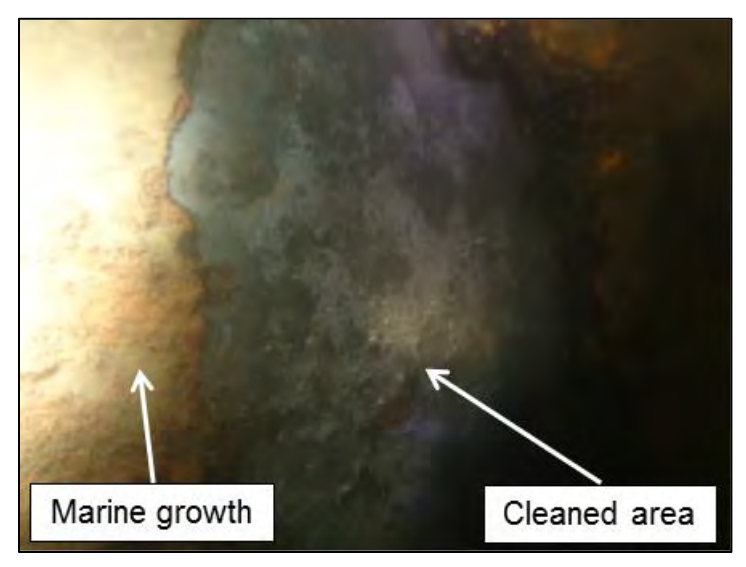


Figure 36. Photo. Steel pile showing marine growth and a level II cleaned area.

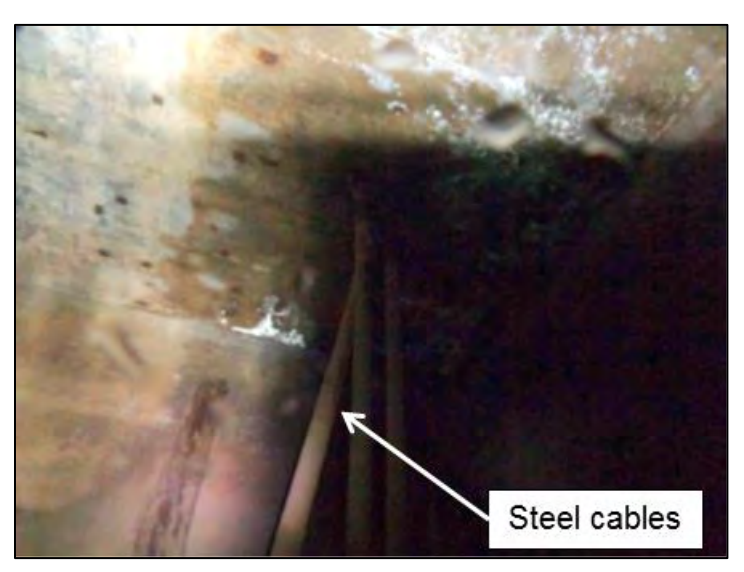


Figure 37. Photo. Above water view of steel cables.

Overall, the divers were able to make detailed observations about the condition of individual structural elements that could not be made by the sonar devices. However, the area covered by the divers was limited.

JAMES E. ROBERTS BRIDGE

The James E. Roberts Bridge is located on California State Highway 49/120 crossing the Tuolumne River at Lake Don Pedro. It consists of five monolithic concrete pier bents and a steel

girder superstructure. Bent 4, shown in figure 38, was selected for inspection. Figure 39 provides an as-built drawing of bent 4. This bent has the greatest height among the 5 bents at 229 ft (70 m). While the water surface varies with season, the depth of water at the bent on the day of testing was approximately 150 ft (46 m).

Access from the deck and bank is nearly impossible. The deck is over 50 ft (15 m) from the water surface and the pier is over 250 ft (76 m)) from the bank. The space around the bent is open, but opportunities for fixing equipment to the pier are limited.

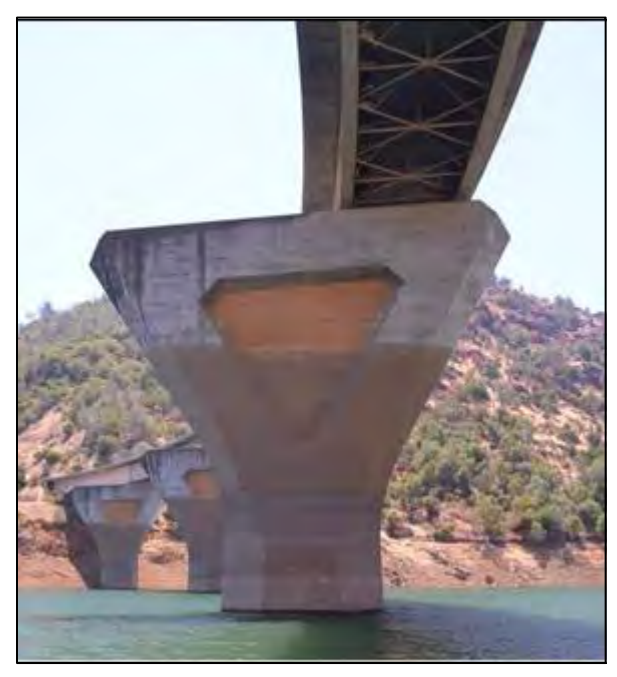


Figure 38. Photo. Northwest face of bent 4.

3D Real-Time Multibeam (Inspection Team A)

James E. Roberts Bridge (bent 4) is in a relatively deep and clear reservoir. At the time of the inspection by team A, water depth at bent 4 was approximately 135 ft (41 m) on the shore side and 150 ft (46 m)) on the channel side.

Figure 40 shows the image of bent 4 captured by the sonar. A symbol representing the data collection boat is also shown to illustrate the range required of the sonar at this site. Figure 41 is a data mosaic showing bents 4 and 5 as viewed from the west side of the bridge. The annotations on the figure demonstrate how structure dimensions can be obtained from the image. Close analysis of the images may reveal reportable observations. For example, a closer view of the base of bent 4 shown in figure 42 provides an indication of scour at the base of the bent.

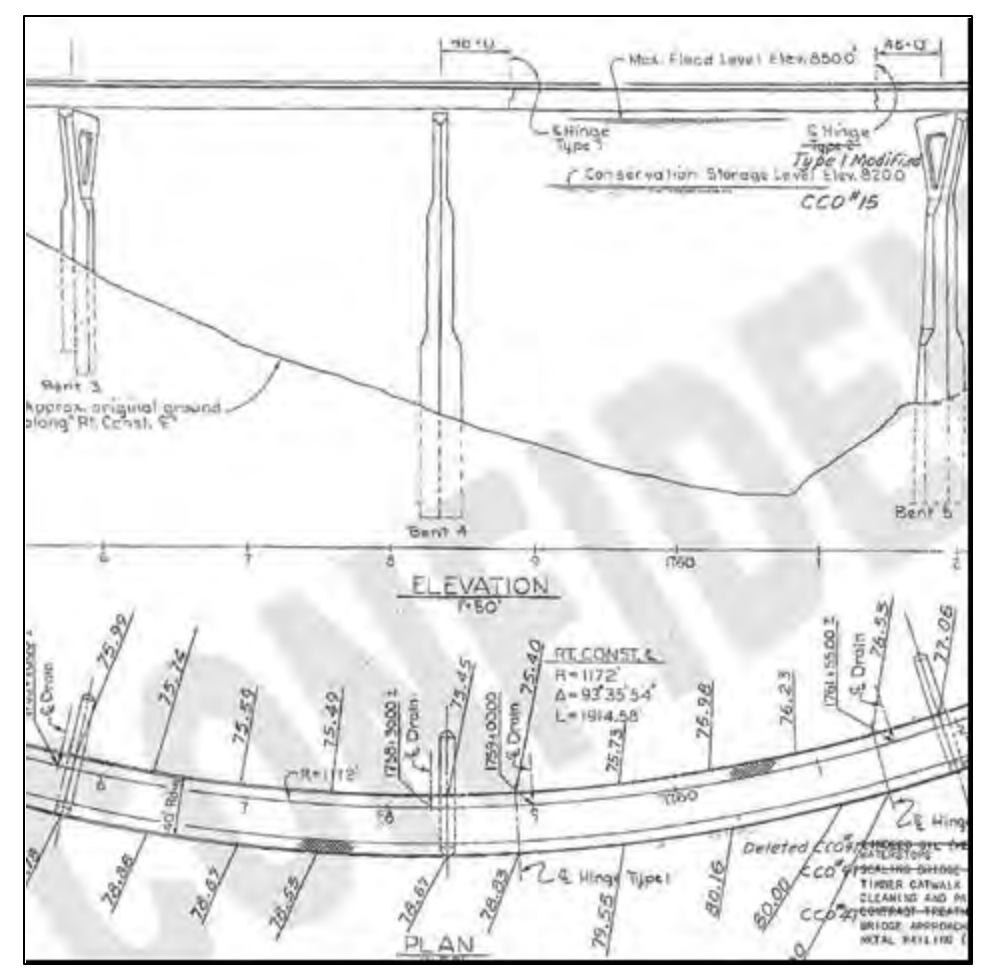


Figure 39. Drawing. As-built drawing of bent 4 of the James E. Roberts Bridge.

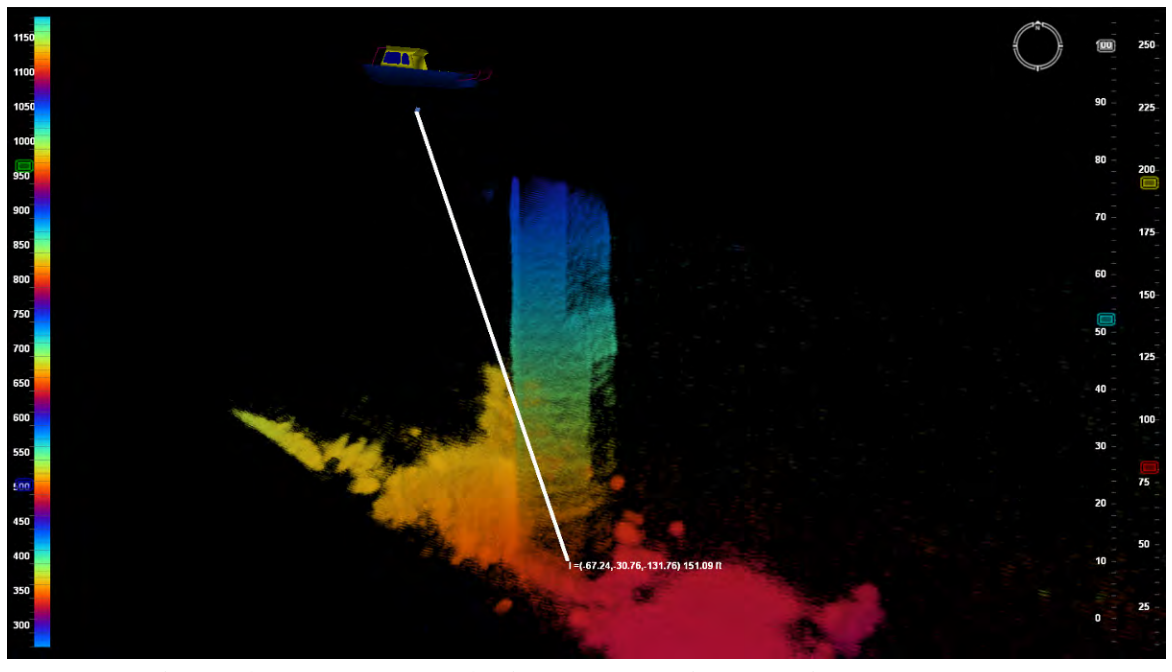


Figure 40. Image. Bent 4 with boat location showing sonar range.



Figure 41. Image. Data mosaic viewed from the west.

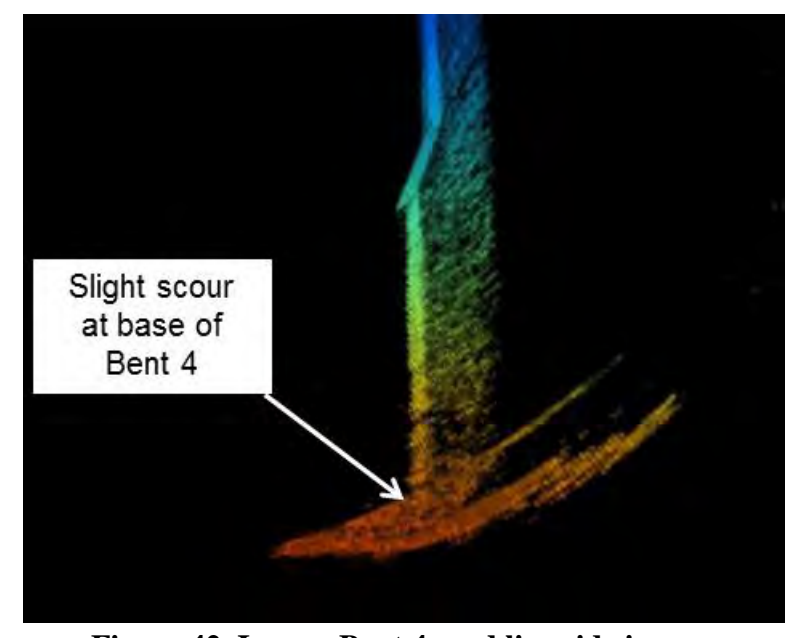


Figure 42. Image. Bent 4 mud line side image.

2D Multibeam and 3D Mechanical Multibeam (Inspection Team B)

Figure 43 displays a plan view of the James E. Roberts Bridge with the naming convention used by inspection team B to label data and images on bent 4. Figure 44 is a sonar wing close-up of the base of face 3 that reveals evidence of an anomaly on the surface.

Overall, the inspection team reported a steep and rocky reservoir bottom at the base of bent 4. Further they observed low scour levels, little debris, and no visible damage to the substructure. They reported that the substructure edges were sharp and the concrete face was smooth.



Original Photo. © 2012 Google®

Figure 43. Image. Bent 4 face naming convention.

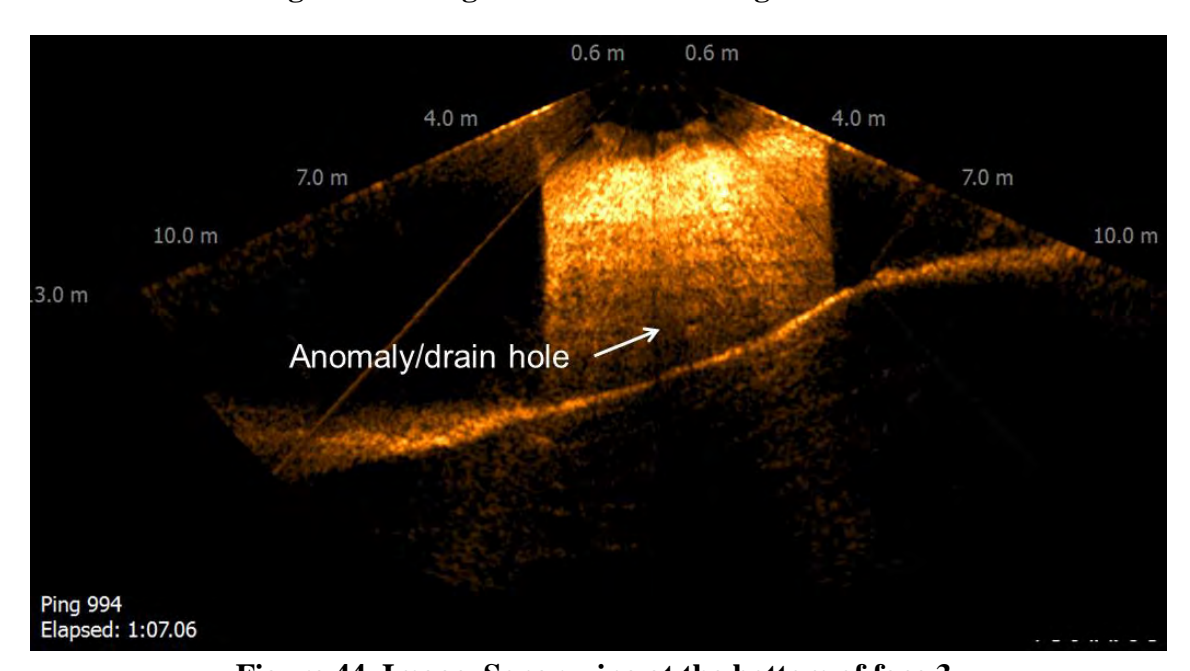


Figure 44. Image. Sonar wing at the bottom of face 3.

2D Sector-scanning and 3D Profiler (Inspection Team C)

Inspection team C used a 2D sector-scanning sonar to inspect bent 4. It was both tripod and frame deployed to collect lakebed and vertical visualization scans of the structure. Bottom scans, taken with the sonar head fitted into a tripod were collected adjacent to the six faces of the structure shown in figure 45.

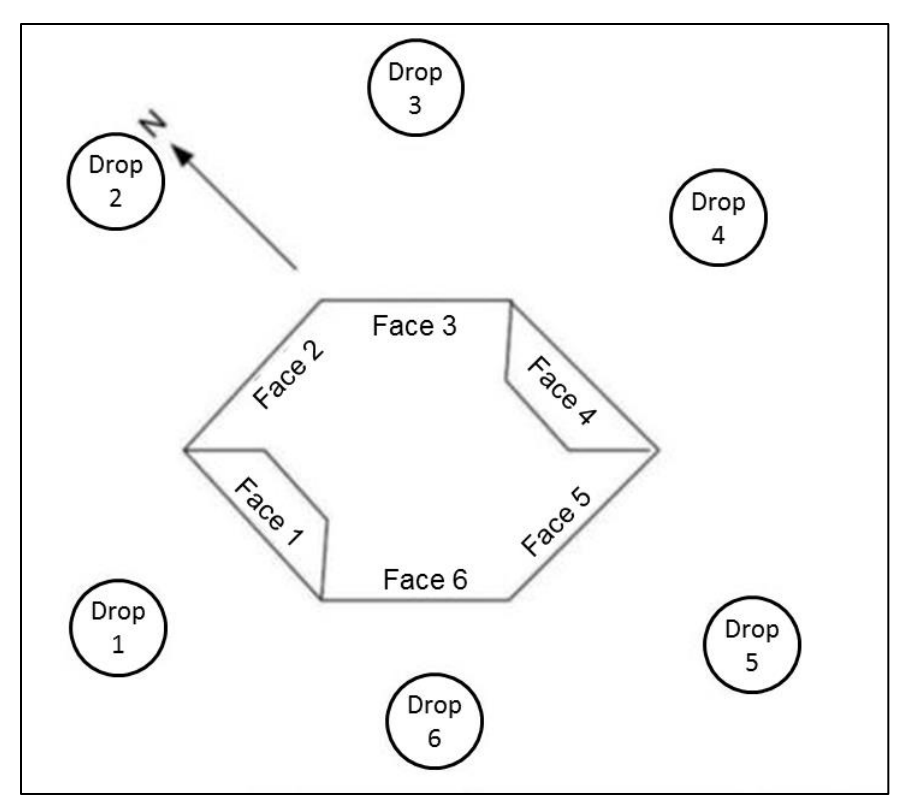


Figure 45. Sketch. Drop and face location key for team B.

A total of six 98 ft (30 m) radius scans were collected. These were combined into a mosaic of the vicinity around bent 4 as shown in figure 46. The bottom shows significant upward elevation change to the northwest of bent 4 (shadowed area). This elevation difference has resulted in some acoustic distortion in plotting the shape of the base of bent 4 as the record cannot be slant-range corrected to a single elevation plane without introducing additional range errors. There are a few angular targets situated close to the structure; their shape suggests they are not natural objects. There is no indication of bottom scour adjacent to the structure or of slope instability in this mosaic.

After completing the bottom scans the head was fitted into a drop frame and lowered along each face of the pier. As an example, figure 47 displays the image for face 6. It appears in good condition with the lakebed slope at the mud line at 24.6 degrees. The circled 'target' is 7.2 ft (2.2 m) above the mud line and may be a small void in the concrete face. Various anomalies were reported on other faces.

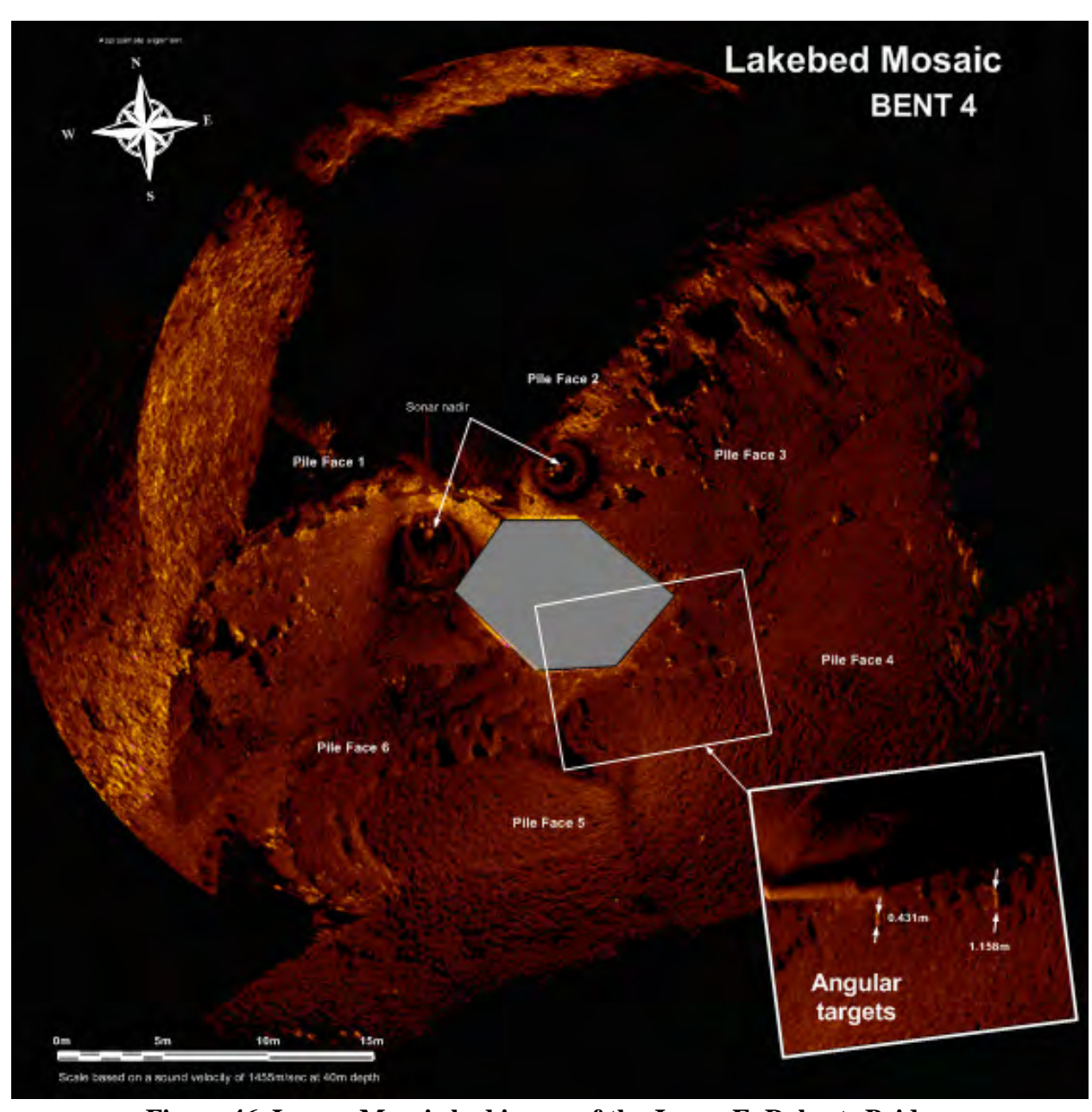


Figure 46. Image. Mosaic bed image of the James E. Roberts Bridge.

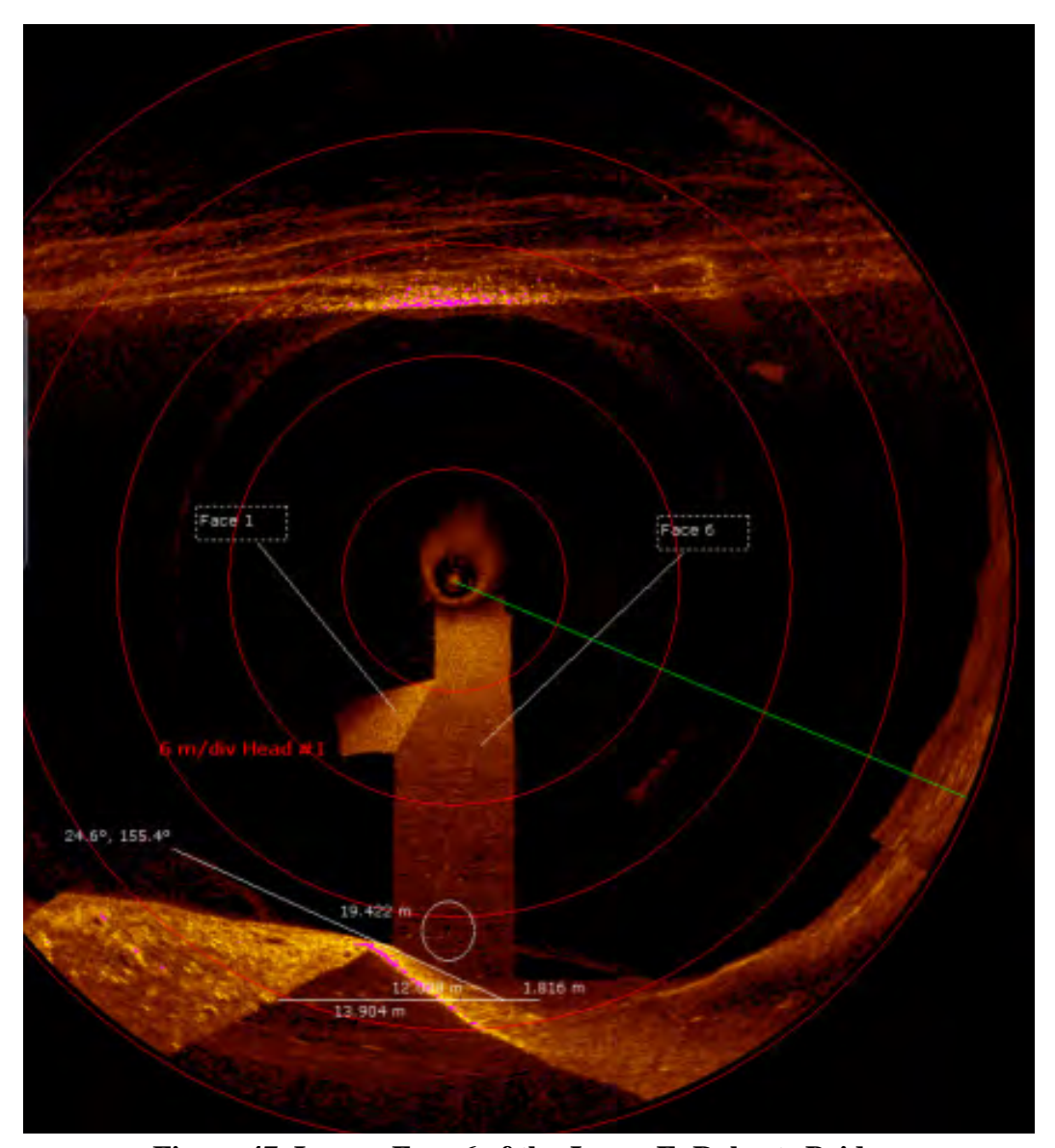


Figure 47. Image. Face 6 of the James E. Roberts Bridge.

Divers

At the time of the dive, the estimated underwater visibility was between 10 and 20 ft (3 and 6.1 m). There was no current. The waterline was approximately located at elevation 777.0 ft (236.8 m) per USGS records. The diver did not inspect below 100 ft (30.5 m) depth because budgetary restrictions associated with compliance to OSHA requirements for an onsite dive chamber at deeper depths. Observations from the inspection included:

- Concrete surfaces were covered with a 1/16-inch to ½-inch (1.6 mm to 6 mm) thick layer of aquatic growth as shown in figure 48.
- The concrete was sound without any detected major defects. The concrete surfaces exhibited scaling with 1/8-inch (3.2 mm) typical and ½-inch (1.6 mm) max penetration over 100 percent of the underwater surfaces. Scaling at the corner edges typically

- exhibited ½-inch (12.7 mm) maximum penetration. Figure 49 shows the typical concrete condition revealed after level II cleaning.
- Horizontal cold joints in the concrete surface were noted at 8, 23, 42, 66, 85, and 110 ft (2.4, 7.0, 12.8, 20.1, 25.9, and 33.5 m) below the waterline. Joints were created during original construction and did not exhibit any major deterioration. Figure 50 shows an example of a joint after level II cleaning at a depth of 23 ft (7.0 m).

Overall, the divers were able to make detailed observations about the condition of the bent and its surfaces that could not be made by the sonar devices. However, the area covered by the divers was limited including not inspecting conditions below 100 ft (30.5 m).

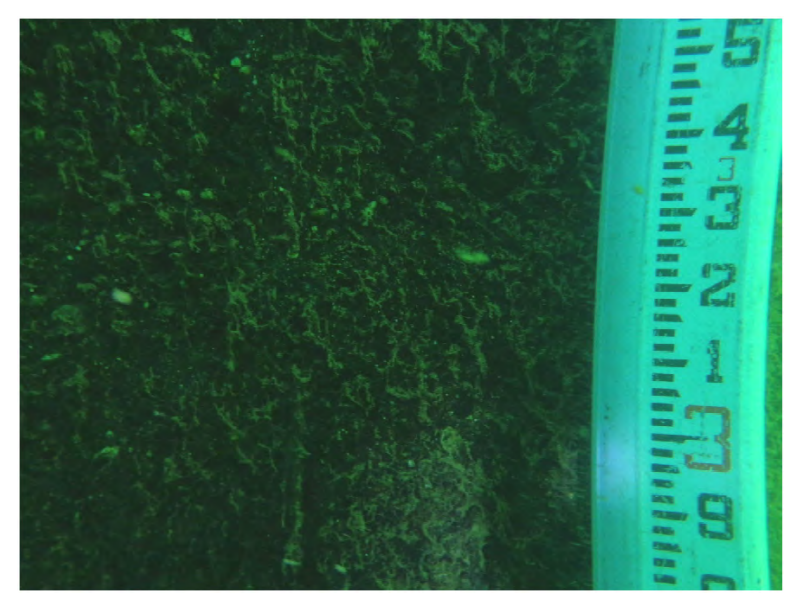


Figure 48. Photo. Marine growth on concrete 15 ft (4.6 m) below the waterline.

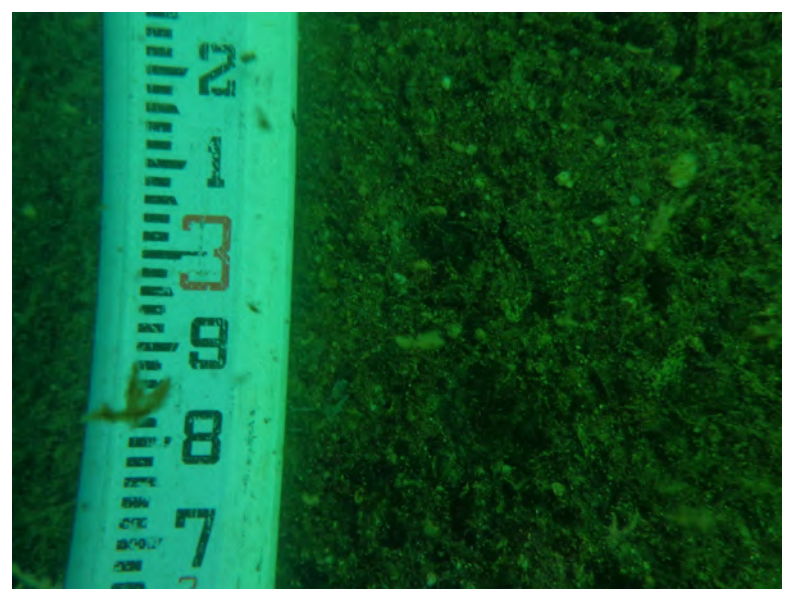


Figure 49. Photo. Typical concrete condition with level II cleaning (15 ft (4.6 m) below the waterline).



Figure 50. Photo. Typical cold joint after cleaning.

CARQUINEZ BRIDGE (1958)

The Carquinez Straight connects San Pablo Bay and Grizzly Bay/Suisun Bay. The older of two parallel spans was built in 1958. The truss bridge is supported at bent 3 on two large concrete footings as shown in figure 51 with a plan view displayed in figure 52. A large concrete fender system surrounds the foundations of the 1958 bridge and a demolished 1927 bridge. The timber fascia of the fender has been removed and part of the fender near the 1927 bridge foundation has been demolished. Swift current and turbid water conditions are common. Figure 53 provides an as-built drawing for bent 3.

3D Real-Time Multibeam (Inspection Team A)

Water depth at the pier at the time of the inspection by team A was approximately 75 ft (23 m) on both the north and south sides of the pier. A plan view of the sonar results is shown in figure 54. The foundation for the 1958 bridge is the dark area on the right; the darker area on the left is the remaining foundation from the demolished 1927 bridge. A fender is shown to enclose both foundations. Figure 55 and figure 56 show views from the north and the south, respectively. The partial demolition of the 1927 foundation is clearly visible.



Figure 51. Photo. Pier 3 of the 1958 Carquinez Bridge (2003 bridge in background).



Original Photo. © 2012 Google®

Figure 52. Photo. Aerial view of pier 3 (1958 bridge on the right).

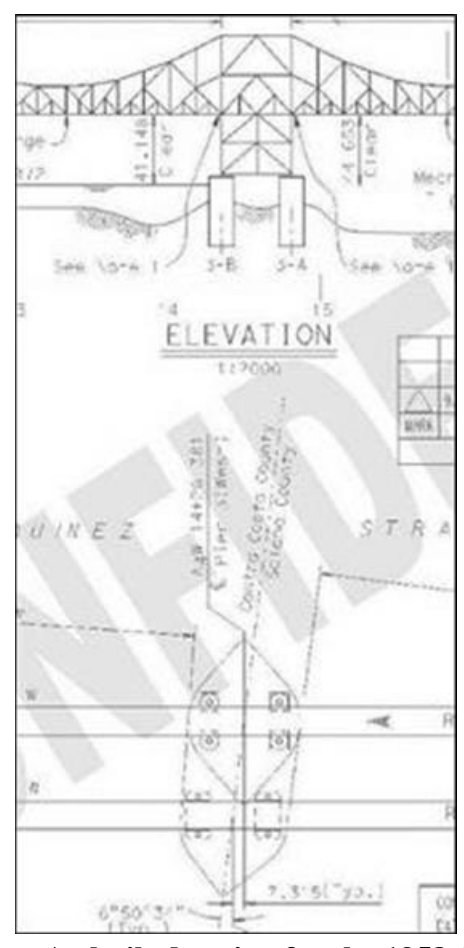


Figure 53. Drawing. As-built drawing for the 1958 Carquinez Bridge.

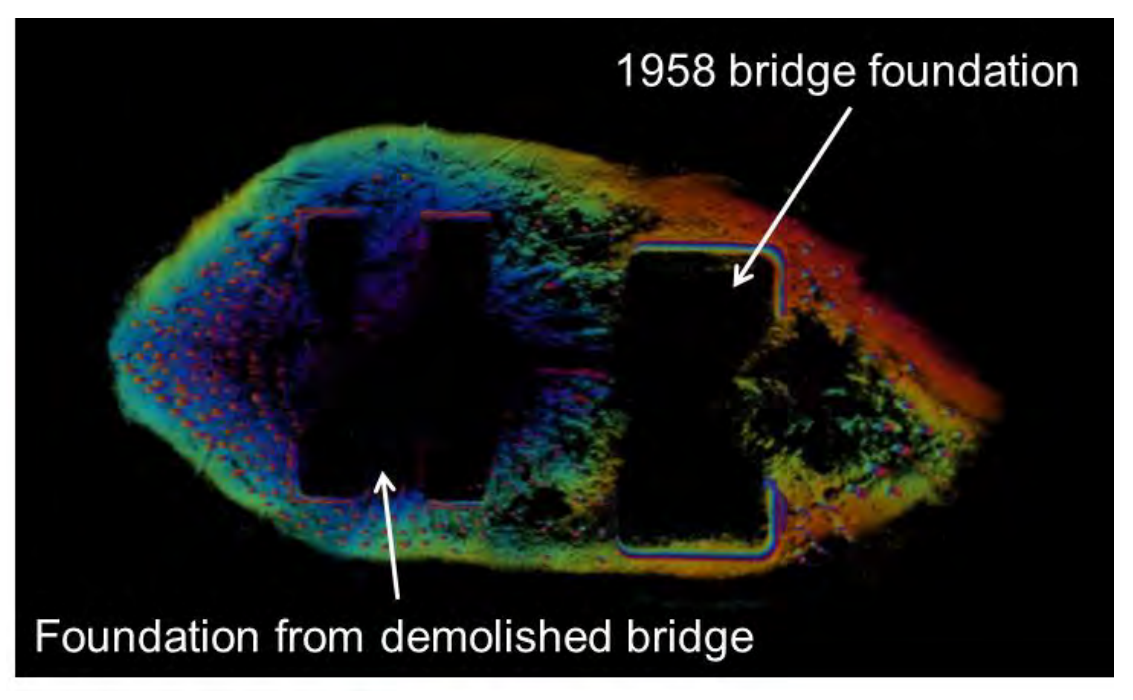


Figure 54. Image. Pier 3 plan view.

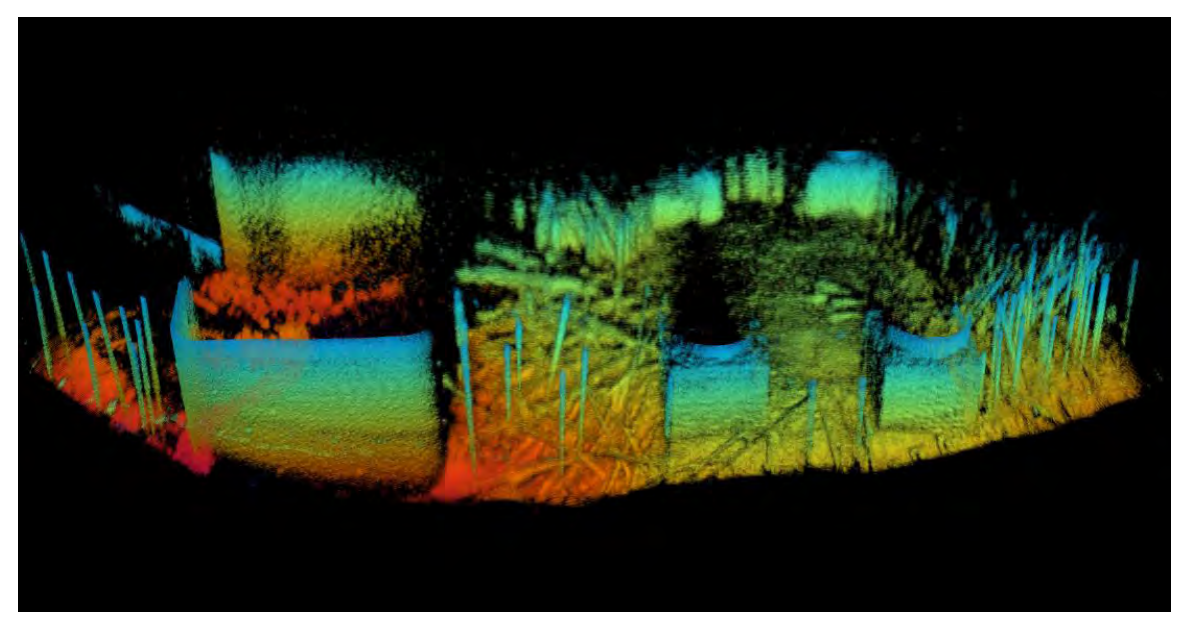


Figure 55. Image. Pier 3 viewed from the north.

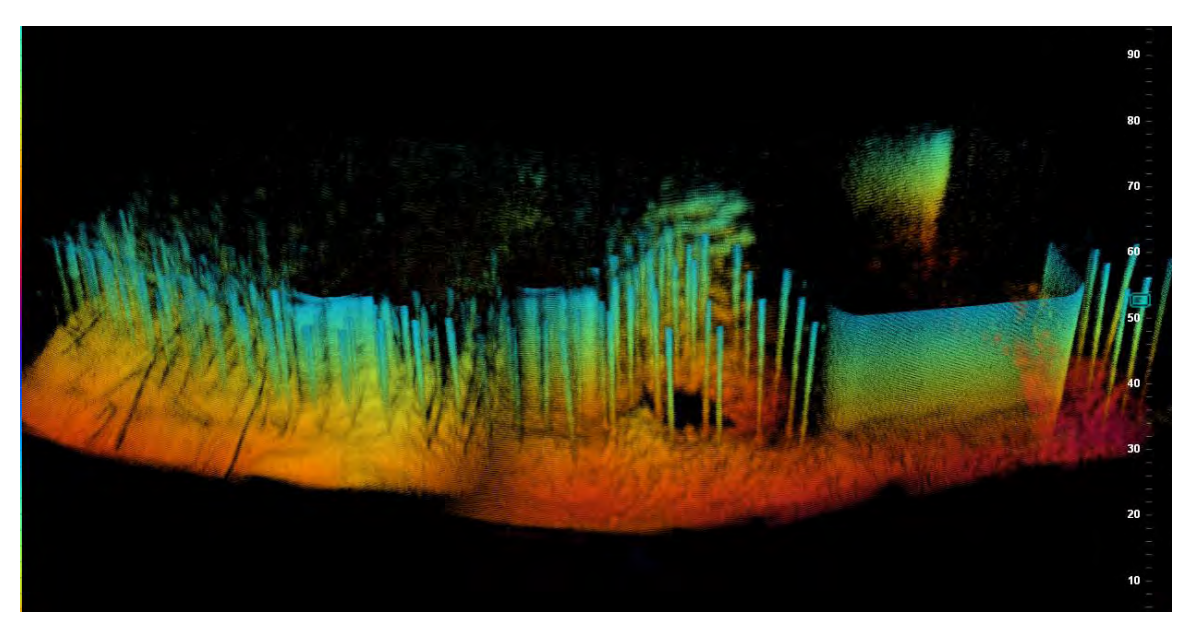


Figure 56. Image. Pier 3 viewed from the south.

2D Sector-scanning and 3D Mechanical Multibeam (Inspection Team C)

Inspection team C performed a combination of 2D and 3D scanning of the 1958 Carquinez Bridge. Figure 57 displays the areas on the pier foundation subject to inspection. An example of the 2D imaging is shown in figure 58. The reference location for this image is indicated in figure 57. An example of one of the 3D images, that among other features reveals a downed pile, is shown in figure 59.

Overall, the inspection team reported little evidence of scour and moderate to high levels of debris. Several small anomalies were noted on the concrete footings and many downed piles were identified.

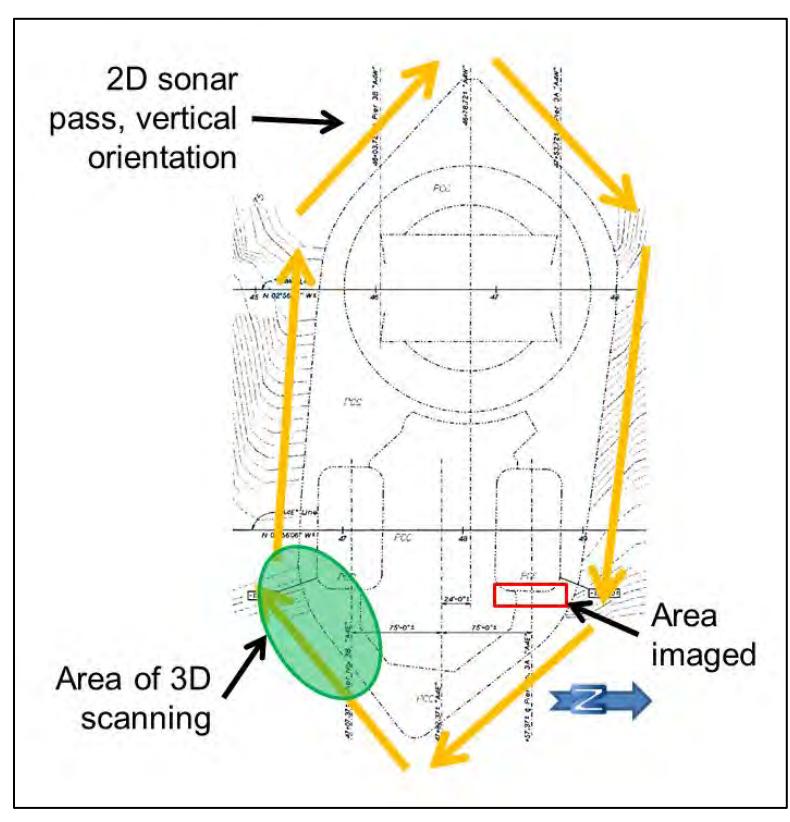


Figure 57. Sketch. Area of 3D scanning and 2D pass alignments.

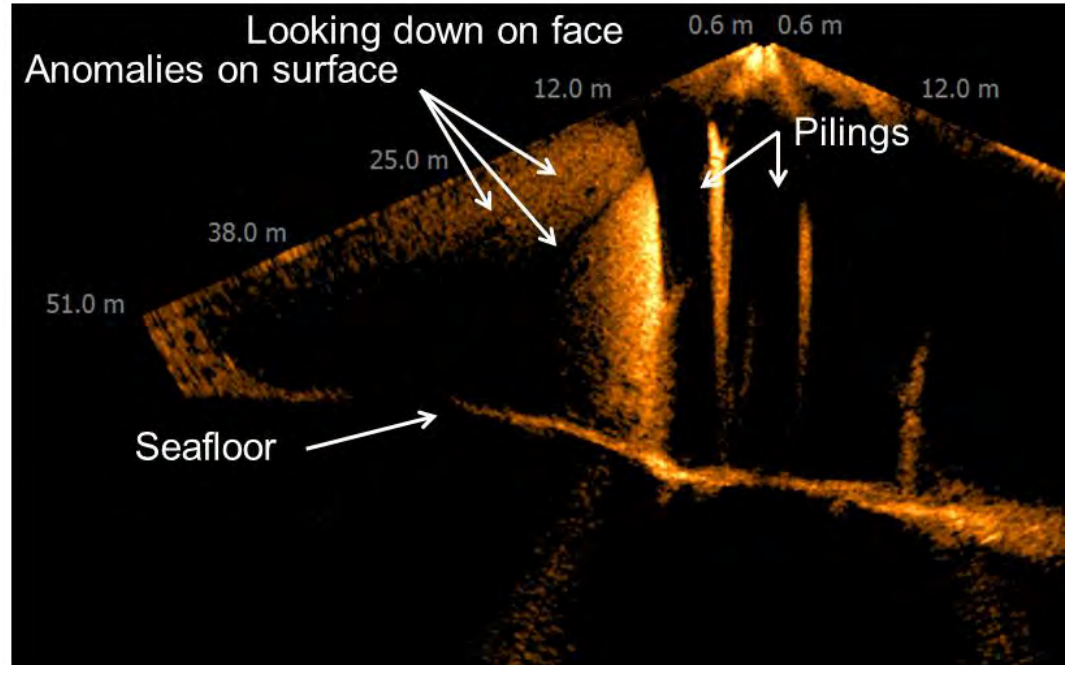


Figure 58. Image. 2D sonar image.

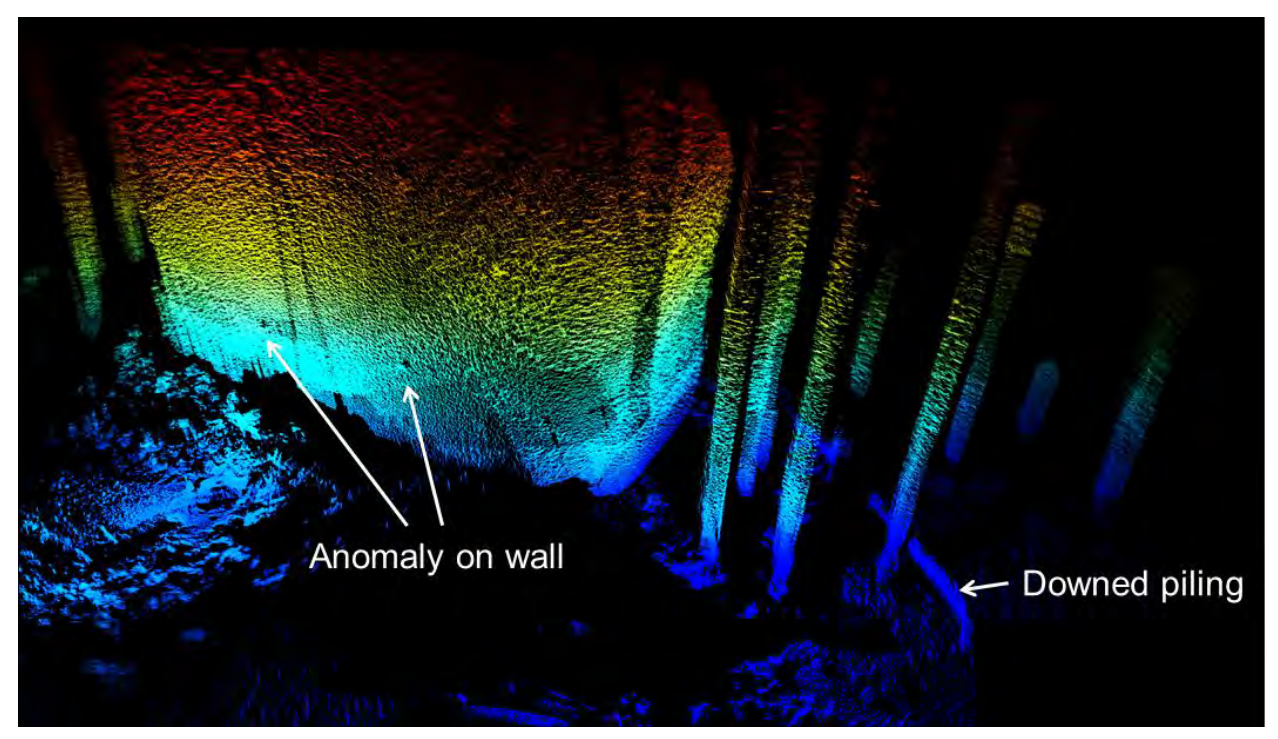


Figure 59. Image. 3D view of base of pier 3.

CARQUINEZ BRIDGE (2003)

A second span crossing of the Carquinez Straight parallel to the 1958 span was built in 2003 and is shown in figure 60. Tower 3 of the 2003 Carquinez Bridge, shown in figure 61, is founded on two prestressed concrete pile caps, each supported on six 10-foot (3.05 m) piles, and linked by a bridging element. Figure 62 shows the pier at the water level. Figure 63 provides the as-built drawing for this location.

This site features swift black water that is also deep, though not exceeding 100 ft (30.5 m). This foundation also offers a large inspection area. A concrete fender system is on the main channel side making accessibility on the water surface limited on the north side (towards the shore) of the foundation. Inspection team C did not inspect the 2003 Carquinez Bridge.



Original Photo. © 2012 Google®

Figure 60. Photo. Aerial view of tower 3 (2003 bridge on the left).



Figure 61. Photo. Tower 3 pile cap.



Figure 62. Photo. Tower 3 pile cap close-up.

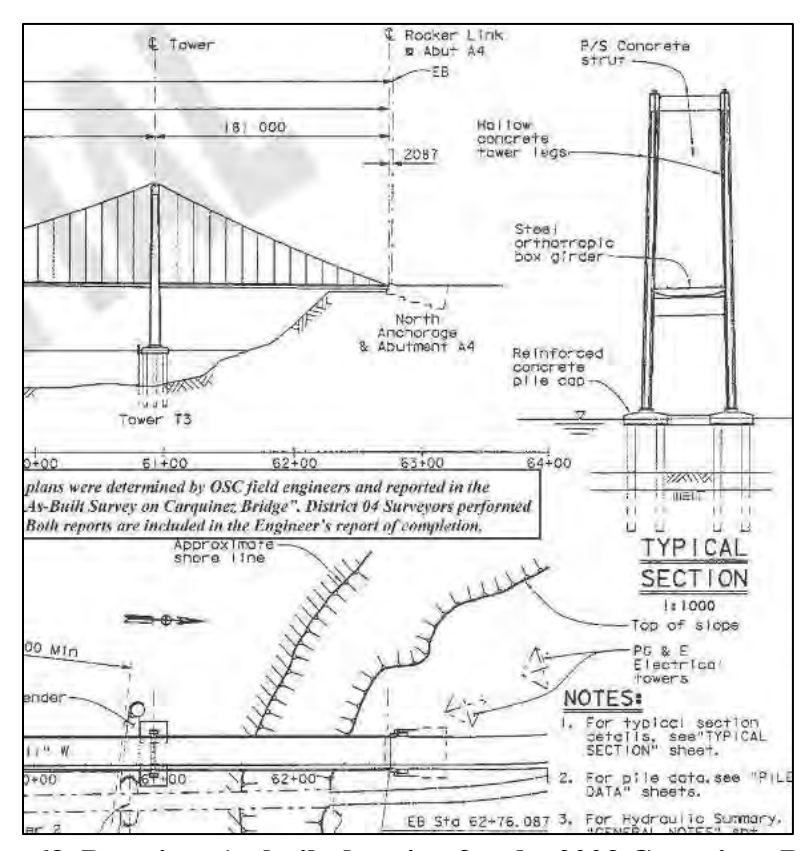


Figure 63. Drawing. As-built drawing for the 2003 Carquinez Bridge.

3D Real-Time Multibeam (Inspection Team A)

Water depth at tower 3 at the time of the inspection by team A was approximately 50 ft (15 m) on the west side and 80 ft (24 m)) on the east side. A plan view of the sonar results is shown in figure 64. Figure 65 and figure 66 show views from the north and the south, respectively.

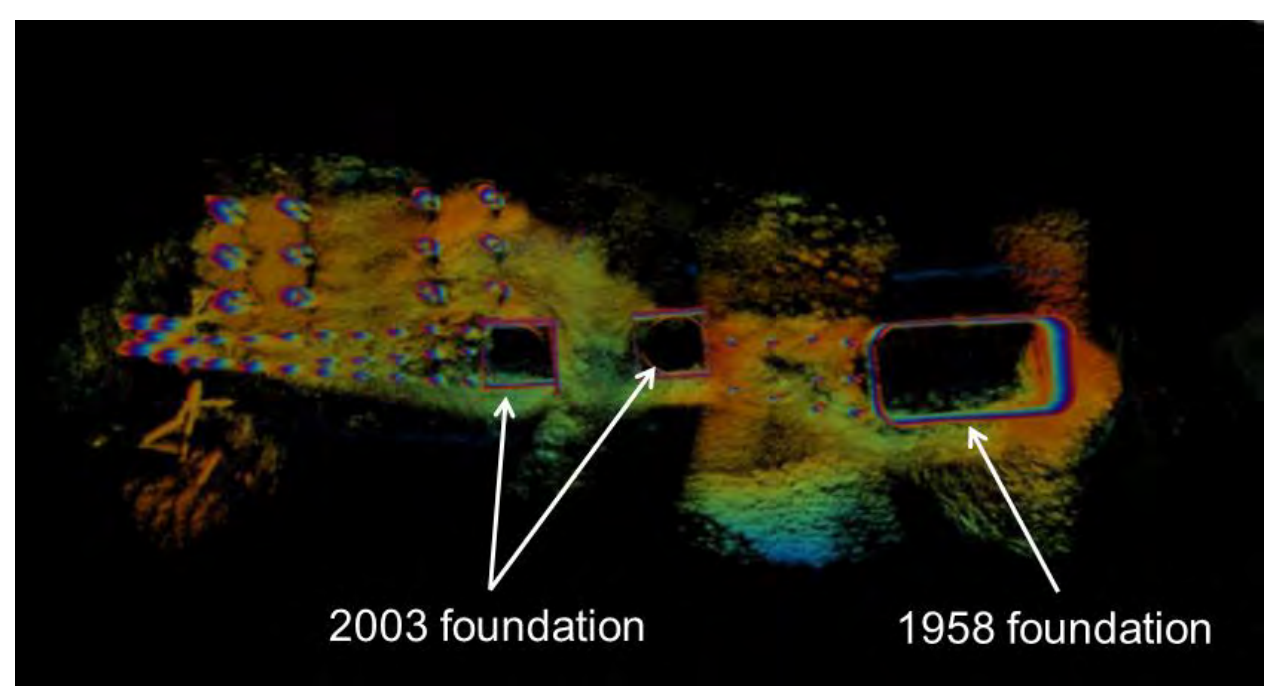


Figure 64. Image. Tower 3 plan view.

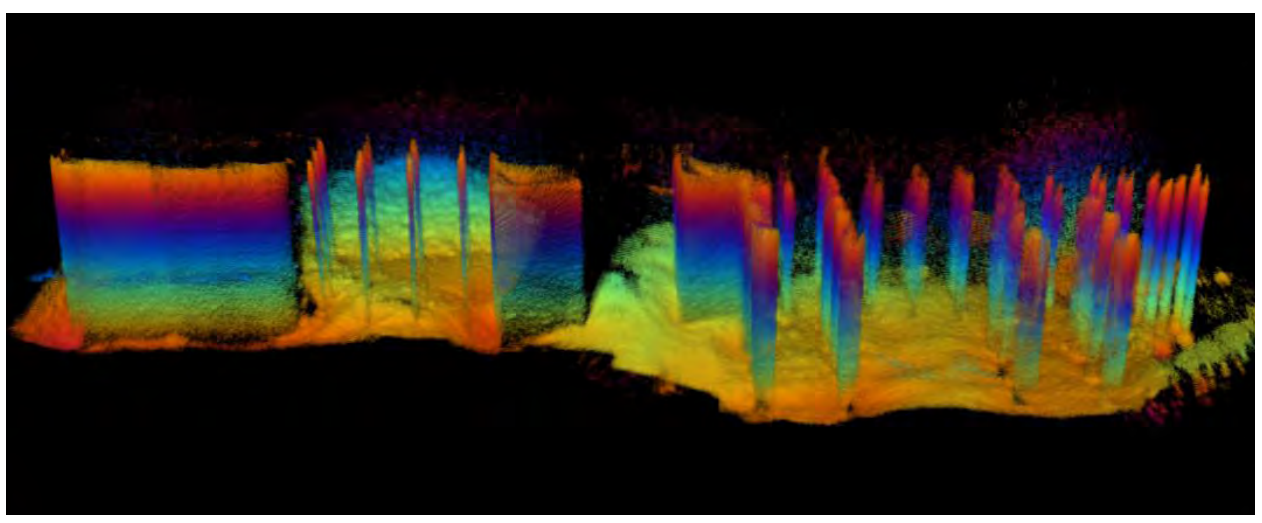


Figure 65. Image. View of tower 3 from the north.

2D Multibeam and 3D Mechanical Multibeam (Inspection Team B)

Inspection team B performed a combination of 2D and 3D scanning of the 2003 Carquinez Bridge. An example of the 2D imaging is shown in figure 67. The figure is an image of the north pilings imaged as the boat was traveling from west to east using the 2D multibeam sonar in the vertical orientation. An example of 3D imaging is shown in figure 68 where several signs of debris are apparent.

Overall, the inspection team reported little evidence of scour and moderate levels of debris to the west with little debris elsewhere. No indication of structural damage was identified.

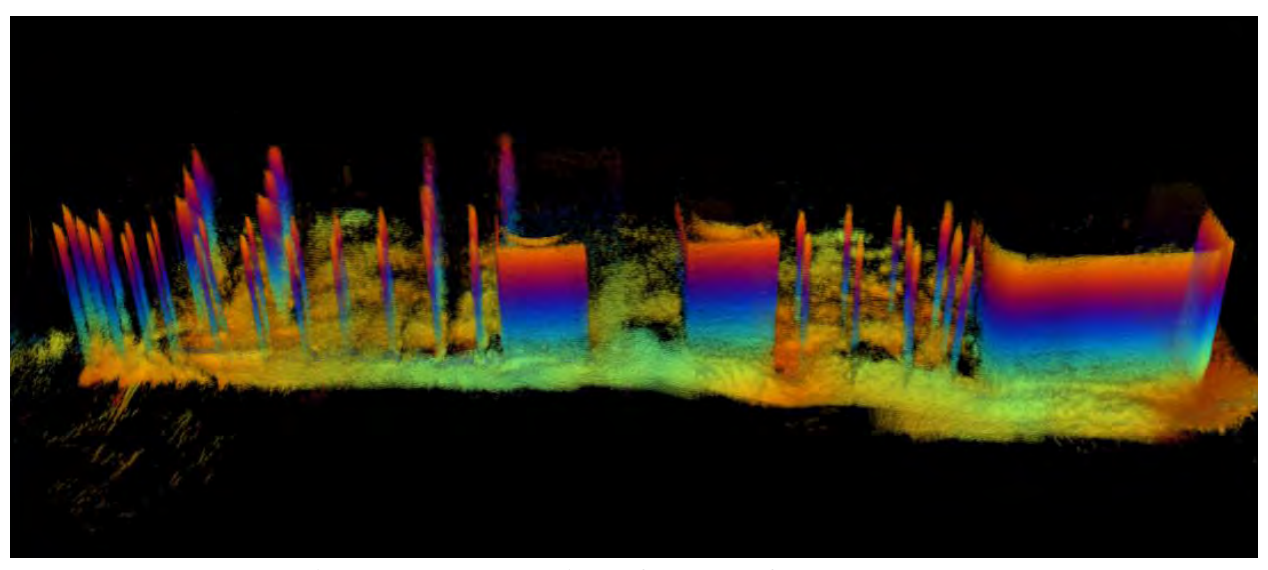
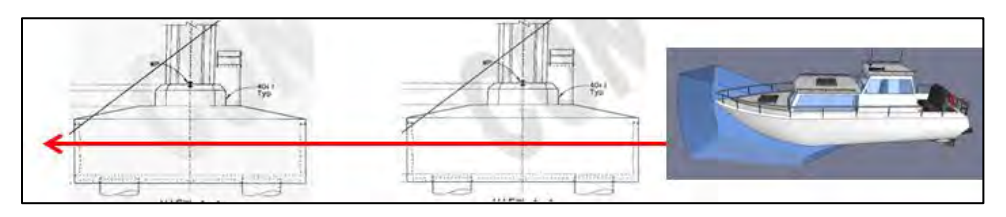
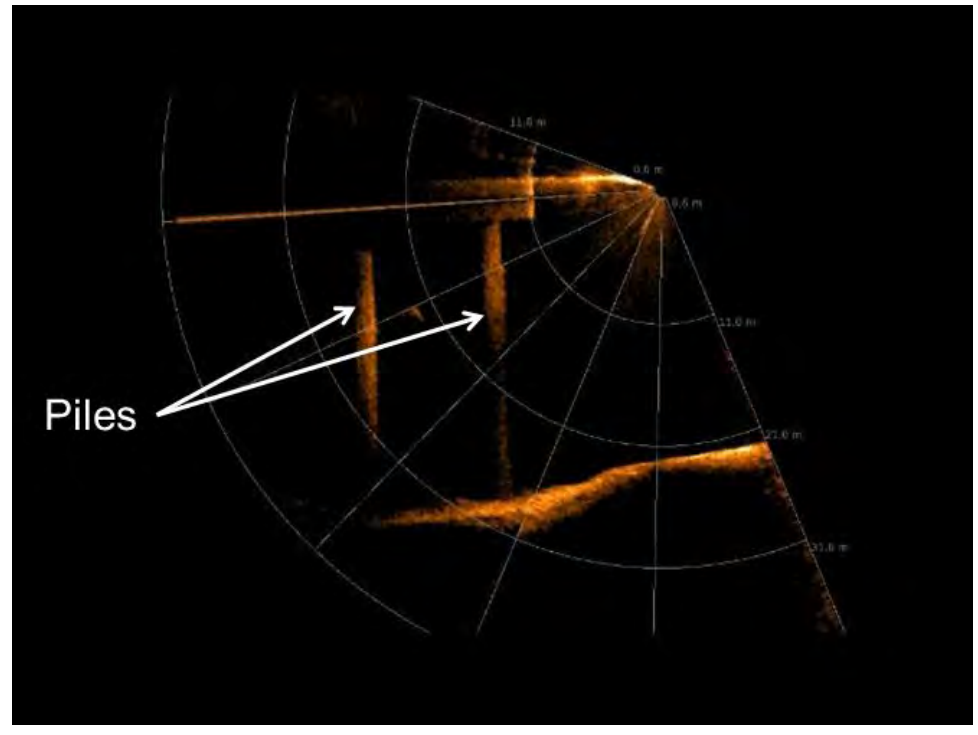


Figure 66. Image. View of tower 3 from the south.



A. Vessel traveling eastward past two pile foundations.



B. Image resulting from eastward pass.

Figure 67. Image. 2D image from an eastward scanning pass.

72

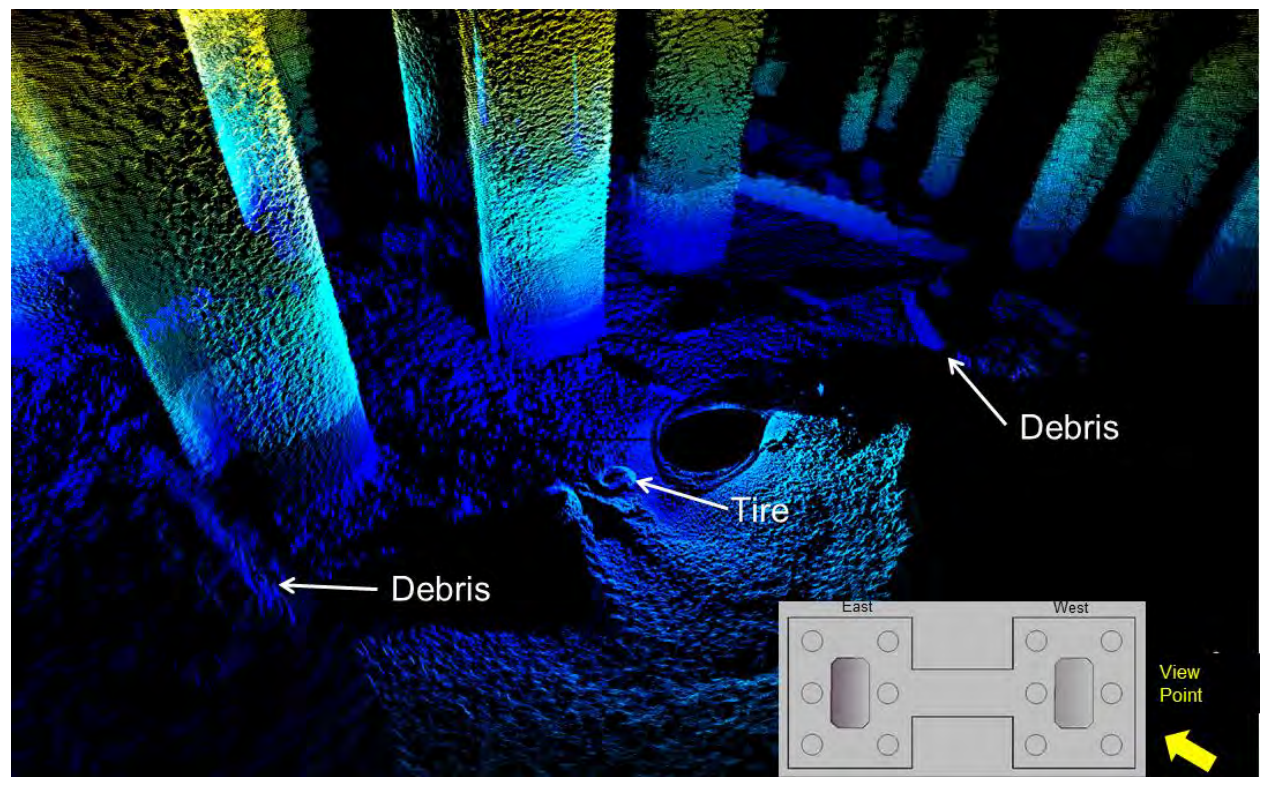


Figure 68. Image. 3D image viewed from the west side of the pier foundation.

Divers

At the time of the inspection the estimated underwater visibility was zero. The current was estimated to be between 3 and 4 ft/s (0.9 and 1.2 m/s). The waterline was located 9.7 ft (3.0 m) below the top of the concrete cap supporting tower 3. This corresponded to a waterline elevation of +2.8 ft (0.85 m).

Because of limited time, the diver only inspected the northeast pile of the east column and the west central pile of the east column. Observations from the inspection included:

- The channel bottom consisted of gravel and cobbles up to 6 inches (152 mm) diameter. The diver noted a 4 ft (1.2 m) by 4 ft (1.2 m) by 1 ft (0.3 m)) high mound of concrete debris on the channel bottom near the northeast pile.
- The steel piles typically exhibited surface corrosion and pitting with 1/16-inch (1.6 mm) maximum penetration.
- All underwater steel surfaces were covered with a ¼-inch (6 mm) to ½-inch (13 mm) thick layer of aquatic growth.
- All underwater concrete surfaces were typically covered with a 1-inch (25.4 mm) to 2-inch (50.8 mm) thick layer of aquatic growth.
- The concrete was sound without any detected major defects.

Overall, the divers were able to make detailed observations about the condition of the bent and its surfaces that could not be made by the sonar devices. However, the area covered by the divers was limited.

EVALUATION OF PHASE I FINDINGS

The various sonar technologies each have their strengths and weaknesses relative to each other as well as compared with divers. The comparison of these approaches is evaluated based on the following criteria: 1) identification of features, 2) performance in adverse environments, 3) data collection/reporting time, 4) equipment costs, and 5) personnel requirements.

Identification of Features

For this evaluation, three types of feature identification are considered: 1) bed forms/scour, 2) objects, and 3) materials defects. These areas include the types of findings that an underwater inspection should reveal about conditions that may threaten the stability or performance of the bridge.

The sonar technologies evaluated in this study can be classified in two groups in terms of mounting and movement in service: boat mount and bed/pier mount. The boat-mounted sonar systems usually provide large coverage in a relatively short time. They can potentially provide quick assessment on the conditions of the bridge foundation and the subsurface bed conditions.

The 3D real-time multibeam provides georeferenced point cloud images while the boat is sailing at a normal speed. The sonar is designed to function as a non-expert oriented system and the interpretation of the image is relatively straightforward.

Figure 28 shows how the size of debris can be obtained such as for the pile-like objects shown in the figure. This assessment can be conducted by a bridge engineer with a small amount of training on the system and software. The precision of dimensional estimates can be affected by a number of factors, but the approach offers a quick assessment of the bridge structure, as well as a complete image of a potential diving site that can be used to guide a subsequent dive to critical locations quickly and safely.

The 2D multibeam sonar mounted on the boat-side pole or on the down-slide wing also provides real-time assessment of the structure/bed condition. Because this is a 2D sonar used in a volume of water without a specific target plane, the interpretation of the image or video requires some experience and/or training. Figure 29 shows an example of a horizontal scan, but other orientations and movements are possible. The sonar can reveal many details. As can be seen in figure 44, the 2D multibeam sonar revealed an anomaly/drain hole. Both the 2D multibeam and the 2D sector-scanning sonar show the bed forms at the mud line.

However, the 2D multibeam and the 2D sector-scanning sonar produce 2D images. The features on the bridge substructure or on the stream bed can be clearly identified, but are difficult to quantify in size. The 3D profiler, 3D mechanical multibeam, and 3D real-time multibeam offer coordinates of all points being scanned. This allows quantification of feature dimensions.

In general, sonar technology is capable of identifying problems on stream bed condition and large-scale structural geometry. Sonar can also identify larger voids or protrusions in underwater substructures. However, it has difficulty detecting minor materials defects, such as small cracks, especially if they are hidden by aquatic growth.

Under good diving conditions, divers can more thoroughly identify and report the onset of deterioration issues—abnormal marine growth, loss of coating, scaling, etc. In adverse environments, such as deep water, swift current, and/or poor visibility the work environment is more challenging making identification of relevant conditions more difficult.

Performance in Adverse Environments

Adverse environments for underwater inspection include rapid flow velocities, deep water, poor visibility or any combination of these. In addition to potentially limiting data collection, these conditions can represent safety concerns for divers and personnel on aquatic craft.

The observed flow velocity at James E. Roberts Bridge was nearly zero during all testing and the flow velocity at Georgiana Slough Bridge varied from approximately 0.5 to 1.5 ft/s (0.15 to 0.46 m/s). These conditions were not a factor for either the sonar or diving teams. However, the current at the Carquinez Bridge varies during the day and was as high as 5 ft/s (1.5 m/s) during the field test period.

The boat-mount sonar systems were not significantly affected by the current since the speed of boat was higher than that of the current. The stationary system that used a heavy plate was heavy and slim so that the hydrodynamic force did not overpower the gravity. This was necessary for proper operation because the stationary type of sonar mounting involved mechanically turning the sonar head. If there was any motion before one scanning cycle was complete, the data were not useful.

With respect to the diving team at the Carquinez Bridge, the first dive was timed close to a slack tide. Overall, the current was manageable, but challenging for the divers. Examples of the water surface conditions are shown in figure 69. In addition, the depth was approximately 90 ft (27 m). The diver used the maximum amount of time allowed for the depth (30 min) to inspect one pile including one level II cleaning. The second dive occurred at a time between slack tide and maximum current. Inspection was nearly impossible because of the current. While the estimated current was likely between 2 ft/s (0.6 m/s) and 3 ft/s (0.9 m/s), the diver reported experiencing an approximately 4 ft/s (1.2 m/s) equivalent current. Based on the post-dive description and observation of the flow condition, it was hypothesized that the blockage caused by the massive pile cap might have produced a high velocity area some distance below the bottom face of the pile cap. This condition was hazardous for the diver.

In order to increase the dive time the depth of the second dive was set at 60 ft (18 m). This allowed a dive time of 57 minutes. However, the diver found it extremely difficult to hold onto the 9.8 ft (3 m) pile to maintain position. The diver managed to complete the inspection of pile 8 down to a 60 ft (18 m)) depth in approximately 10 minutes. The diver then attempted to switch to pile 9, but found it extremely difficult to maintain a position. After approximately 20 minutes, the diver was exhausted and requested pull-back.

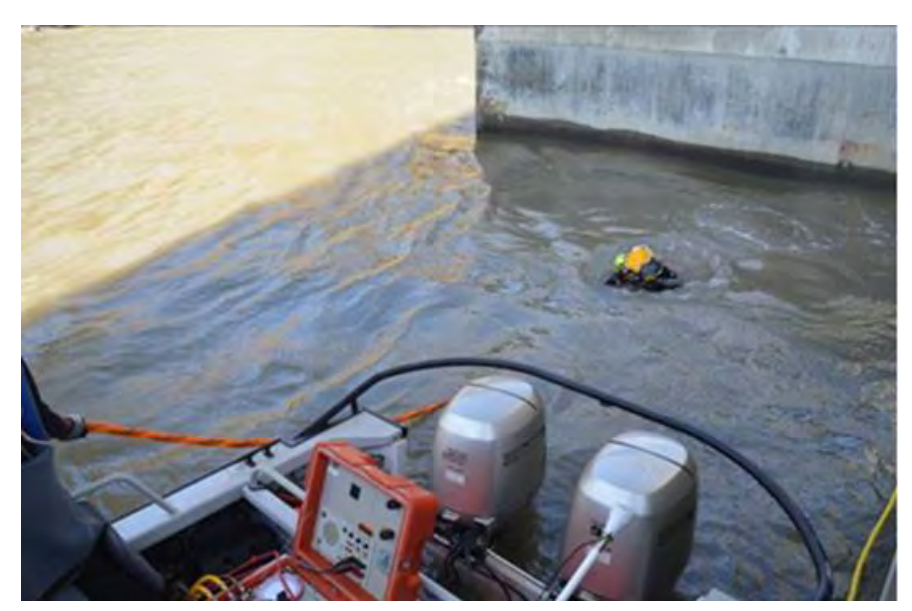


Figure 69. Photos. Wave and current condition during the diving operation.

All three sonar teams at the four phase I sites collected data without significant difficulty, even in conditions of swift water, deep water, and low visibility. The sonar systems could be easily operated through periods of high current with no clear degradation in quality. Boat-mounted sonar would have certain limitation in depth because of the limitation in their range. This limitation is offset by two types of techniques: denser measurement and stationary-mounting/elevator mounting. The 3D real-time multibeam sonar can compress the sound beams to a narrower angular range, and can scan the same area with multiple passes. Another strategy is to use tripods or heavy plates for stationary mounting with elevators that allow vertical scanning for deep sites.

The bottom time limit for divers can significantly hamper inspection progress at deep water sites. Sonar systems can provide assistance to a diver or can be used in situations that are difficult for divers to access safely.

Data Collection/Reporting Time

Inspection time includes mobilization, data collection, and reporting time. Reporting time includes required data processing and preparation of reports documenting the inspection findings.

Onsite Mobilization and Data Collection

Time measurements were recorded with the arrival of the inspection team at a bridge inspection site with all equipment. Table 8 summarizes inspection time requirements for the phase I field work. The table provides approximate summaries of preparation time, packing time, data collection, troubleshooting, and processing time. It is expected that these times will greatly vary depending on the nature of the site and personnel experience. Troubleshooting, in particular, is expected to be highly variable depending on the issues that may arise. Troubleshooting issues may include user-errors, as well as mechanical, electrical, or software difficulties. The time

estimates in the table for troubleshooting represent the average daily time for these inspection teams at the phase I sites.

Table 8. Summary of time requirements.

Component	Sonar Team A	Sonar Team B	Sonar Team C	Divers
Preparation (Initial	45/15	60/30	60/60	30-60/30-60
day/subsequent days)				
(minutes)				
Packing (final day/previous	15/30	15/30	30/90	30/na
days) (minutes)				
Data collection (each spot)	5-10	10-30	5-70	30-99
(minutes)				
Data collection (complete	60-90	35-225	120-360	Depends on
site) (minutes)				number of
				dives
Troubleshooting (daily	50	15	25	Resolved on
average) (minutes)				go
Data processing (hours)	1-5	1-5	1-5	0
Interpretation/report	>1	>1	>1	>1
preparation (hours)				

Preparation times are distinguished between the initial day and subsequent days using the same equipment. A range is sometimes given when different equipment was used. Similarly, two estimates of packing time are provided. Generally, packing on the final day was more time consuming.

The time for data collection depends on the number of locations required for an inspection. Therefore, the estimates include time at each location as well as time at the entire site. For the divers, the collection time is governed by bottom time. Bottom time for shallow water is limited to 99 minutes while the limit for deep water is 30 minutes.

Post-Processing

As shown in table 8, the overall processing and report preparation time for the sonar technologies ranges from 1 to 4 hours depending on the nature of the observations and the detail required to properly document findings. Some data can be used with no processing, but processing allows for more detailed measurements and visualization. In general, bathymetry, debris identification, and 2D images are available almost immediately. If it is necessary to stitch together 3D mosaics or models or if georeferencing is required, processing time is generally 1 to 5 hours. Image interpretation and report preparation can vary widely ranging from an hour and up.

For the sonar technologies there is a tremendous amount of raw data available immediately following completion of the field work. All 2D acoustic images and videos are seen in real time as the inspection progresses. For the 3D real-time multibeam, 3D data were ready for display immediately. It was the only technology tested that generated large area images without image stitching. It uses a "mosaic" technique that lumps all point clouds to enhance accuracy on the fly. However, the coverage size appeared to be limited by the video memory of the computer, which is a minor cost component of the entire system.

Similar 3D data can be generated by the 3D mechanical multibeam sonar with modest processing times (one to five hours). The images are generated from multibeam sonar on a stationary mounting that is not georeferenced. Therefore, it requires stitching to produce large area overviews and to compensate for the reduction in resolution at larger distances.

Additional data processing allows more formalized presentation of information and, possibly, more detailed and accurate characterizations and interpretations. Generally, with extensive processing (greater than five hours) more refined reports can be produced. Additional post-dive analysis may also enhance reporting from dive inspections.

Equipment and Personnel Costs

Costs of underwater bridge inspection include equipment and personnel. Table 9 summarizes the estimated equipment and personnel costs for each team at the time of the phase I work in 2012. Costs are likely to change with evolving technology. Equipment cost reflects the primary sonar unit while the total cost includes all supporting equipment and software used in the phase I field work. The manufacturers reported that typical daily rental rates depend on rental duration and are 1 percent, 0.75 percent, and 0.5 percent for rental durations for 1 to 3 days, 4 to 21 days, and greater than 21 days, respectively. Costs of the boat and travel costs to the site are not included. However, these costs are the same for all inspection teams.

	Sonar Team	Sonar Team	Sonar Team	Sonar	
Component	A	B (2D)	B (3D)	Team C	Divers
Equipment cost (\$)	260,400	27,157	113,945	65,000	n.p.
Total (\$)	385,200	35,300*	148,000*	81,000	n.p.
Daily rental (\$/day)**	2,900	300	1100	600	n.p.
Personnel (\$/day)	~4,000	~4,800	~4,800	~4,800	n.p.
Cost/day (\$/day)	6,900	5,100	5,900	5,400	6,805-10,800

Table 9. Cost summary for phase I field work.

The equipment cost for the 3D real-time multibeam sonar used by team A includes the sonar head and other system components. The sonar head ranged from \$235,200 for a single frequency head to \$260,400 for a dual frequency (375/610 kHz) 1970 ft (600 m) rated head. Total cost of the system was \$385,200. This included power supply, cables, etc. (\$10,000), software (\$4,800 - \$16,800 depending on modules included), and an F185+ GPS/inertial measurement unit that allows for accurate positioning (\$94,400). Daily rental of this package is \$1,500.

Sonar team B used two types of equipment. The 2D multibeam sonar cost was \$27,157 while the 3D mechanical multibeam sonar) was \$113,945. Estimates of the cost of supporting equipment and software was not provided.

Total cost for the 2D sector-scanning and 3D single beam profiler sonar used by sonar team C, including all software and ancillary features, was \$81,000. This estimate includes the required computer.

^{*} Total cost not provided. Estimated at approximately 30 percent higher than the equipment cost.

^{**} Daily rental estimated as 0.75 percent of total cost.

Personnel Requirements

Diver qualifications and certifications were described in chapter 1. In addition, the diver requires training on what to look for during inspections at each level.

Use of sonar for underwater bridge inspection is relatively new. Requirements for successful bridge inspections include training and competency in the following:

- Working on or near water.
- Operating sonar equipment.
- Interpreting sonar images.
- Processing sonar images.
- Identifying features important for bridge inspection.

Summary

Sonar technologies and divers each offer benefits and challenges for underwater bridge inspection. Based on the phase I evaluation, there are opportunities for improving underwater inspection through the joint use of sonar and diving. Such combinations may yield much more useful information on the bridge conditions while effectively managing costs and safety. Based on this phase I evaluation, potential effective use and limitations of sonar include:

- **Swift current**. In this study, it was observed that when current flow velocity approaches or exceeds 3 ft/s (0.9 m/s), diver mobility and safety are reduced. As a result, inspection time and the ability of the diver to effectively inspect target conditions are reduced. It was further observed that tidal currents can be amplified as they pass by or through the bridge substructure at constricted locations. In swift currents it is difficult for divers to maintain their position near large scale structural elements (such as the 9.8 ft (3 m) pile of the new Carquinez Bridge) and conduct a full-coverage inspection. Waiting for more moderate velocity conditions might significantly reduce the window available for inspection work or even completely eliminate the window in steady high flow conditions. The data collection capabilities of sonar systems have not been found to be affected by high velocity currents. However, the safety of boat operations in swift currents must be considered.
- Deep water. While a surface-supplied diver can reach depths of up to 100 ft (30.5 m) without a decompression chamber, bottom time is limited at greater depths. For the shallow depths at the Georgiana Slough site submerged inspection periods of 1.5 hours were achieved. However, at the deeper depths at the Carquinez Bridge and the James Roberts Bridge sites submerged inspection times of only 30 minutes were possible. For the James Roberts Bridge, 30 min was sufficient to circle the pier at the deeper depths, but the diver could only visually inspect up to approximately 120 ft² (11.1 m²) during that period under good visibility. At that rate, inspection of the entire bridge substructure with a diver would be time consuming. Because 2D scanning sonar systems can visualize the surface of the pier in good detail sonar inspections could be a cost-saving opportunity. However, it would increase the confidence level for both diving inspections and acoustic

inspections if a correlation between diver and sonar findings could be established. If possible, this could extend the diver-verified inspections at shallower depths to greater depths by the use of acoustic technologies.

- Real-time assistance and safety oversight for difficult diving. The 2D systems and georeferenced 3D system can show environmental conditions around the diver and the diver's position and movement to the dive tender. This information can be used to guide the diver in conducting safe and efficient inspection work in conditions with swift currents and deep water. In such situations the sonar can be used to scan the entire underwater structure target and surrounding stream bed to identify specific areas that may require visual and hands-on inspection.
- Large coverage area. Acoustic imaging techniques share similar advantages in covering a large area in a relatively short time.
- **Georeferencing**. Georeferencing and object recognition are used in sonar technology to produce compound images or 3D models. Both increase the likelihood of identifying significant problems in an inspection. However, the precision of such techniques requires quantification.

CHAPTER 7. PHASE II FIELD TESTING

The objective of the phase II field testing was to conduct a level I underwater inspection on two towers on the west span of the San Francisco-Oakland Bay Bridge (SF-OBB) and two piers of a nearby Third Street Bridge to evaluate the use of sonar in underwater inspection. The phase II work was designed to determine the efficacy of sonar in identifying possible defects and deterioration that a bridge inspector (diver) would report in a routine Level I underwater inspection. The phase II work was also intended to identify other potential benefits and limitations of sonar for maintenance and inspection work.

BACKGROUND AND APPROACH

Caltrans provided access to two tower foundations on the west span of the SF-OBB and piers on the Third Street Bridge to provide information and visualization on the underwater structural and foundation elements using sonar. The west span of the SF-OBB is shown in figure 70. The W2 and W6 towers were identified for this phase II work because the substructures for these towers are located in deep water with swift black water conditions. The other inspection site is the Third Street Bridge shown in figure 71. The substructure for this site is located in shallow water with limited freeboard subject to tidal change. Table 10 provides a summary of characteristics for the phase II sites.



Figure 70. Photo. SF-OBB viewed from the south.



Figure 71. Photo. Third Street Bridge.

Table 10. Phase II site information.

Information	W2 Tower SF-OBB	W6 Tower SF-OBB	Third Street Bridge
Coordinates	37°47'26.22"N 122°23'8.35"W	37°48'20.4"N 122°22'11.0"W	37°46'36.48"N 122°23'24.91"W
Access	Boat	Boat	Boat/deck
Depth	< 65 ft (19.8 m)	< 130 ft (39.6 m)	6 to 20 ft (1.8 to 6.1 m)
Daily Maximum Current (knots)	Approximately 3 to 4	Approximately 3 to 4	Approximately 3 to 4
Approx. freeboard	200 ft (61 m)	200 ft (61 m)	~5 ft (1.5 m)
Type of substructure	Steel tower on concrete caisson	Steel tower on concrete caisson	Steel truss movable span on concrete foundation
Approximate size of foundation	92 by 197 ft (28 by 60 m)	92 by 197 ft (28 by 60 m)	varies

Inspection Conditions

The phase II field work employed a set of known conditions to explore the strengths and limitations of the acoustic technologies. The known conditions included two components:

- Reference sites with conditions documented in previous dive inspections.
- Targets planted specifically for this study.

Known artifacts from prior Caltrans inspections included such features as a tire embedded in the concrete of the substructure of the Third Street Bridge. According to a 2007 inspection report the

tire was found in the concrete of the southeast section of the north channel pier approximately 2.3 ft (0.7 m) above the mudline.

In addition, Caltrans (with in-house personnel) performed an inspection of pier W2 and the south face of pier W6 of the SF-OBB from October 22 through November 7, 2013. The findings from this inspection related to pier W2 were used as reference information for this study. Other known conditions include concrete voiding in pier W2 supporting the SF-OBB based on a 1995 inspection of the pier.

On October 22, 2013, a Caltrans dive team planted several targets on pier W6. The targets were relatively small to avoid suspicion that they were intentionally placed. However, they were also made to appear to be out of context so that inspectors would consider them relevant for reporting. Regardless of the intent, a risk of the strategy of planting targets is that it is possible that the dive and sonar inspection teams could notice a target, but not report it because it did not appear to represent a threat to the bridge substructure.

As will be apparent in the discussion of pier W6 on the SF-OBB, there is a clear interface between smooth concrete and timber formwork at approximately 35 to 45 ft (10.7 to 13.7 m) below the water surface. The vertical location of the planted targets is referenced to this datum. The planted targets and their locations are summarized as follows:

- Target 1: A 1-inch (25.4 mm) diameter, 62-inch (1570 mm) long, orange plastic coated cable with a welded loop on one end (see figure 72). This target was bolted to W6 east face (3 ft (0.9 m) from the south corner and 3 ft (0.9 m) below the smooth concrete/formwork interface).
- Target 2: A 3/8-inch (9.5 mm), 7-ft (2.1 m) long rusty chain, looped at one end with a bolt (see figure 73). This target was bolted to W6 south face (12 ft (3.7 m) from the east corner and 10 ft (3.05 m) below the smooth concrete/formwork interface).
- Target 3: A 13-ft (4.0 m) overall, 8.5 ft (2.6 m) length of ¼-inch (6 mm) cable with an 18 inch by 1 inch (460 mm by 25 mm) chrome bar, 28 inch (711 mm) accordion hose, and a 4-inch by 2-inch (102 mm by 51 mm) tube attached to a 5-inch (127 mm) square steel plate (see figure 74). This target was bolted to W6 north face (15 ft (4.6 m) from the west corner and 13 ft (4.0 m) below the smooth concrete/formwork interface).
- Target 4: A steel pin with handle, 6 inches (150 mm) overall with 3.5-inch (90 mm) by 1.25-inch (32 mm)) pin and a 4-inch (102 mm)) by 2.5-inch (63 mm) handle (see figure 75). This target was bolted to W6 west face (15 ft (4.6 m) from the north corner and 15 ft (4.6 m) below the smooth concrete/formwork interface).

Dive Inspection

As part of the phase II study, Caltrans hired a contract dive inspection team to conduct inspections of the SF-OBB and the Third Street Bridge using the standard dive inspection protocols for underwater inspection. The contractor inspected piers W2, W5, and W6 of the SF-OBB between November 4 and 6, 2013. They also inspected the north and south channel piers of the Third Street Bridge on November 14, 2013. The contract dive inspection team was not aware of the results of previous dive inspections of these locations or of the planted targets on pier W6.

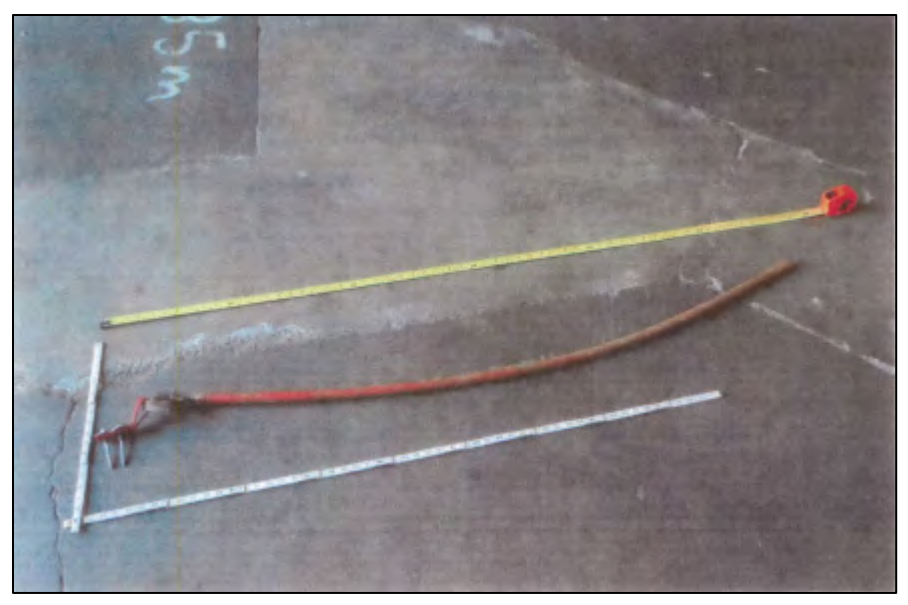


Figure 72. Photo. Target number 1: plastic coated cable.

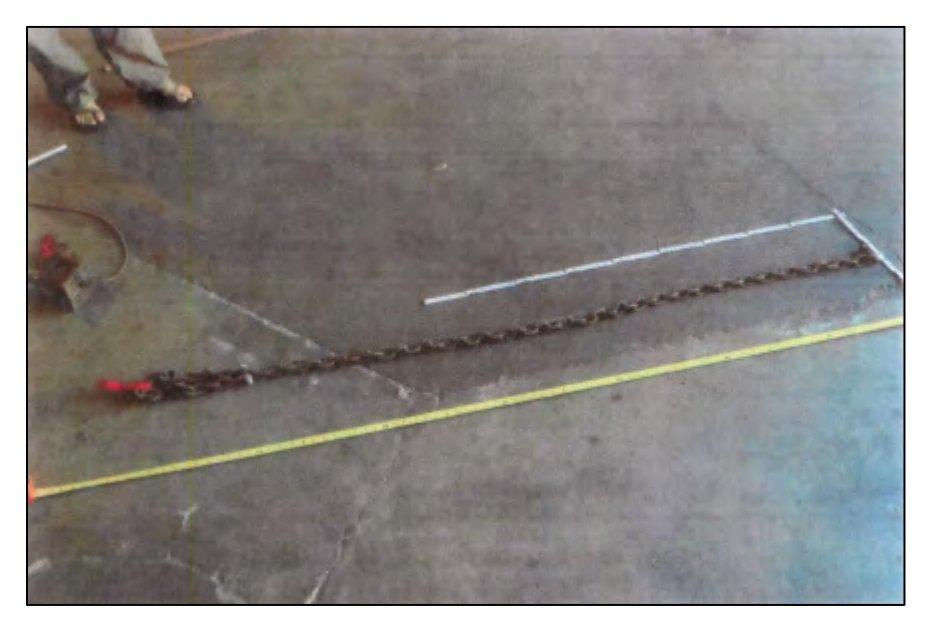


Figure 73. Photo. Target number 2: a chain.

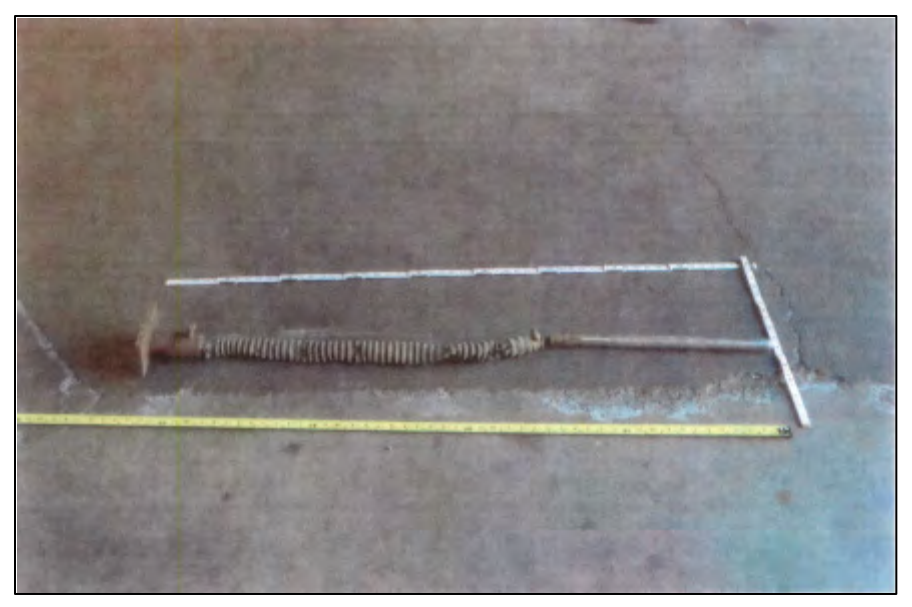


Figure 74. Photo. Target number 3: chrome bar and accordion hose.



Figure 75. Photo. Target number 4: a steel pin with handle.

Sonar Inspection Teams and Reporting

Three sonar inspection teams were formed to independently apply a range of acoustic imaging equipment types described in a subsequent section. Table 11 summarizes the inspection dates and operating windows for each team. Some of the teams operated in larger windows than others.

Table 11. Phase II sonar field test schedule.

		Third	Third Street	
	SF-OBB	Street	Bridge	
SF-OBB	Operating	Bridge	Operating	
Date	Window	Date	Window	Sonar Inspection Team
4/14/14	1 pm - 5 pm	4/15/14	9 am -12 noon	Team A
4/16/14	7 am – 7 pm	4/15/14	12 noon -7 pm	Team B
4/17/14	8 am – 8 pm	4/18/14	8 am – 6 pm	Team C

Because the underwater inspection of bridges and the interpretation of findings are subject to engineering judgments related to threats to structural stability, a qualified bridge inspector was identified to lead each sonar team as the inspection team leader. The same individual from Infrastructure Engineers, Inc. was assigned to work with the acoustic imaging teams to identify potential anomalies and areas of interest during the inspection and to produce typical underwater bridge inspection reports following the inspection.

An advantage of using the same bridge inspection team leader for all three teams is the consistency that the inspector would bring regarding what to look for at each site. A risk in this approach is that the inspector will learn about the substructures from earlier inspections and apply that knowledge to later inspections.

The inspection team leader conducted pre-inspection meeting(s) for each sonar team to review the capability of the acoustic imaging team and plan the required work. Each acoustic imaging team (team leader and team members) was responsible for:

- Providing the acoustic imaging hardware.
- Operating the equipment including operational and post-processing software.
- Providing a boat suitable for: 1) carrying acoustic imaging equipment, 2) operating in San Francisco Bay, and 3) carrying the acoustic team, an assigned team leader, and Caltrans observers.
- Reporting results of the inspection, including technical support for extracting data and images, in a format consistent with underwater bridge inspection reports.

Inspection teams were encouraged to organize their reporting of element condition based on the AASHTO classification of commonly-recognized (CoRe) bridge elements. However, this was not required because the focus of the level 1 inspections for this phase II field work targeted the identification of large anomalies, such as significant section loss, missing elements, or large scale misalignment. The AASHTO descriptions are as follows:

Reinforced Concrete

- Little or no deterioration. No effect on strength and/or serviceability.
- Minor cracks and spalls, no exposed rebar.
- Some delamination and/or spalls may be present and some reinforcing may be exposed. Loss of section does not significantly affect the strength and/or serviceability.

• Advanced deterioration. Corrosion of reinforcement and/or loss of concrete section require analysis to ascertain the effect on the strength/serviceability of either the element or the bridge.

Prestressed Concrete

- Little or no deterioration. Discoloration, efflorescence, and/or superficial cracking, but without effect on strength and/or serviceability.
- Minor cracks and spalls, and exposed reinforcing with no corrosion. No exposure of the prestressed system.
- Some delamination and/or spalls. Minor exposure, but no deterioration of the prestressed system. Corrosion of non-prestressed reinforcement, but loss of section is incidental and does not significantly affect the strength and/or serviceability.
- Delamination, spalls, and corrosion of non-prestressed reinforcement are prevalent. There may also be exposure and deterioration of the prestressed system (loss of bond, broken strands or wire, failed anchorages, etc.). An analysis is warranted.

Steel Painted

- Paint system sound and functioning.
- Little or no active corrosion. Surface or freckled rust. Paint system chalking, peeling, curling (paint system distress), but there is no exposure of metal.
- Surface or freckled rust prevalent. Exposed metal, but no section loss.
- Active corrosion, section loss resulting from active corrosion does not require structural analysis.
- Section loss warrants structural analysis for ultimate strength and/or serviceability.

Steel Unpainted

- Little or no corrosion. Oxide film for weathering steel is uniform and tightly adhered.
- Surface rust or surface pitting. Weathering steel color is yellow orange to light brown. Oxide film has a dusty to granular texture.
- Measurable section loss, but does not warrant structural analysis. Weathering steel is dark brown or black. Oxide film is flaking.
- Oxide film has a laminar texture with thin sheets of rust. Section loss is sufficient to warrant structural analysis.

Sonar Technologies

Several sonar technologies were employed in the phase II field testing. The technologies used by each of the three sonar teams introduced in table 11 are described in the following sections.

3D Real-Time Multibeam

Inspection team A used a 3D real-time multibeam sonar, supported by GPS and inertial instrumentation, for the investigation. The equipment was mounted on a 30-ft (9.1 m) long forward cabin vessel. Once the 3D real-time multibeam components were assembled and calibrated, the boat operator made multiple low speed passes around the perimeter of the piers. The sonar apparatus produced 3D images in real time for review by the technician and team leader.

2D Multibeam and 3D Mechanical Multibeam

Inspection team B used both 2D multibeam and 3D mechanical multibeam sonar for the underwater inspections in phase II. The sonar and supporting instrumentation were deployed from a 50-ft (15 m) forward cabin vessel at both locations and a 30-ft (9.1 m) forward cabin vessel at the Third Street Bridge. In several cases at the SF-OBB and at the majority of cases at the Third Street Bridge, the pier faces were inspected from stationary locations on the channel bottom. For these stationary locations the 3D mechanical multibeam sonar apparatus was attached to various mounting assemblies and lowered to the channel bottom.

Inspection team B also used two 2D multibeam sonar products. Scans near the surface were taken from stationary locations with the 2D multibeam sonar used in phase I mounted to a pole and operated manually by an assistant on the boat. The position of the sonar transducer was adjusted according to water depth and structure orientation. Additionally, team B employed a second 2D multibeam sonar (Reson 7125), which was attached to a vertical support mounted to a rotating bracket on the starboard gunwale of the vessel.

Depending on the specific equipment, the sonar apparatus produced 2D or 3D images in real time for review by the technicians and team leader. The sonar technicians and boat operator coordinated the location and heading of the vessel to maximize the resulting image detail and perspective angle.

2D Sector-scanning and 3D Profiler

Inspection team C employed 2D sector-scanning and 3D profiler sonar for the phase II inspections. The sonar and supporting instrumentation were deployed depending on the situation. In some situations, the sonar was deployed from a 50-ft (15 m), rear cabin, flat deck vessel. The majority of the pier faces were inspected from a stationary location at the surface. In situations with sufficient access, the sonar head was mounted to a davit crane at the bow of the vessel. In cases of limited access for surface scanning, such as the Third Street Bridge, the sonar was mounted to a remote operated vehicle (ROV) and maneuvered to an optimal scanning location. The position of the sonar transducer was adjusted according to the water depth and structure orientation. When scanning the channel bottom and base of the pier at the Third Street Bridge, the sonar was mounted to a tripod and lowered to the channel bottom.

The fan beam of the 2D sector-scanning sonar sensor was directed along the surface plane of each side and each nose of the piers from multiple positions in order to provide substantial imagery of the bridge piers. The 3D profiling beam was utilized to produce pier-to-water bottom interface measurement in order to determine and describe any localized scour.

The underwater investigation for inspection team C consisted of sonar imaging of the visible substructure unit surfaces from the high water mark to the channel bottom. Potential anomalies and areas of particular interest were identified from the initial results on site. Localized data were then collected by focusing the sonar trajectory on these areas. The inspection team also assessed the waterway and streambed conditions in the bridge vicinity, noting the location and extent of any observed scour, riprap, or debris.

In each configuration, the sonar produced high resolution, 2D images in real time for review by the technicians and team leader. For boat-mounted configurations, the sonar technicians and boat operator coordinated the location and heading of the vessel to maximize the resulting image detail and perspective angle.

SAN FRANCISCO-OAKLAND BAY BRIDGE

The SF–OBB, west span carries traffic over the San Francisco Bay between Yerba Buena Island and San Francisco. The bridge consists of six suspension spans. The superstructure is supported by two abutments and five intermediate piers. The piers consist of submerged concrete cofferdams beneath concrete pedestals that support the steel towers. The piers are numbered from west to east, with pier W2 (figure 76) adjacent to San Francisco and pier W6 (figure 77) adjacent to Yerba Buena Island.

The caisson on pier W2 includes remnants of sheet pile, probably from the construction of the coffer dam. Also contained within close proximity to the west side of pier W2 are piles supporting a remnant of the old Wharf Pier 24, which had been truncated during the construction of the west span of the SF-OBB.

The San Francisco Bay is tidally influenced and flowed with a velocity of up to 2.0 knots during the inspections. The maximum water depths were estimated to be approximately 65 ft (20 m) at pier W2 and 130 ft (40 m) at pier W6.



Figure 76. Photo. Pier W2 viewed from the east.



Figure 77. Photo. Pier W6 viewed from the west.

The scope of the field work included a sonar inspection of all accessible submerged substructure units located in the water from the high water mark to the channel bottom. The objectives of the inspections were to identify conditions relevant for a level I underwater inspection and to provide recommendations for further maintenance and inspection work, when applicable.

Inspection Findings at Pier W2

A schematic of pier W2 is provided in figure 78. The directional faces referenced in the inspection reports are also defined in the figure. Inspection findings from the dive inspection and the three sonar inspections performed as part of this study are described in this section and are summarized in table 12. The summary includes overall conclusions of the inspection, observations related to bed forms, scour, or objects identified, as well as materials conditions and defects.

The report from the 2013 dive inspection concluded that there were no structural deficiencies that could jeopardize the structural integrity of pier W2. The dive inspection report also stated that there was no evidence of notable scour around pier W2.

The dive inspection report noted that at water depths down to 16 ft (4.9 m) the concrete pier surfaces were typically found to be smooth and in sound condition. At depths greater than 16 ft (4.9 m), the concrete exhibited random voids and vertical or horizontal seams of section loss having typical penetrations between 0.5 to 1.0 ft (0.15 to 0.3 m) in depth, with maximum penetrations of 3 ft (0.9 m). On the south face, the inspector reported a large void at a depth of approximately 29 ft (8.8 m) approximately 10 ft (3.05 m) wide by 1.5 ft (0.45 m) high with a penetration depth of up to 5 ft (1.5 m).

The dive inspection report noted occurrences of exposed reinforcing steel. On the south face, random reinforcing steel measuring up to 1.5 inches (38 mm) in diameter was encountered in some voids. The report also noted exposed reinforcing steel on the north face.

All three sonar inspection teams reported that the submerged portion of pier W2 was in fair to good condition. Each noted that the general concrete condition is normal for in-service, sheet pile formed concrete piers of this size and age. They noted bands of voiding in pier W2, but concluded they were not sufficient to independently pose a significant threat to the integrity of a pier of this size. The teams made no repair recommendations.

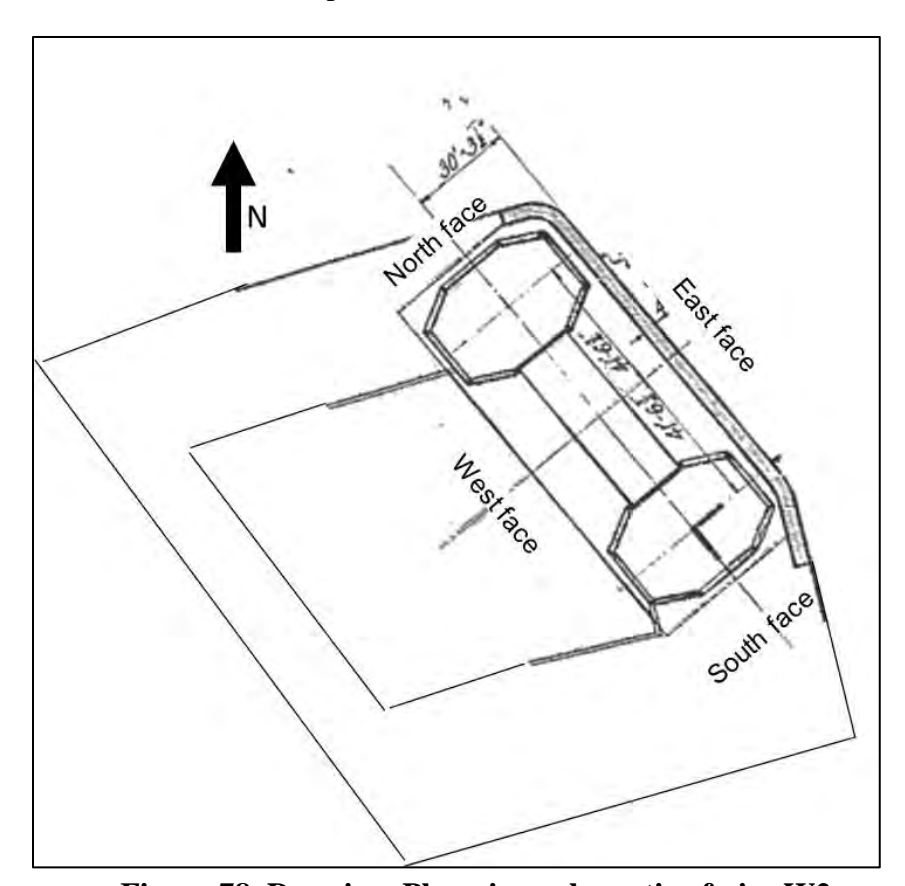


Figure 78. Drawing. Plan view schematic of pier W2.

All three of the sonar inspection teams also noted significant aggradation along the southwest quadrant of pier W2, which is protected from tidal ebb by nearby Port of San Francisco Pier 26. The minimum depth in this area was approximately 11 ft (3.4 m), while the maximum depth along the east face of pier W2 was approximately 65 ft (20 m).

The piles from old Wharf Pier 24 prevented access to the south and west faces of the concrete caisson for inspection team A. Team A reported that sheet pile form impressions were visible on all inspected faces (east and north) of pier W2. As shown in figure 79, the underwater acoustic imaging results show areas of voiding along the east face of pier W2. These horizontal bands varied in size, up to a maximum of 50 ft (15 m) long by 4 ft (1.2 m) high by 1.5 ft (0.46 m) deep, and are located near the center of the east face, ranging from approximately 10 ft (3 m) above the channel bottom to approximately 30 ft (9 m) above the channel bottom.

Table 12. SF-OBB pier W2 inspection comparison summary.

Inspection/	Conclusions/	Bed forms/ Scour/	
Location	Recommendations	Objects	Materials Conditions and Defects
Diver (2013)/ Overall	No structural deficiencies that could jeopardize the structural integrity.	No evidence of notable scour.	Concrete exhibited random voids and vertical or horizontal seams of section loss having typical penetrations between 0.5 to 1.0 ft (0.15 to 0.3 m) in depth, with maximum penetrations of 3 ft (0.9 m).
Diver (2013)/ South Face			Large void at a depth of approximately 29 ft (8.8 m) approximately 10 ft (3.05 m) wide by 1.5 ft (0.45 m) high with a penetration depth of up to 5 ft (1.5 m). Exposed reinforcing steel measuring up to 1.5 inches (38 mm) in diameter encountered in some voids
Sonar Team A	Submerged portion of pier in fair to good condition. General condition normal for inservice, sheet pile formed concrete piers of this size and age. Old Wharf Pier 24 prevented access to the south and west faces of the caisson.	Significant aggradation along the southwest quadrant of pier. No evidence of notable scour.	Sheet pile form impressions visible on east and north faces. Areas of voiding identified on the east face. These horizontal bands varied in size, up to a maximum of 50 ft (15 m) long by 4 ft (1.2 m) high by 1.5 ft (0.46 m) deep, and are located near the center of the east face, ranging from 10 ft (3 m) to 30 ft (9 m) above the channel bottom.
Sonar Team B	Submerged portion of pier in fair to good condition. General condition normal for inservice, sheet pile formed concrete piers of this size and age.	No evidence of notable scour. Identified debris on the bed near pier including an axle with a pair of wheels.	Much of the sheet pile appears to have deteriorated from the submerged portions of the caisson. Intermittent horizontal bands of voiding in the concrete caisson throughout the lengths of the entire east and west faces, with a maximum height of 6 ft (1.8 m) and a maximum depth of 1 to 2 ft (0.3 to 0.6 m). On the east face, voids were most prominent at 15 ft (4.6 m) and 30 ft (9.1 m) above the channel bottom. On the west face, voids were evident beginning just below the top of the sheet pile form and extending down to approximately 8 ft (2.4 m) above the channel bottom. Voids were also visible on the northeast and southeast corners of the caisson.

Inspection/	Conclusions/	Bed forms/ Scour/	
Location	Recommendations	Objects	Materials Conditions and Defects
Sonar	Submerged portion of	No evidence of notable	Much of the sheet pile appeared to have deteriorated from the
Team C	pier in fair to good	scour.	submerged portions of the caisson. Intermittent horizontal bands of
	condition. General		voiding in the concrete caisson that varied in size, up to a maximum of
	condition normal for in-		50 ft (15 m) long by 8 ft (2.4 m) high by 2 ft (0.6 m) deep. On the east
	service, sheet pile formed		face, voiding was visible beginning near the top of the sheet pile form,
	concrete piers of this size		and extended down 15 ft (4.6 m). On the west face, voiding was found
	and age.		throughout the entire submerged height of the sheet pile formed caisson.
			Voids were most prominent on the east and west faces of the pier, but
			were visible on all of the scanned faces. The remaining sheet pile
			appeared to be delaminating from the pier.

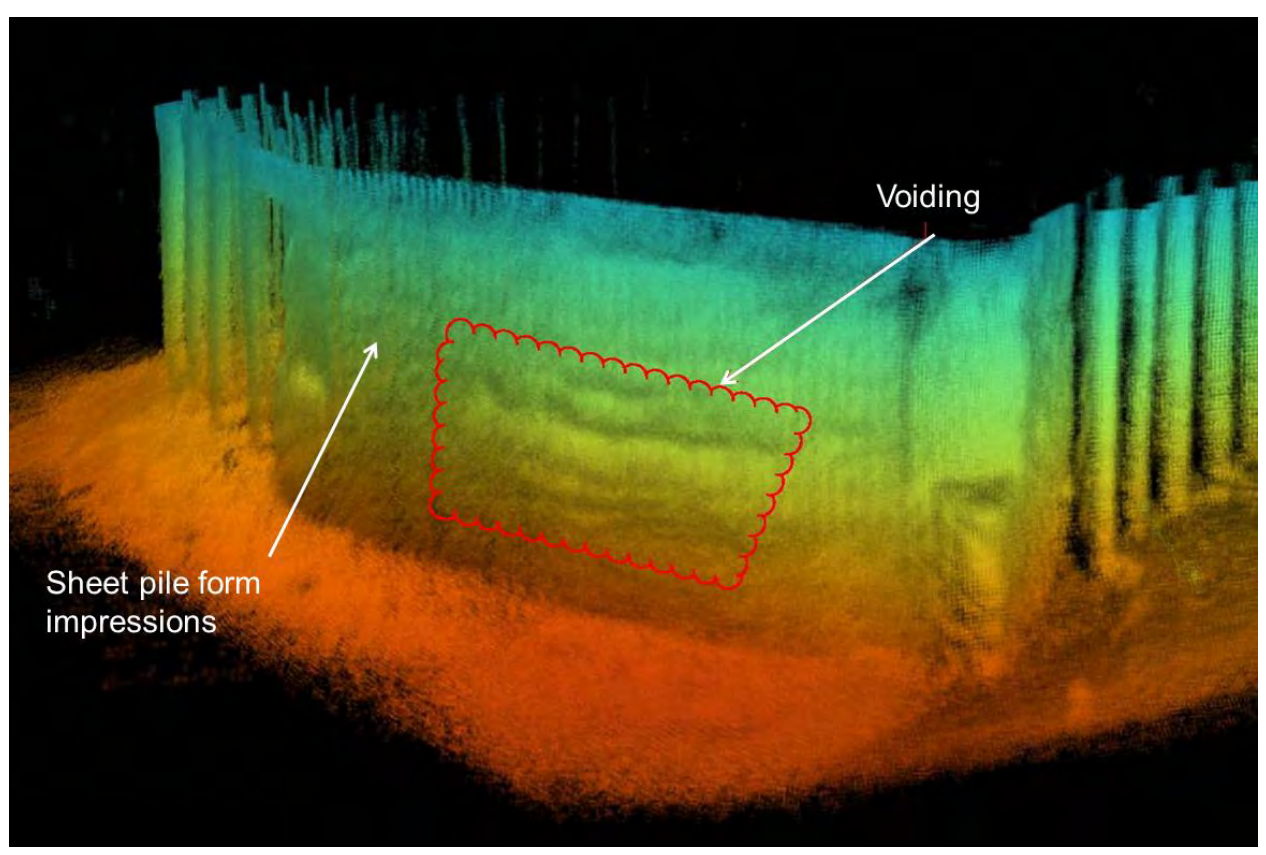


Figure 79. Image. Pier W2 viewed from the east.

Inspection team B reported that much of the sheet pile appears to have deteriorated from the submerged portions of the caisson at pier W2. As shown in figure 80, there were intermittent horizontal bands of voiding in the concrete caisson throughout the lengths of the entire east and west faces, with a maximum height of approximately 6 ft (1.8 m) and a maximum depth of approximately 1 to 2 ft (0.3 to 0.6 m). On the east face, the voids were most prominent at approximately 15 ft (4.6 m) and 30 ft (9.1 m) above the channel bottom. On the west face, the voids were evident beginning just below the top of the sheet pile form and extending down to approximately 8 ft (2.4 m) above the channel bottom near the center of the face. These voids were also visible on the northeast and southeast corners of the caisson.

Inspection team B also identified debris on the bed near pier W2. The image in figure 81 shows evidence of debris including an axle with a pair of wheels.

Inspection team C reported that the imaging results showed sheet pile form impressions at pier W2. They noted that much of the sheet pile appeared to have deteriorated from the submerged portions of the caisson at pier W2 as shown in figure 82. They further observed that there were intermittent horizontal bands of voiding in the concrete caisson and that they varied in size, up to a maximum of approximately 50 ft (15 m) long by 8 ft (2.4 m) high by 2 ft (0.6 m) deep. On the east face, the voiding was visible beginning near the top of the sheet pile form, and extended down approximately 15 ft (4.6 m). On the west face, the voiding was found throughout the entire submerged height of the sheet pile formed caisson. These voids were most prominent on the east

and west faces of the pier, but were visible in varying degrees on all of the scanned faces. The remaining sheet pile appeared to be delaminating from the pier.

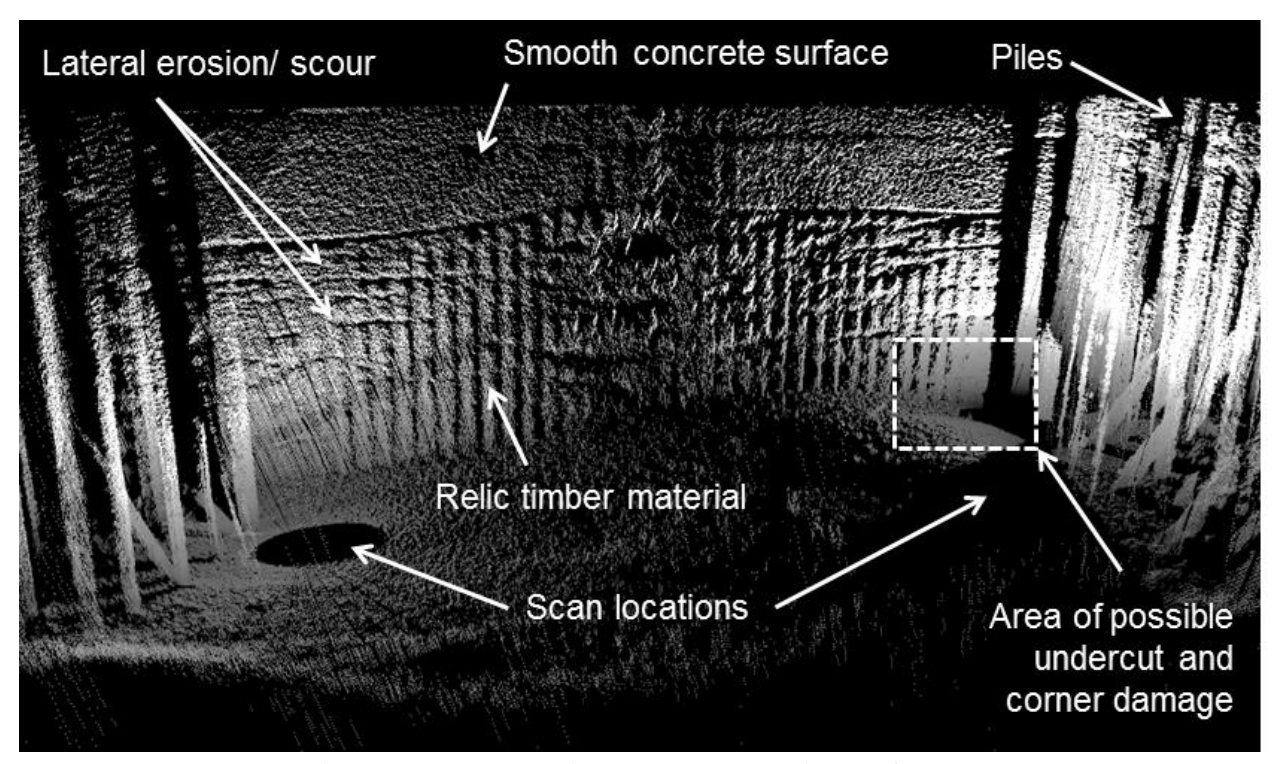


Figure 80. Image. Pier W2 3D data viewed from west.

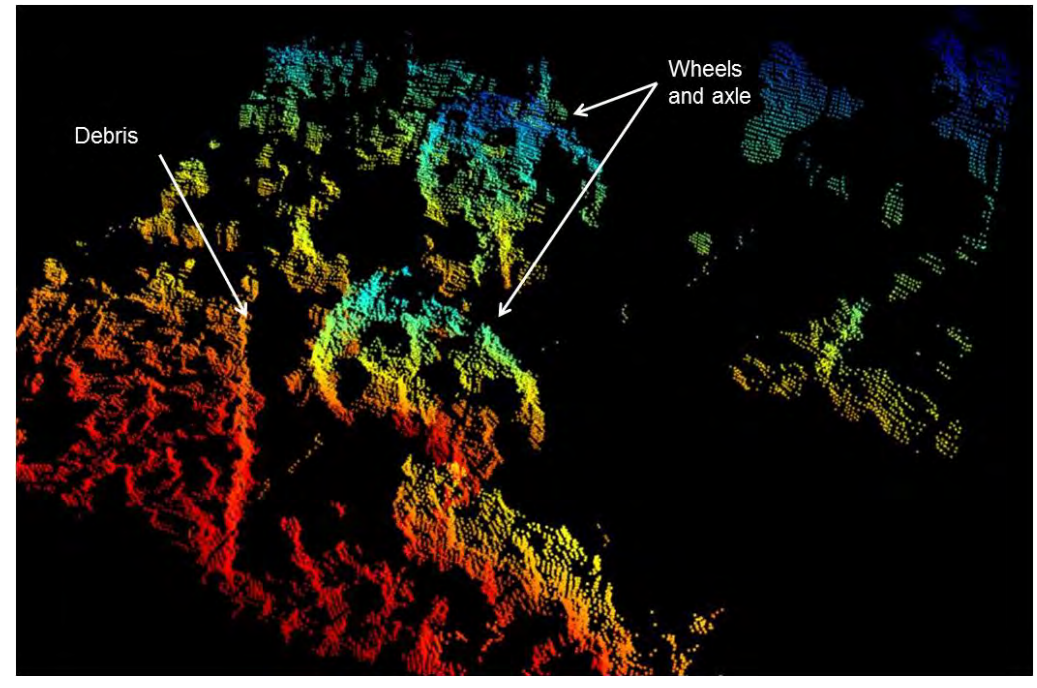


Figure 81. Image. Detail at bed near pier W2.

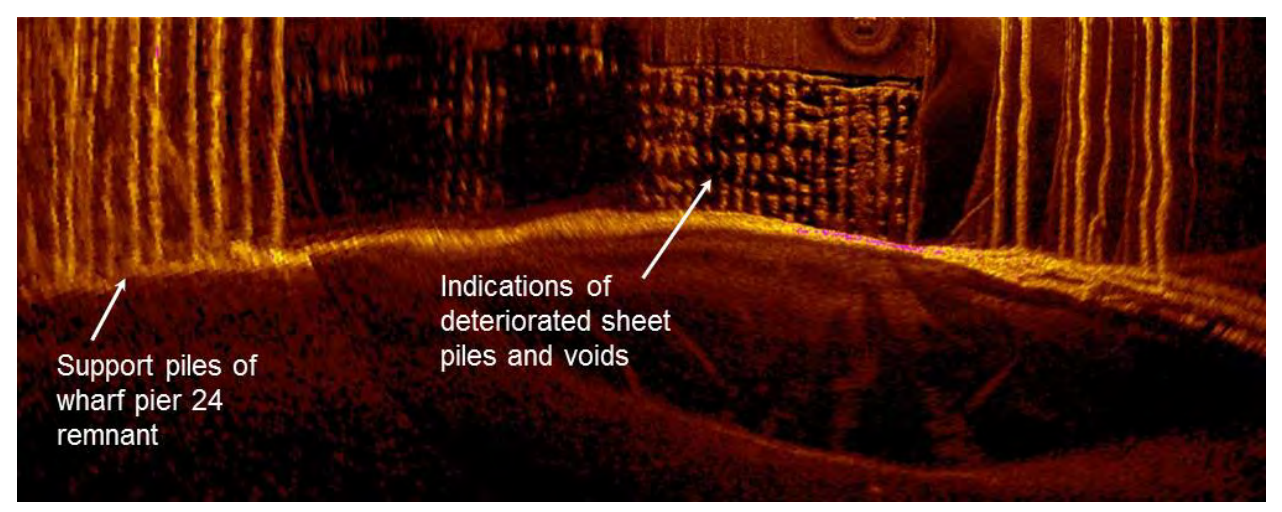


Figure 82. Image. Southeast corner of pier W2.

The dive team and all three sonar teams drew the same general conclusions regarding the overall stability of the underwater portions of pier W2: voids were common, but nonthreatening, and scour was not evident. The sonar teams also noted aggradation at the southeast corner of the pier (visible in figure 82), but this was not reported by the dive team. Except for sonar team A, all inspection teams were able to access all four pier faces.

The largest void reported by the dive team had up to 5 ft (1.5 m) of penetration at a depth of 29 ft (8.8 m) on the south face. The deepest penetrations reported by the sonar teams were 1.5 ft (0.46 m) (east face), 2 ft (0.6 m) (east and west faces), and 2 ft (0.6 m), for teams A, B, and C, respectively. While the sonar teams were able to identify the locations and scale (width and length) of voids, none of the voids reported by the sonar teams had the depth of penetration reported by the dive team.

Sonar team B noted debris adjacent to the pier that was not reported by the other sonar teams or the dive team. This may be either because the debris was not detected or was observed, but not considered relevant to the inspection.

Finally, the dive team noted several instances of exposed reinforcing steel. None of the dive teams identified any of these occurrences.

Inspection Findings at Pier W6

A schematic of pier W6 is provided in figure 83. The directional faces referenced in the inspection reports are defined in the figure and are the same as those for pier W2. Inspection findings from the dive inspection and the three sonar inspections conducted as part of this study are described in this section and summarized in table 13

The summary includes overall conclusions of the inspection, observations related to bed forms, scour, or objects identified, as well as materials conditions and defects.

The report from the 2013 dive inspection concluded that there were no structural deficiencies that could jeopardize the structural integrity of pier W6. However, the inspection could draw no

conclusions regarding scour because the dive range was limited to a depth of 100 feet and the channel bottom was at a depth of approximately 130 ft (40 m). The lower 30 ft (9.1 m) of the pier surface and the channel bed were not inspected by the divers.

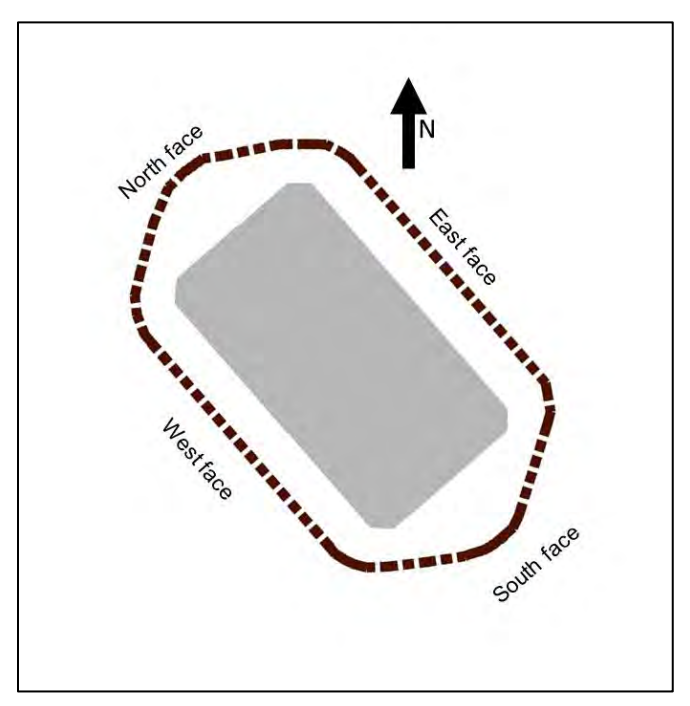


Figure 83. Drawing. Plan view schematic of pier W6.

For the surfaces of pier W6 that were inspected, the dive inspection report noted that the concrete surfaces were typically smooth and sound with no significant deterioration noted down to a depth of 35 ft (10.7 m). Below 35 ft (10.7 m) timber formwork was observed around the concrete to the lower dive limit of 100 ft (30.5 m). The formwork, while deteriorating in some areas, covered 95 percent of the pier face between depths from 35 to 80 ft (11 to 24 m) and covered 90 percent between depths from 80 to 100 ft (24 to 30 m). The report described the formwork as a well-defined surface of diagonal 1 ft by 1 ft (0.3 m by 0.3 m) members on the south and north faces and as more irregular with mostly 1 ft (0.3m) vertical timber members on the west and east faces.

Overall, the three sonar inspection teams reported that the submerged components of pier W6 were in fair to good condition. They noted that the general concrete condition is normal for inservice, sheet pile formed concrete piers of this size and age. The teams made no repair recommendations. The images generated by the inspection teams covered the full depth of the pier to the bed. Although the bed was visible in the images, no comments on scour were made.

Table 13. SF-OBB pier W6 inspection comparison summary.

Inspection/	Conclusions/	Bed forms/ Scour/	
Location	Recommendations	Objects	Materials Conditions and Defects
Diver (2013)/ Overall	No structural deficiencies that could jeopardize the structural integrity.	No conclusions regarding scour could be made because the dive range was limited to a depth of 100 feet and the channel bottom was at a depth of approximately 130 ft (40 m). Planted objects not found.	Below 35 ft (10.7 m) timber formwork was observed around the concrete to the lower dive limit of 100 ft (30.5 m). (Inspection was not conducted below this depth.) The formwork, while deteriorating in some areas, covered substantial surface areas. The formwork was described as a well-defined surface of diagonal 1 ft by 1 ft (0.3 m by 0.3 m) members on the south and north faces and as more irregular with mostly 1 ft (0.3m) vertical timber members on the west and east faces.
Sonar Team A	Submerged portion of pier in fair to good condition. General condition normal for inservice, sheet pile formed concrete piers of this size and age. The images covered the full depth of the pier.	Images showed the bed, but no comments were made in the report. Planted objects not found.	Identified formwork impressions visible on all submerged faces of the caisson. The change from smooth concrete to the formwork is visible in the images.
Sonar Team B	Submerged portion of pier in fair to good condition. General condition normal for inservice, sheet pile formed concrete piers of this size and age. The images covered the full depth of the pier.	Images showed the bed, but no comments were made in the report. Planted objects not found.	Noted formwork impressions visible on the submerged caisson. A possible area of abrasion is distinguishable at the southeast corner, near the top of the caisson, just below the step-out.

Inspection/	Conclusions/	Bed forms/ Scour/	
Location	Recommendations	Objects	Materials Conditions and Defects
Sonar	Submerged portion of	Images showed the bed,	Noted formwork impressions visible on the submerged caisson at pier.
Team C	pier in fair to good	but no comments were	There are also possible diagonal sheathing remnants or impressions
	condition. General	made in the report.	visible on the south and west faces near the southwest corner
	condition normal for in-	Planted objects not	
	service, sheet pile formed	found.	
	concrete piers of this size		
	and age. The images		
	covered the full depth of		
	the pier.		

Inspection team A reported that there were no significant deficiencies visible at pier W6. The report identified that formwork impressions are visible on all submerged faces of the caisson as shown in figure 84. The change from the smooth concrete to the formwork is visible in the figure.

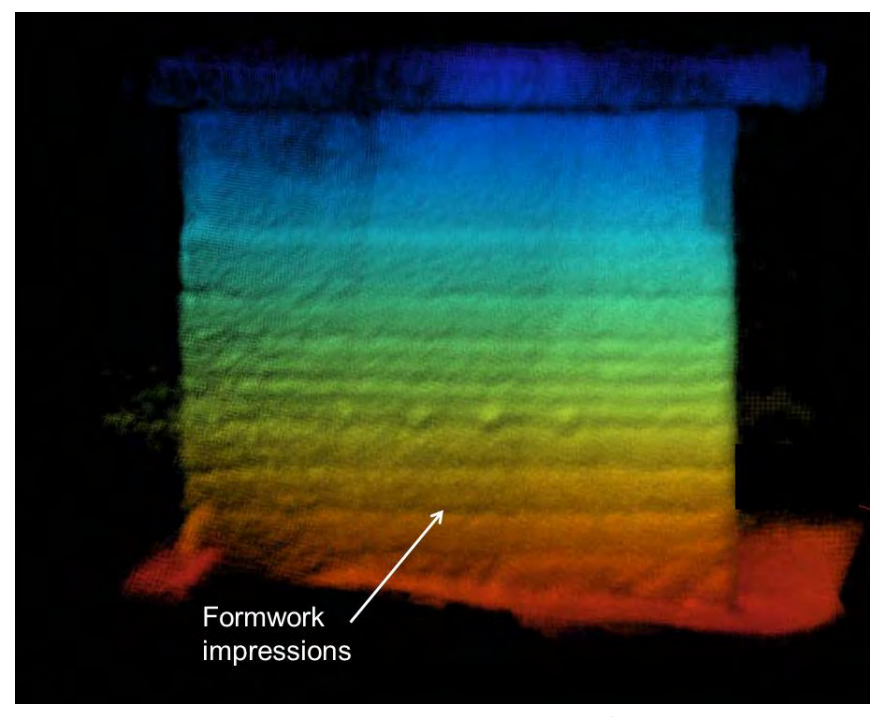


Figure 84. Image. Pier W6 viewed from the west.

Inspection team B noted formwork impressions visible on the submerged caisson as shown in figure 85. A possible area of abrasion is distinguishable at the southeast corner, near the top of the caisson, just below the step-out.

Inspection team C also noted formwork impressions visible on the submerged caisson at pier W6 as shown in figure 86. There are also possible diagonal sheathing remnants or impressions visible on the south and west faces near the southwest corner.

The dive team and all three sonar teams drew the same general conclusions regarding the overall stability of the underwater portions of pier W6: the top portions of the pier were smooth and the lower portions displayed formwork impressions. The sonar teams also noted the presence of the bed, but did not report anything regarding scour. The dive inspection did not reach the depth of the bed and could not comment on scour.

The dive team reported diagonal formwork on the south and north faces with vertical formwork on the east and west faces. All sonar images displayed predominantly vertical and horizontal formwork.

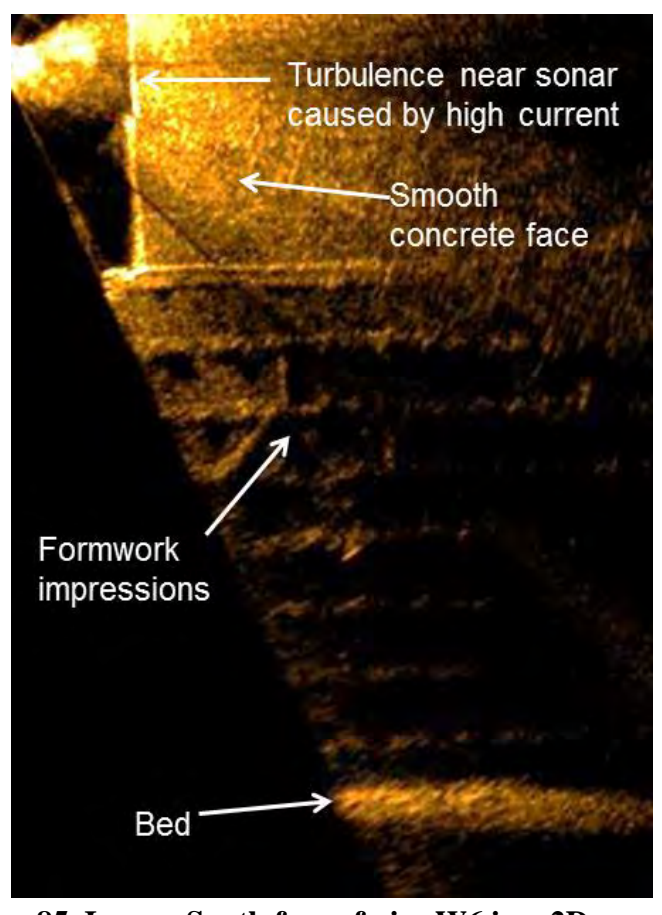


Figure 85. Image. South face of pier W6 in a 2D sonar image.

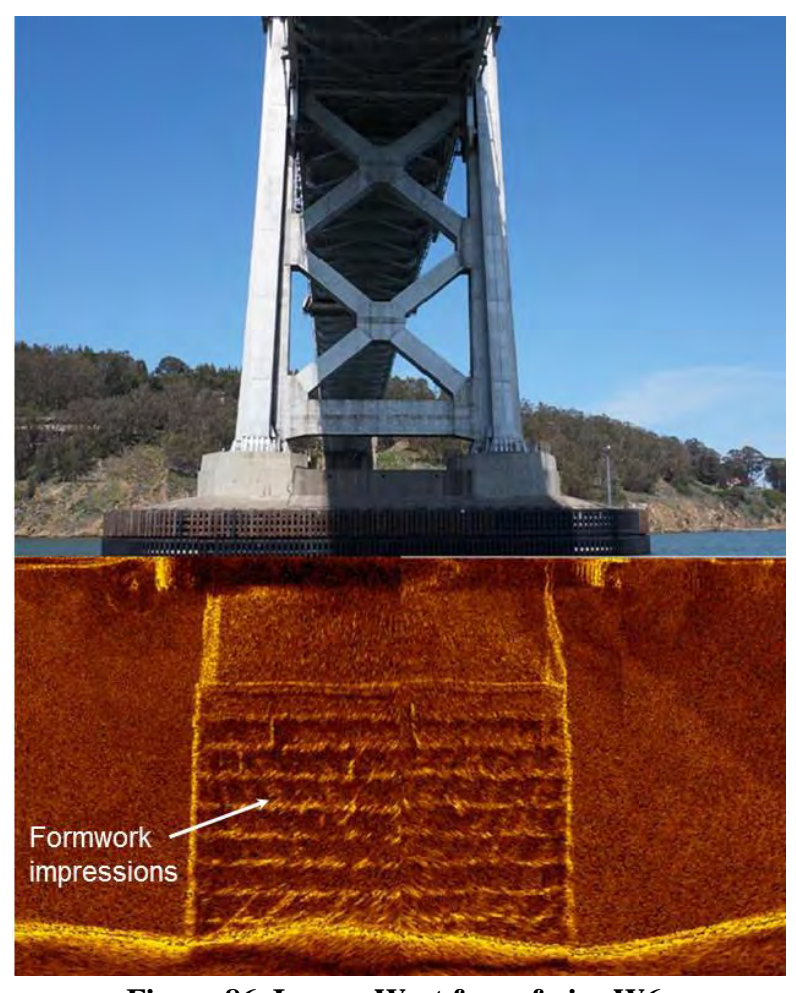


Figure 86. Image. West face of pier W6.

Post-Inspection Review

There was general consistency between the dive reports and the sonar reports for piers W2 and W6 on the larger scale findings. The inspections for this phase II field work were also generally consistent with findings from the previous (1995) inspection of pier W2. However, neither the dive report nor the sonar reports identified any of the planted targets on pier W6. After being informed of the prior inspection report and the planted targets, the sonar teams were asked to review their data for the possibility that these could be identified retrospectively.

After further review, inspection team A stated it was not able to identify these features. The inspection team further noted that while targets of the size presented are detectable by the 3D real-time multibeam, they are very hard to discern when placed against larger structures, especially at the large range required at these depths.

Analysts from sonar team B noted that the 1995 dive inspection report pertaining to pier W2 showed many linear features as shown in figure 87. They stated that similar features are readily noticeable in both the 2D multibeam images and the 3D mechanical multibeam point cloud data. For example, the analyst estimated that the lateral erosion was approximately 2 to 3 ft (0.6 to 0.9 m) deep from the image shown in figure 88. In addition, using the image shown in figure 80, the

analyst identified the transition from smooth concrete in the upper portion of the image to where the original concrete forms had been removed. They further identified numerous lateral erosion pockets, which were easily discernable in the data.

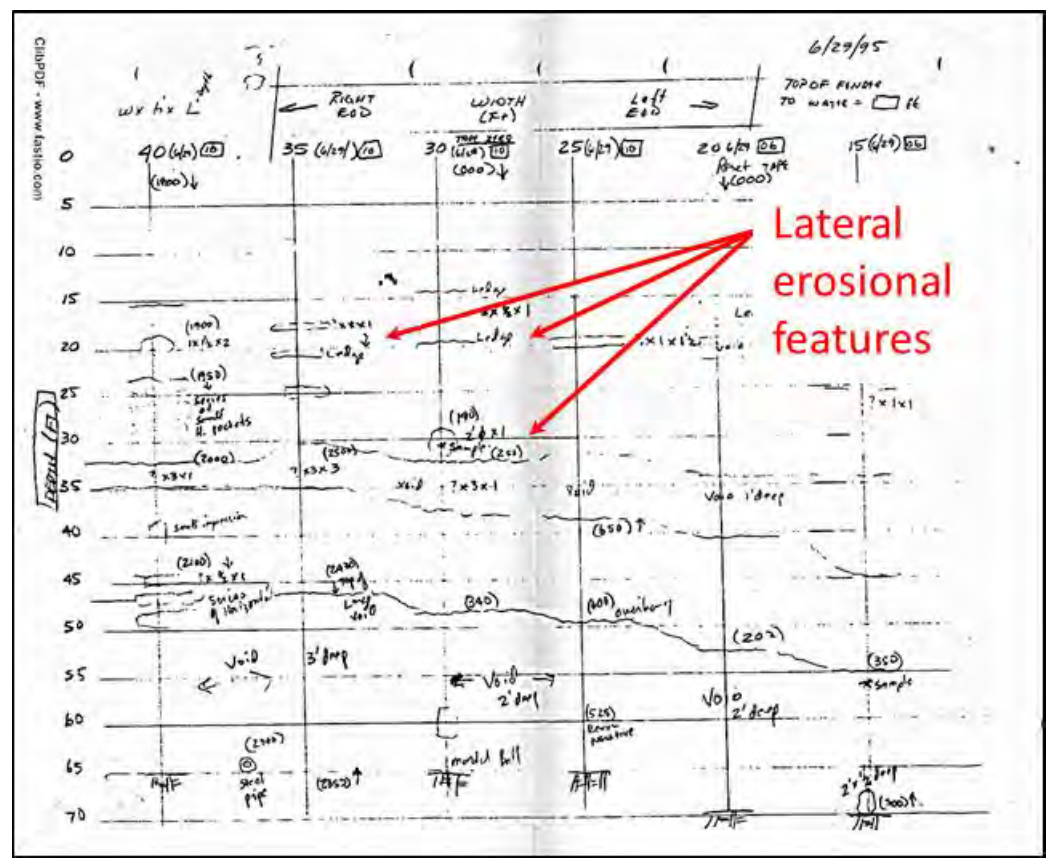


Figure 87. Image. Page from the 1995 diver inspection report on SF-OBB pier W2.

On further review, team C reported that the imagery depicted in their inspection report for pier W2 detailed the observed deteriorating concrete and patterns produced from the deteriorated and deteriorating sheet pile encasement. They stated that the concrete showed no signs of exposed steel reinforcement that would be observable if this were structural concrete and a part of the pier monolith or column. Therefore, it was surmised that this was tremie concrete placed between a sheet pile coffer dam and the actual pier monolith during construction.

The reanalysis noted that the close up views, such as the one shown in figure 89, revealed the deteriorated concrete and voids that number far more than the dive reports indicated and are too numerous to detail in light of the lack of structural significance. However, they maintained that it is possible to estimate penetration depths and to document each specific spall and void with the equipment and software used by team C.

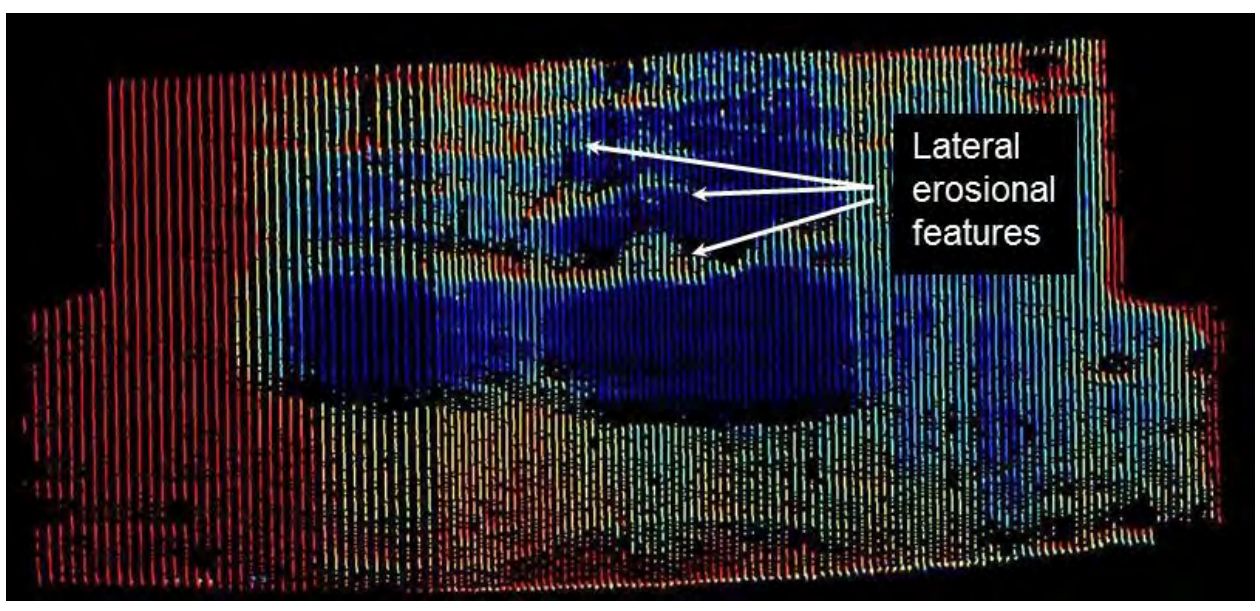


Figure 88. Image. 2D multibeam point cloud data of the east face of the W2 pier.

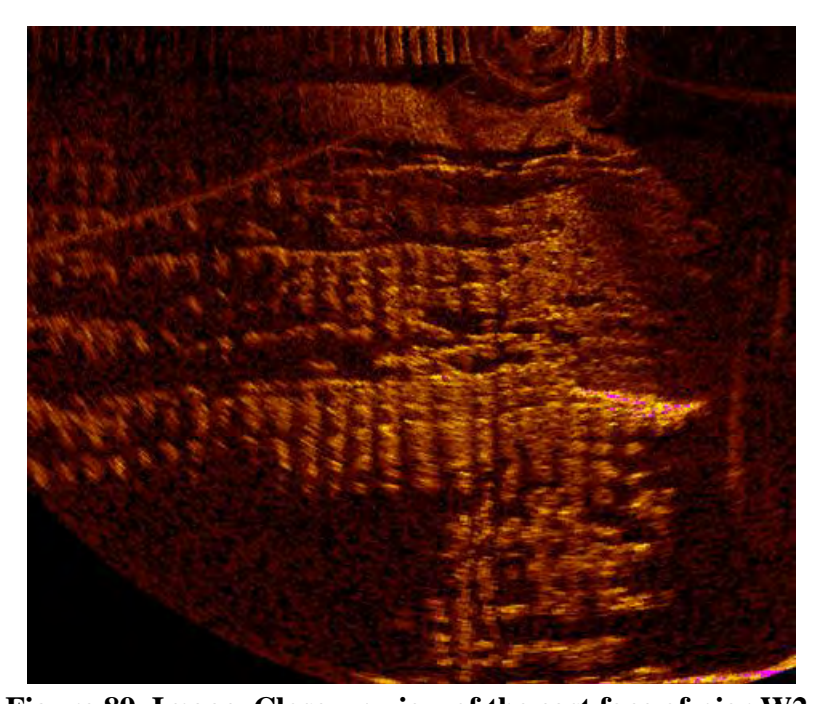


Figure 89. Image. Close-up view of the east face of pier W2.

The reanalysis by inspection team C also resulted in several observations regarding the planted targets on pier W6. The analyst observed that while there is a signature shown in figure 90 that is in the correct location and exhibits the appropriate dimensions for planted target 2 (a 7 ft (2.1 m), 3/8-inch (9.5 mm) chain), the nature of the object, if present, could not be identified. Several other linear articles of debris hanging on the pier are observed in the sonar images. The analyst noted that this is typical so it is not practice to call out each article of debris if it is not of consequence to the structural integrity.

In addition, the analyst speculated that the targets were not placed on pier W6, but on a different pier. The targets were planted in 2013 and the analyst notes that there was a pier designation change for the pier W6 inspection that occurred in early March of 2014 the month before the sonar inspection. However, there is no documentation supporting this assertion.

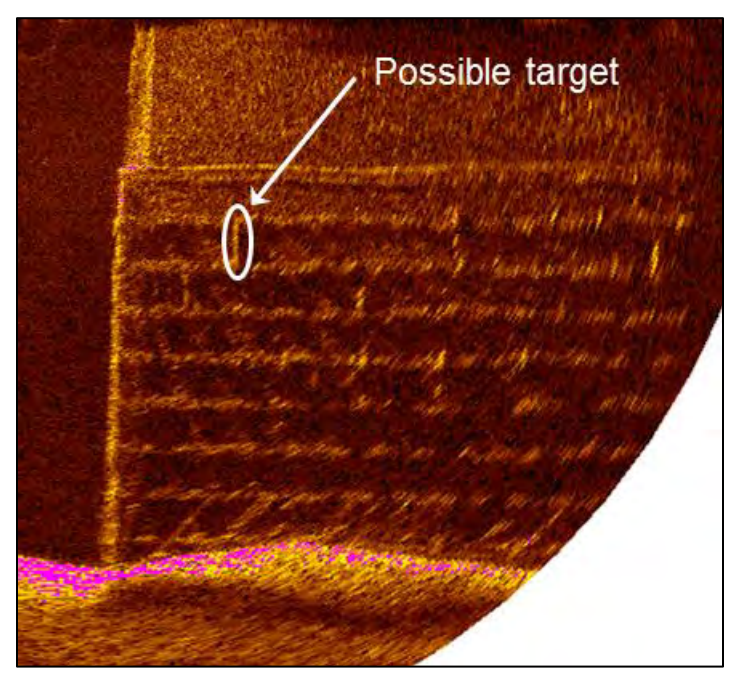


Figure 90. Image. South face of pier W6.

Further, the analyst from team C observed that there is no indication in the sonar imagery of the diagonal wood formwork around the caisson reported by the dive team. To the contrary, there is the observed characteristic typical of remnants of a concrete pour that has squeezed through horizontal formwork. The analyst suggested that the sonar indicated that the formwork is no longer surrounding the pier.

THIRD STREET BRIDGE

The Third Street bascule bridge, shown in figure 91, carries traffic over China Basin in downtown San Francisco. The bascule bridge has less than 3 ft (0.9 m) of vertical clearance at high tide and lifts from the north end when additional clearance is needed. The inspections focused on the piers adjacent to the main channel: pier 2 (the north channel pier) and pier 3 (the south channel pier). The south channel pier consists of two rectangular concrete supports founded on timber piles with a third concrete box between the two supports. The north channel pier consists of two rectangular concrete supports founded on timber piles connected by a concrete buttress wall.

Figure 92 highlights the location and orientation of the pier columns subject to inspection for this study. The inspection reports also refer to specific columns supporting the piers. The middle concrete box is not shown in the figure.



Original Photo. © 2012 Google®

Figure 91. Photo. Third Street Bridge in San Francisco.

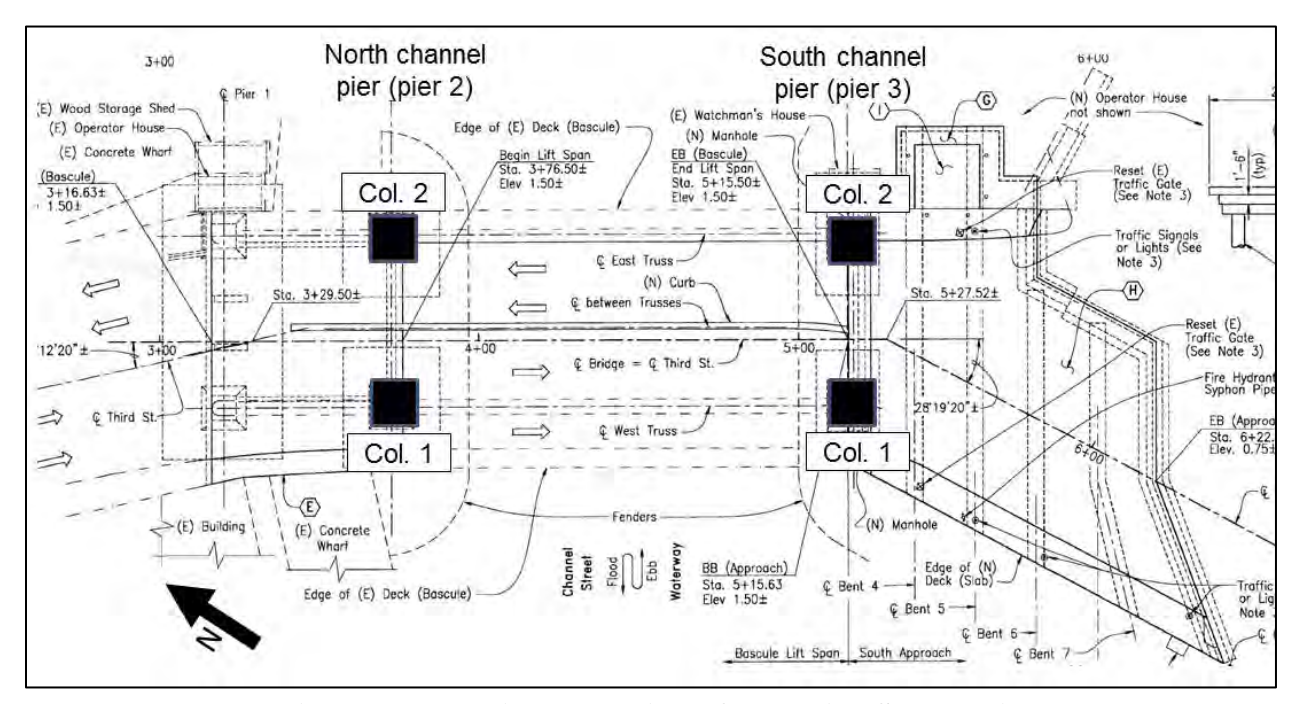


Figure 92. Drawing. Plan view of the Third Street Bridge.

The scope of the field work for each sonar team included inspection of all accessible submerged portions of the north and south channel piers from the high water mark to the channel bottom. The intent was to identify conditions relevant to bridge integrity that a bridge inspector would

report in a routine level I underwater inspection, as well as recommendations for maintenance and inspection work, if appropriate.

The San Francisco Bay and China Basin are tidally influenced, but no flow was noted during the inspections. According to the sonar results, the maximum water depths were less than 15 ft (4.6 m) at both piers during the inspections. Findings from each inspection team are provided in the following sections.

Inspection Findings at the Third Street Bridge

Inspection findings from the dive inspection and the three sonar inspections performed as part of this study are described in this section and summarized in table 14. The summary includes overall conclusions of the inspection, observations related to bed forms, scour, or objects identified, as well as materials conditions and defects.

The report from the 2013 dive inspection concluded that piers 2 and 3 were in mostly satisfactory condition with no defects of structural significance that would adversely affect the bridge. The report notes that, though pier 2 is in poor condition, its condition does not threaten the bridge. More specifically, the dive report noted that the concrete of the pier columns for both piers was relatively smooth and sound from the waterline to the channel bottom with minor random areas of section loss along vertical corners of the columns having typical penetrations of up to 1 inch (25 mm). Random 1 to 3 inch (25 to 76 mm) horizontal seams (mostly at cold construction joints) were noted throughout the columns and buttress wall with penetrations into the concrete of up to 6 inches (150 mm).

The dive inspection report included observations regarding the channel bottom noting that in the vicinity of the piers and bents the bed was primarily composed of 12-inch (300 mm) and smaller rocks and coarse gravel, with random scattered timber and steel formwork that allowed only minimal probe rod penetrations by the diver. The report noted that the shorelines under the bridge were both armored with riprap measuring up to 3 ft (0.9 m) in diameter and that the riprap appeared stable.

In addition to general observations, the dive inspection report provided observations for each column of each pier. The report noted that the columns of pier 2 were in fair to poor condition with various structural defects observed that could adversely affect structural integrity. Numerous random seams were noted along the south and west faces of column 1 with penetrations of up to 6 inches (150 mm), but with no reinforcing steel bars exposed. It went on to say that at the southwest corner of column 1, an area of greater section loss was observed just off the channel bottom measuring 1.5 ft (0.46 m) wide on each side of the corner, up to 1 ft (0.3 m) high, with a maximum penetration of 1 ft (0.3 m) with no exposed steel reinforcing. Other sections of loss were reported with one area identified where a heavily corroded reinforcing steel bar was exposed.

Table 14. Third Street bridge inspection comparison summary.

Inspection/	Conclusions/	Bed forms/ Scour/	
Location	Recommendations	Objects	Materials Conditions and Defects
Diver (2013)/ Overall	Piers 2 and 3 were in mostly satisfactory condition with no defects of structural significance that would adversely affect the bridge. The report notes that, though pier 2 is in poor condition, its condition does not threaten the bridge.	In the vicinity of the piers and bents the bed was smaller rocks and coarse gravel, with random scattered timber and steel formwork. Shorelines under the bridge were both armored with riprap that appeared stable. Partially buried tire not noted.	Noted that the concrete of the pier columns for both piers was relatively smooth and sound from the waterline to the channel bottom with minor random areas of section loss along vertical corners of the columns having typical penetrations of up to 1 inch (25 mm). Random 1 to 3 inch (25 to 76 mm) horizontal seams (mostly at cold construction joints) were noted throughout the columns and buttress wall with penetrations into the concrete of up to 6 inches (150 mm).
Diver (2013)/ Pier 2	The report noted that the columns of pier 2 were in fair to poor condition with various structural defects observed that could adversely affect structural integrity. The report recommended that the areas with exposed reinforcing steel should be addressed and repaired to inhibit those areas from further deterioration.		Numerous random seams were noted along the south and west faces of column 1 with penetrations of up to 6 inches (150 mm), but with no reinforcing steel bars exposed. At the southwest corner of column 1, an area of greater section loss was observed just off the channel bottom measuring 1.5 ft (0.46 m) wide on each side of the corner, up to 1 ft (0.3 m) high, with a maximum penetration of 1 ft (0.3 m) with no exposed steel reinforcing. Other sections of loss were reported with one area identified where a heavily corroded reinforcing steel bar was exposed. At column 2 of pier 2, the report identified additional areas of section loss. The largest void identified had a penetration of 1.5 ft (0.46 m) with one horizontal reinforcing steel bar exposed. In addition, concrete inside the void could be broken apart with a gloved hand. A 12 ft (3.7 m) long horizontal seam on the east face (and wrapping around the southeast corner) about 7 ft (2.1 m) below the water surface had maximum penetration of 1.5 ft (0.46 m). Delamination of the concrete face at the southeast corner was also noted.

Inspection/	Conclusions/	Bed forms/ Scour/	
Location	Recommendations	Objects	Materials Conditions and Defects
Sonar	Submerged portion of	Partially buried tire not	No major deficiencies. Because of limited access, in-depth scanning was
Team A	pier in fair to good condition. General condition normal for in- service, sheet pile formed concrete piers of this size and age. No remedial recommendations were made.	noted.	limited to the east support (column 2) of the north channel pier
Sonar Team B	Submerged portion of pier in fair to good condition. General condition normal for inservice, sheet pile formed concrete piers of this size and age. No remedial recommendations were made.	Partially buried tire not noted.	No major deficiencies. Because of limited time and access, in-depth scanning was limited to the east support (column 2) of the north channel pier (pier 2). At the north channel pier (pier 2), possible abrasion damage or voiding was identified along the west end of the south face. This area was reported as 3 ft (0.9 m) long by 2 ft (0.6 m) high and positioned 5 ft (1.5 m) above the channel bottom. On the northwest corner of the same support column, two possible areas of corner spalling or abrasion were reported. On the south face of column 2 formwork lines as well as an area of voiding at the east end was reported to be 6 ft (1.8 m) long by a maximum of 1 ft (0.3 m) high and positioned 1 to 2 ft (0.3 to 0.6 m) above the channel bottom. At the southeast corner a corner spall 6 inches (150 mm) high by 6 inches (150 mm) deep located 8 ft (2.4 m) above the channel bottom was noted. On the east face, an area of voiding 3 ft (0.9 m) long by a maximum of 1 ft (0.3 m) high located 6 to 8 ft (1.8 to 2.4 m) above the channel bottom was reported. Also on the east face, several possible areas of voiding approximately 1 ft (0.3 m) in diameter and ranging 3 to 8 ft (0.9 to 2.4 m) above the channel bottom were identified.

Inspection/	Conclusions/	Bed forms/ Scour/	
Location	Recommendations	Objects	Materials Conditions and Defects
Sonar	Submerged portion of	Acoustic imaging of the	Several horizontal and vertical cold joints in the imaging, including a
Team C	pier in fair to good condition. General condition normal for inservice, sheet pile formed concrete piers of this size and age. No remedial recommendations were made.	east channel profile and overall east channel bottom were performed in conjunction with this investigation. Nothing of concern was reported related to the channel. Partially buried tire not noted.	pronounced vertical cold joint or form line on the westernmost concrete support structure on the south face near the west end were noted. At the north channel pier, the inspection report noted horizontal cold-joints and associated latent concrete visible on the supports as well as vertical and horizontal formwork impressions. The report noted voiding on the east support of the north channel pier. On the east face a void ranging from 0.5 ft (0.15 m) to 2 ft (0.6 m) high located 12 ft (3.7 m) below the top of the concrete support was identified. This voiding extended intermittently along the entire length of the east face and continued around the northeast corner to the north face for 5 ft (1.5 m). Additional voiding at the east end of the south face 5 ft (1.5 m) long by 6 inches (150 mm) high positioned 19 ft (5.8 m) below the top of the concrete
			support was reported.

At column 2 of pier 2, the report identified additional areas of section loss. The largest void identified had a penetration of 1.5 ft (0.46 m) with one horizontal reinforcing steel bar exposed. In addition, the report noted that concrete inside the void could be broken apart with a gloved hand. A 12 ft (3.7 m) long horizontal seam on the east face (and wrapping around the southeast corner) about 7 ft (2.1 m) below the water surface had maximum penetration of 1.5 ft (0.46 m). Delamination of the concrete face at the southeast corner was also noted.

At the south channel pier, the dive report noted that the columns were in satisfactory condition with no significant structural defects observed that could adversely affect the bridge. The concrete was in similar condition to that at the south channel pier, but to a less extensive degree. No reinforced steel was reported to be exposed.

As a result of the inspection findings the report recommended that the areas with exposed reinforcing steel should be addressed and repaired to inhibit those areas from further deterioration.

All three sonar inspection teams reported that the submerged components of the north and south channel piers were in good condition. They reported that the general concrete condition appeared to be normal for in-service concrete piers of this size and age. In contrast to the dive inspection report, the sonar inspection teams did not recommend any repairs.

An image of both piers from sonar inspection team A is shown in figure 93. The report from sonar team A states that acoustic imaging of both the south channel pier (figure 94) and the north channel pier (figure 95) revealed no major deficiencies. The team reported that because of limited access, in-depth scanning was limited to the east support (column 2) of the north channel pier.

Inspection team B noted that because of limited access and time constraints, scanning of the south channel pier was limited to a few scans of the east support (column 2). These images, such as found in figure 96, revealed no significant deficiencies.

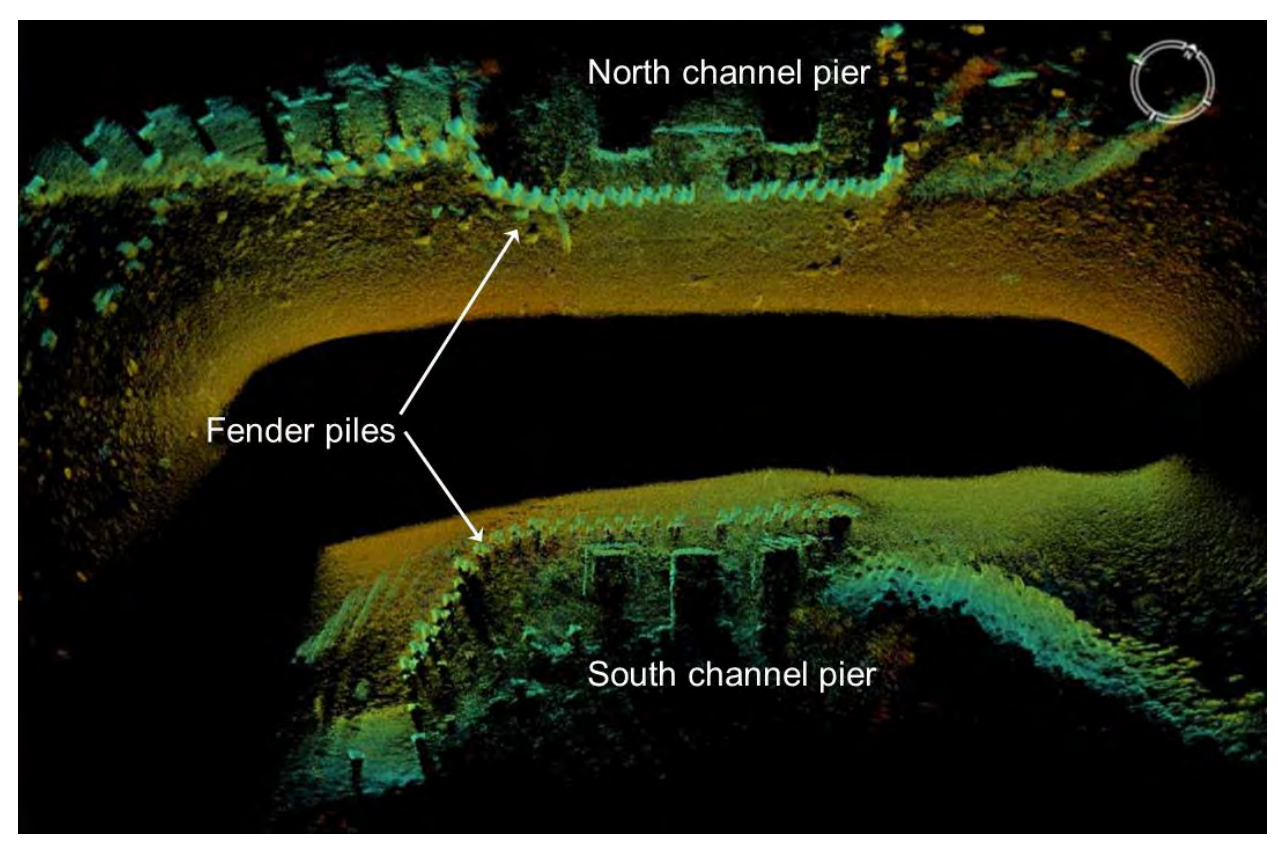


Figure 93. Image. North and south piers of the Third Street Bridge.

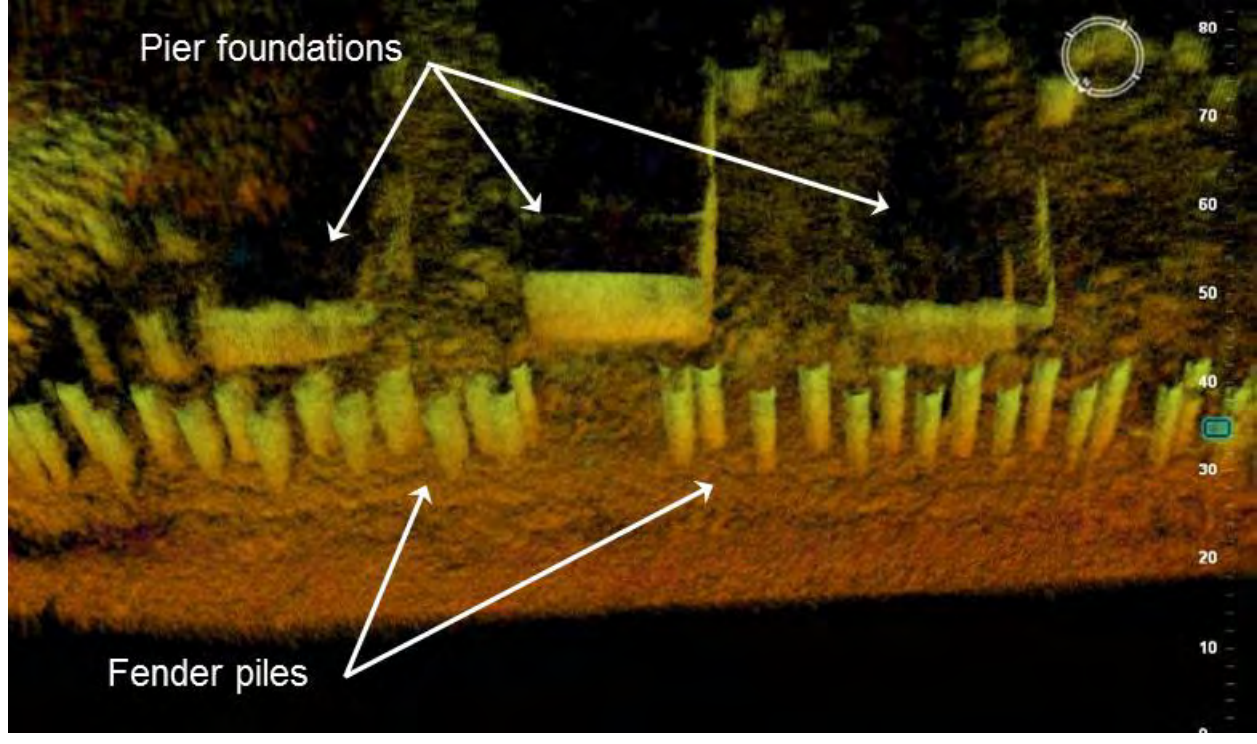


Figure 94. Image. Close-up of the south channel pier (Third Street Bridge).

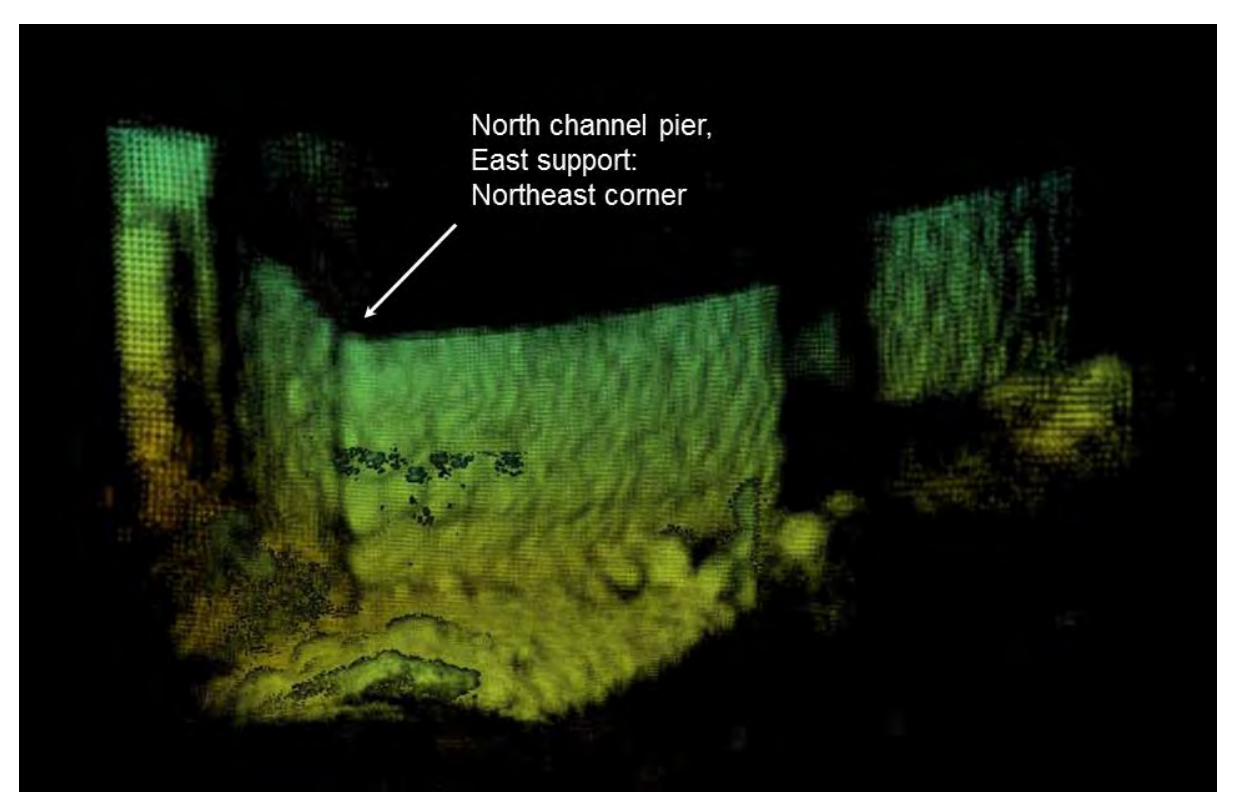


Figure 95. Image. Detail of east support for the north channel pier.

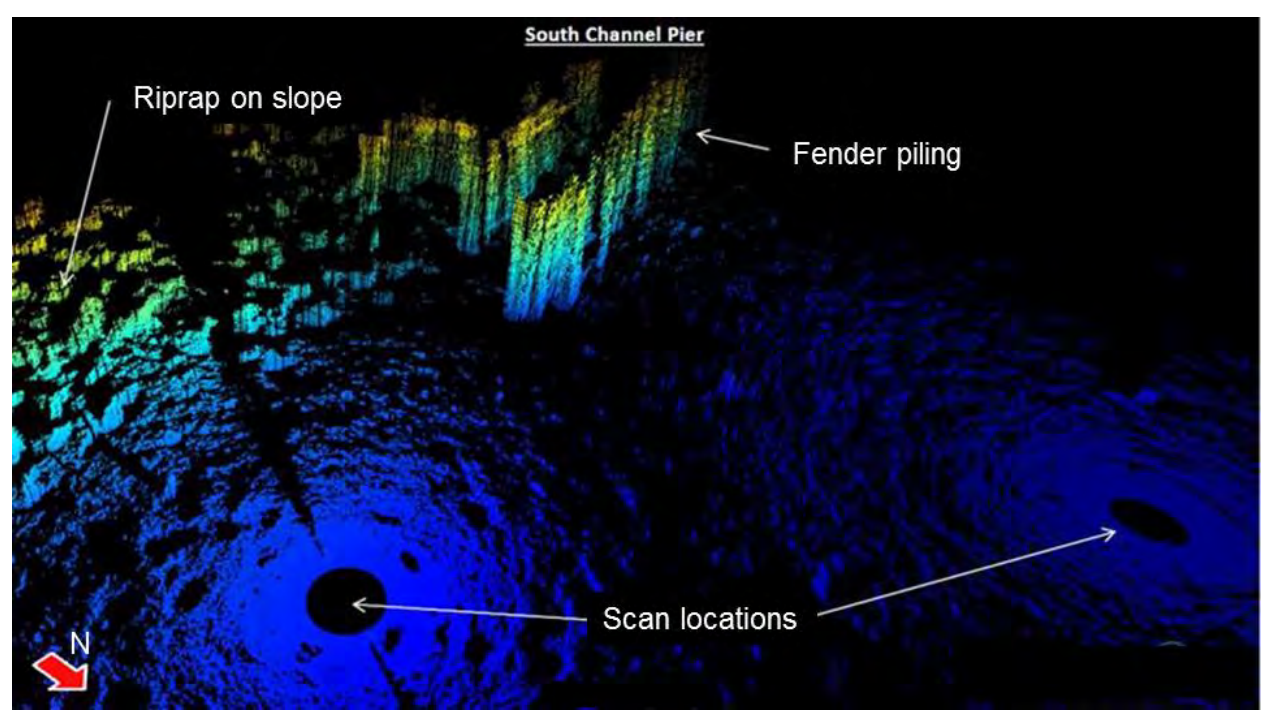


Figure 96. Image. South channel pier viewed from the northeast.

With respect to the west support (column 1) of the north channel pier, team B did identify possible abrasion damage or voiding along the west end of the south face as shown in figure 97. This area was reported as approximately 3 ft (0.9 m) long by 2 ft (0.6 m) high and positioned

approximately 5 ft (1.5 m) above the channel bottom. On the northwest corner of the same support column, the report also noted two possible areas of corner spalling or abrasion. These areas were reported as being approximately 1 to 2 ft (0.3 to 0.6 m) high by up to approximately 3 inches (76 mm) deep and located approximately 5 to 8 ft (1.5 to 2.4 m) above the channel bottom.

Inspection team B reported several observations for the east support (column 2) of the north channel pier. On the south face the report noted formwork lines as well as an area of voiding at the east end. The void was reported to be approximately 6 ft (1.8 m) long by a maximum of 1 ft (0.3 m) high and positioned approximately 1 to 2 ft (0.3 to 0.6 m) above the channel bottom. At the southeast corner the report noted a corner spall approximately 6 inches (150 mm) high by 6 inches (150 mm) deep located approximately 8 ft (2.4 m) above the channel bottom. On the east face, an area of voiding approximately 3 ft (0.9 m) long by a maximum of 1 ft (0.3 m) high located approximately 6 to 8 ft (1.8 to 2.4 m) above the channel bottom was reported. Also on the east face, the report identified several possible areas of voiding approximately 1 ft (0.3 m) in diameter and ranging approximately 3 to 8 ft (0.9 to 2.4 m) above the channel bottom.

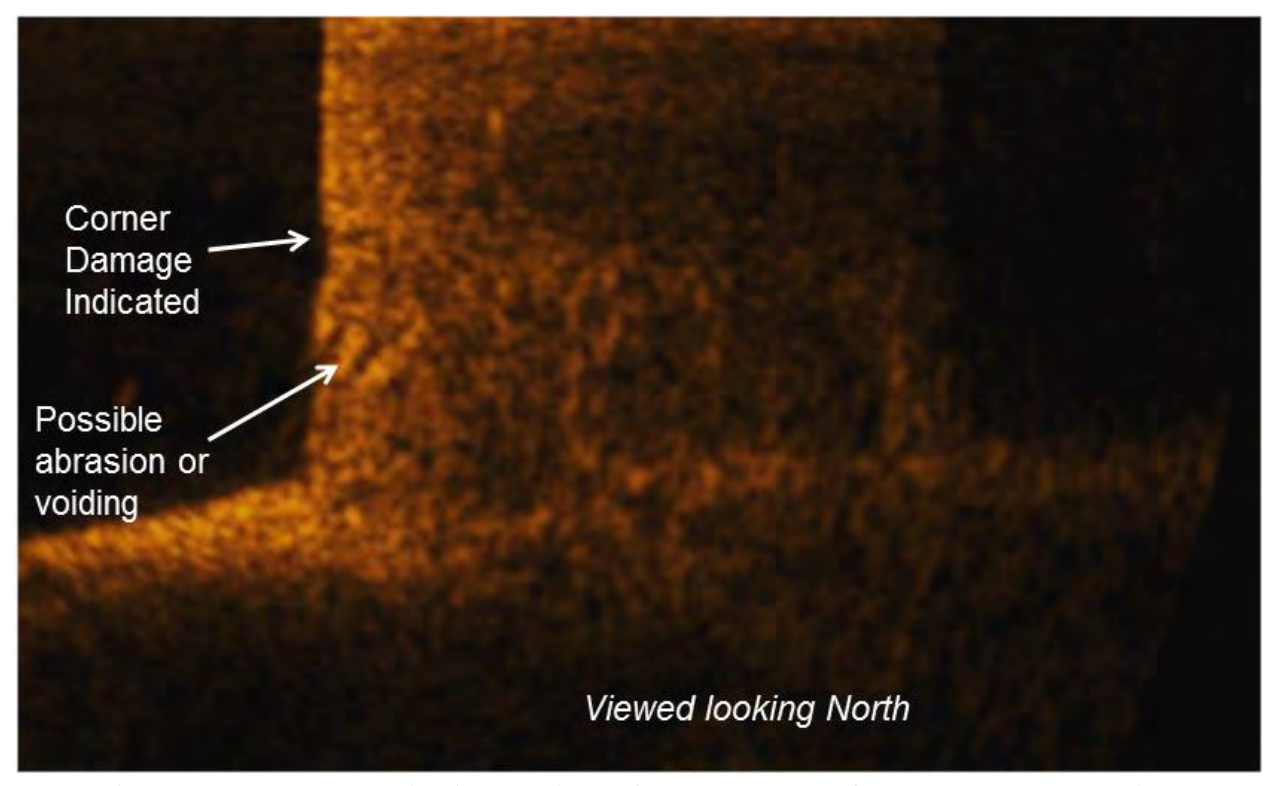


Figure 97. Image. Detail of south face of west support of the north channel pier.

Sonar inspection team C reported that the underwater acoustic imaging revealed no significant deficiencies at the south channel pier. Their report noted several horizontal and vertical cold joints in the imaging, including a pronounced vertical cold joint or form line on the westernmost concrete support structure on the south face near the west end.

At the north channel pier, the inspection report noted horizontal cold-joints and associated latent concrete visible on the supports as shown in figure 98 as well as vertical and horizontal

formwork impressions as shown in figure 99. In addition, the report noted voiding on the east support of the north channel pier. On the east face a void ranging from approximately 0.5 ft (0.15 m) to 2 ft (0.6 m) high located approximately 12 ft (3.7 m) below the top of the concrete support was identified. The report noted this voiding extended intermittently along the entire length of the east face and continued around the northeast corner to the north face for approximately 5 ft (1.5 m). Additional voiding at the east end of the south face approximately 5 ft (1.5 m) long by 6 inches (150 mm) high positioned approximately 19 ft (5.8 m) below the top of the concrete support was reported.

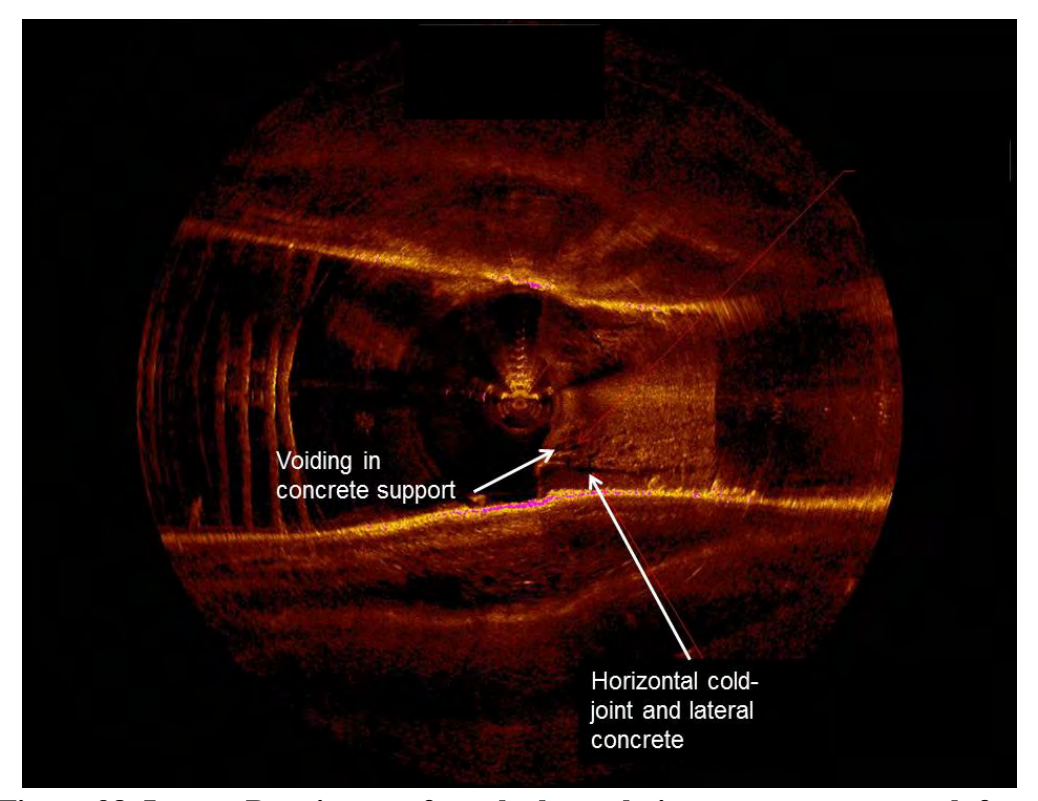


Figure 98. Image. Raw image of north channel pier, east support, south face.

In addition to inspecting the two piers, acoustic imaging of the east channel profile and overall east channel bottom were performed in conjunction with this investigation. Nothing of concern was reported related to the channel.

The dive inspection report and all three sonar inspection reports concluded that the north and south channel piers were in satisfactory condition. The dive report noted that the north channel pier was in generally worse condition than the south channel pier and that observation mirrored the sonar reports which noted very little on the south channel pier, but voiding and abrasion on the north channel pier. The sonar teams also noted limited access and time as reasons for limiting the evaluation of the south channel pier.

The dive inspection report included identification of several areas of exposed reinforcing steel and recommended that these areas be repaired. The sonar inspection reports did not mention exposed reinforcing steel and did not include any repair recommendations. All reports noted several areas of concrete voiding on the north channel pier. However, the details of size,

location, and penetration varied. The dive inspection report included the deepest void at approximately 1.5 ft (0.46 m).

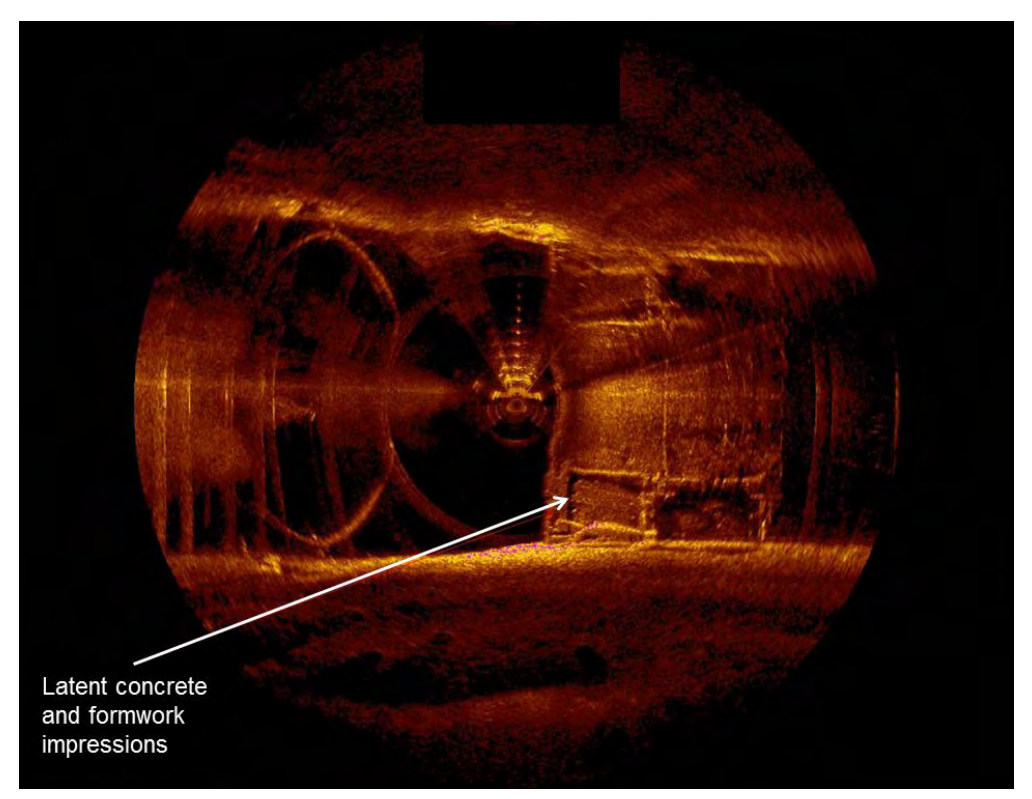


Figure 99. Image. Raw image of north channel pier, west support south face.

The dive and sonar reports included some commentary on the channel bottom in the vicinity of the two piers. None of the reports identified any scour issues. In addition, none of the teams reported the tire that was previously reported to be embedded in the concrete of the north channel pier. Two possible reasons this known condition may not have been identified are: 1) the tire was observed, but not considered relevant to substructure integrity and 2) it was buried beneath the mudline and not observable.

Post-Inspection Review

After the inspections of the Third Street Bridge were completed, each sonar inspection team was provided with an opportunity to reassess the collected data and images. With respect to void depths, the sonar inspection teams stated that it was beyond the scope of the inspection to define the depth of voids, but that this is within the capabilities of the equipment.

With respect to the sonar observations (April 2014) compared with the dive inspection (November 2013), one sonar inspection team noted that rehabilitation of the bridge occurred from May 2013 to March 2015 and could explain the observation differences. The scope and schedule of any bridge rehabilitation was not confirmed.

EVALUATION OF PHASE II FINDINGS

As with the phase I inspections, the results for this phase II are evaluated based on the following criteria: 1) the ability of the inspection teams to identify features important for underwater bridge inspection and 2) performance in adverse environments. The phase I evaluation also considered data collection and reporting time, equipment/personnel costs, and personnel requirements. These factors were not part of the phase II study.

Identification of Features

This evaluation considered the three types of features previously evaluated in phase I: 1) bed forms/scour, 2) objects, and 3) materials defects. An effective underwater inspection should reveal these types of features if they have the potential to threaten the stability or performance of a bridge.

With respect to bed forms and scour, the inspection of pier W6 of the SF-OBB revealed an important benefit of sonar for underwater inspection. Because the dive inspection was limited to 100 feet in depth, the dive inspection did not include inspection of the full depth of the pier and did not reach the bed. Therefore, no observations could be made regarding scour conditions at the pier base. The images from all three sonar inspection teams provided information to the inspection teams. With respect to pier W2 of the SF-OBB and the Third Street Bridge, the dive and sonar reports provided similar conclusions regarding bed forms and scour.

In the initial inspection reports, the sonar inspection teams provided significant insights into the underwater conditions, but did not identify the known conditions or planted objects. In some cases, the images captured unusual objects reasonably well, but the tire in the concrete at the Third Street Bridge was not identified nor were any of the planted objects. On re-analysis of the sonar data, some of the inspection teams identified visuals on the images that could be the known conditions or planted objects. However, they could not be definitely identified as those objects. The dive inspection reports also failed to reveal these conditions.

One explanation for not identifying the targets in the inspection reporting is that the inspector considered them a "normal" condition of a structural member submerged for a long time. That is, the condition was observed, but not considered a threat to the integrity of the bridge substructure.

With respect to materials defects and structural integrity, the dive and sonar inspection teams reported variations in concrete surfaces and voiding at both bridges. While there were differences in the numbers, gross dimensions, and precise locations, the inspection reports generally drew the same conclusions regarding the qualitative conditions of the substructure surfaces.

However, the dive inspection reports for both bridges reported deeper void penetration than did the three sonar inspection teams. The dive inspection reports for both bridges also identified locations with exposed steel reinforcing. At the Third Street Bridge, the dive report recommended repairs to protect the steel reinforcing. The sonar inspections did not report exposed reinforcing and made no repair recommendations.

Performance in Adverse Environments

Adverse environments for underwater inspection with divers have been previously described to include those with rapid flow velocities, deep water, poor visibility or any combination of these conditions. In addition to potentially limiting data collection, these conditions can pose safety concerns for divers and personnel on aquatic craft.

For deep water conditions, as found at pier W6 of the SF-OBB, dive inspection below 100 ft (30.5 m) deep did not occur. Sonar technology provided images below this depth that were used to assess the pier condition and to identify potential for scour at the base of the pier. In these conditions, sonar technology provides clear benefits.

Neither the dive inspection team nor the sonar inspection teams for the phase II sites experienced high velocity conditions that hampered inspection work. However, sonar technology may be helpful in such situations especially if it can be deployed from fixed locations. Boat-mounted sonar may also be an asset if the flow velocity does not make operation of the vessel hazardous.

In the case of the Third Street Bridge, visibility was limited compared to the SF-OBB. Neither the dive team nor the sonar inspection teams reported difficulties because of visibility. The dive inspection team used tactile techniques (probes and gloved hands) to test concrete integrity.

The detail from the acoustic technologies was impressive even when the data were collected relatively quickly from technologies such as the real-time 3D multibeam sonar. In all environments, including those with adverse conditions, this technology provides potential for identifying macro features quickly. Based on the phase II results, these technologies can be used to inspect underwater structural elements where divers cannot work effectively, to guide divers for a closer look, and to provide independent inspection insights.

CHAPTER 8. SUMMARY, CONCLUSIONS, AND RECOMMENDATIONS

This study applied multiple approaches to assess the strengths and limitations of underwater acoustic imaging technology for bridge inspection. Opportunities that these technologies may provide were assessed through the following field and office activities:

- Blind inspection (phase I) of four bridge sites (Georgiana Slough Bridge, James E. Roberts Bridge, Carquinez Bridge (1958), and Carquinez Bridge (2003)) using multiple sonar technologies and diver inspections.
- Neutral observation and logging of the effort and difficulties experienced in the phase I inspections.
- Blind inspection (phase II) of two additional bridge sites (SF-OBB and the Third Street Bridge) with a set of known conditions to evaluate multiple sonar technologies for defect detection capability.
- Post-field test analyses of data collected in both field phases to evaluate each technique and to develop recommendations.

Through both phase I and phase II field studies, the range of sonar technologies exhibited strengths and weaknesses relative to each other as well as compared with divers. The comparison of these approaches was evaluated based on the following criteria:

- Identification of features
- Performance in adverse environments
- Data collection/reporting time
- Equipment costs
- Personnel requirements

The following sections summarize the findings and provide recommendations for further activities.

SUMMARY

With respect to the identification of features, this study considered three types of relevant features: 1) bed forms/scour, 2) objects, and 3) materials defects. These three areas include the types of findings that an underwater inspection should reveal about conditions that may threaten the stability or performance of a bridge.

The tested sonar technologies were effective at providing representations of general bed conditions and large scale representations of the underwater structures. Closer examination of underwater structural elements with sonar also revealed important conditions such as large voids. Sonar imaging technology demonstrated broad capability for revealing large scale structural conditions and stream bed conditions, often in real time.

The scope of this study did not include evaluation of whether the tested sonar technologies could identify refilled scour holes as none of the phase I or phase II sites included such a condition. As

described in summaries of various sonar methods (Chapter 3) some technologies, such as geophysical sub-bottom profilers, can identify refilled scour holes if the refilled materials are different in some way from the original bed surface, e.g. less densely packed. Other sonar technologies have little or no capability for identifying refilled scour holes. Dive inspection relying primarily on visual means may also fail to identify refilled scour holes.

Under most of the environmental conditions experienced by the dive and sonar inspection teams during both field phases of this study, the dive and sonar inspection reports were generally consistent in reporting the overall larger scale condition of substructure elements. These conditions included section loss and voids; anomalies and debris; and riprap and scour. However, neither the dive nor sonar phase II inspection teams reported finding the known conditions reported in previous inspections or the targets (anomalies) planted prior to the phase II inspections, but unknown to the inspection teams in this study. This may point to weaknesses in both approaches because these items were not reported or it could be that the items were observed, but not reported because they posed no threat to the substructure.

At the conclusion of the phase II field work, the three sonar teams were asked to review their data and attempt to identify the known conditions and planted targets. While one of the teams highlighted areas on specific images that might be the target, they could not do so with any confidence. However, the exercise demonstrated that once the sonar data are collected, it can be analyzed in greater detail at a later time. If the sonar data are georeferenced, data from one inspection can be compared with earlier or later inspections to identify changes. With dive inspections, this is not possible beyond the written report, unless there is a collection of photos and/or videos taken during the inspection.

With respect to smaller scale observations and quantitative measurements that would be more commonly associated with Level II or Level II inspections, the dive inspection reports differed from the sonar inspection reports in two ways. First, while both consistently noted the general location of voids, the precise location, number, and size of voids varied between the reports. With respect to void penetration (depth), the diver reports consistently estimated deeper void penetrations than did the sonar inspection reports.

Second, several of the dive inspection reports identified locations of exposed steel reinforcing. In some of those situations, the inspection reports made recommendations for repair to prevent or slow further deterioration. None of the sonar reports identified exposed steel at any of the sites. Because exposed steel was not identified, repair recommendations were not made in any of the sonar reports.

Confirmed by observations of the phase I and phase II field work, dive inspections become more difficult under adverse environmental conditions. These conditions include black water, swift currents, and deep water. When only one unfavorable condition was present (swift currents, deep water, or black water), experienced dive inspectors could safely, efficiently, and effectively accomplish the inspection work. When two or more adverse conditions existed at the same time it became potentially hazardous and difficult to conduct a thorough and accurate inspection.

In the case of the inspection of pier W6 of the SF-OBB, the inspection was not completed by the dive team because depths exceeded 100 ft (30.5 m). All three sonar teams were able to secure

good images of the base of the W6 pier as well as the bed surrounding the pier. This was a condition in which the sonar showed a clear advantage.

The swiftest currents during the field work were encountered during phase I at the Carquinez Bridge. At this site, the divers reported difficulty in maintaining their position to conduct the inspection, though they did complete their work. The sonar teams completed their data collection efforts with only the challenge of maintaining vessel stability when boat-mounted sonar was used.

The site with the poorest visibility conditions, with zero visibility reported by the dive team, was at the Carquinez Bridge (2003) site. Although visibility was poor, detailed observations were completed by the dive team. However, progress was relatively slow. The sonar teams did not report any difficulty attributable to poor visibility at this site.

All of the inspections were limited to some extent by project budget and schedule. The result of this was that each inspection team placed limits on the scope of the inspection at each site. However, in some cases, the sonar teams reported that they could not complete inspection of a particular underwater element because of limited access. For example, sonar team A reported that access prevented inspection of parts of pier W2 at the SF-OBB and parts of the Third Street Bridge substructure. Sonar team B reported limited accessibility during the inspection of the Third Street Bridge. The dive inspection team did not report any access issues resulting from low clearances or the presence of protective elements such as fenders.

Related to the topic of time and budget, it was observed that the inspection area at the SF-OBB was extensive. Inspection of the entire underwater area would have made significant physical and time demands on dive inspection teams. With good access, the sonar teams could collect data from the entire underwater area more quickly than the dive team would have been able to accomplish. However, the sonar inspections did not yield the same detail of conditions that could threaten a bridge, e.g. void penetration depths and exposed reinforcement.

Finally, the field testing demonstrated that the post-processing capability and data record of acoustic imaging technology might provide critical information when new questions arise or new knowledge/techniques become available after an inspection is completed. The acoustic record might also be used to compare inspections with results from earlier inspections, especially when the data are georeferenced. These data and images might also be an asset for QA/QC practices. With respect to dive inspections, photos and videos may provide this same function, if visibility at the time of inspection permits.

CONCLUSIONS

The results of this study, particularly the experience gained from the field work, lead to two broad conclusions. First, sonar inspections have not demonstrated the ability to identify some smaller scale elements of substructure condition, as described in the following paragraph, that may be important in assessing the bridge and recommending maintenance. Second, sonar technologies offer significant opportunities for improving underwater bridge inspections, especially in adverse environments or to inspect extensive areas.

The preceding summary section highlighted that both the dive and sonar inspection teams made similar observations on the general and large-scale conditions at the underwater substructures, such as the location and predominance of concrete voiding. However, the dive inspection reports for both the SF-OBB and the Third Street Bridge reported deeper void penetrations than any of the sonar teams. The dive inspection reports also identified locations of exposed reinforcing steel and provided maintenance recommendations. None of the sonar inspection reports identified exposed reinforcing steel or identified any maintenance needs. These differences suggest that current sonar techniques do not offer the "up-close" ability that dive inspection does.

However, as is best illustrated in the inspection of pier W6 of the SFF-OBB, the dive inspection did not include any part of the pier or bed below a depth of 100 ft (30.5 m). If conditions of concern existed, they would have remained undiscovered. In contrast, all three sonar teams provided useful images of conditions at depth. Scour and other potentially threatening conditions, if they had existed, might well have been identified.

This example highlights one of many opportunities that sonar technology offers for improving underwater bridge inspection. Significant depth, such as at pier W6, is one of several conditions adverse to diving where sonar can be useful. Other adverse conditions include swift currents and poor visibility (black water). While diving can still be accomplished under difficult conditions, progress may be slowed and risks to divers may increase. Under such conditions, sonar can be used to complement dive inspections. Sonar might also be used to scan large areas to identify locations of potential concern that warrant a closer look by divers.

RECOMMENDATIONS

The findings and conclusions of this study lead to recommendations that support the expanded use of sonar technology to improve the safety of bridges, including, but not necessarily limited to, Level I inspections, for broad characterization of bed conditions, and in conditions adverse to diving. These recommendations assume that the technology will continue to improve and the opportunities for sonar applications will increase further.

The first recommendation is to develop guidance or benchmarking information for the use of sonar technologies in underwater bridge inspection, as well as interpretation of the results. Extensive guidance exists for the use of sonar in bathymetric surveys. Guidance documents that specifically address underwater structure inspection and best practices are needed. In addition, guidance in the evaluation and selection of specific technologies as they relate to different types of situations and conditions is also needed. The time consumption log, troubleshooting record, and cost data in this study can be used to inform such guidance. As part of the development of guidance, benchmarking information on acoustic signature identification of specific types of bridge defects in specific types of materials might aid in the accurate interpretation of sonar data.

The second recommendation is for a program of training for bridge inspectors in the use of acoustic technologies. Currently, dive inspectors go through extensive training in the protocols for inspection and the types of findings that are relevant to report. Analogous training for sonar inspections is needed. The sonar inspection teams involved in the phase I and phase II field work included well established subject matter experts in both acoustic technology and bridge inspection. However, they had to adapt throughout the process because there were not

established protocols in place for sonar inspections. Each sonar inspection team expressed that more rigorous inspections would likely result with an appropriate training program.

Finally, sonar technologies show promise for improving underwater inspection of bridges and, therefore, for increasing the safety and longevity of those bridges. Expanded use of sonar technologies should be encouraged to complement dive inspections.

APPENDIX A – RECENT RESEARCH

This appendix summarizes recent research efforts relevant to the current study.

U.S. ARMY CORPS OF ENGINEERS (2006, 2007)

A series of case studies were conducted by the USACE to evaluate the use of sonar technologies for detecting scour of hydraulic control structures, specifically navigation dams. (21, 22) A lens-based multibeam sonar unit and a multibeam swath sonar system were used in the studies.

The first study was to evaluate the degree of scour underneath the apron leading to the stilling basin below the Starved Rock Dam near Ottawa, Illinois. The lens-based sonar indicated with sufficient certainty that there was no evidence of the apron being undermined. The lens-based multibeam was also able to identify several small defects in the concrete such as areas of section loss. However, the depth of penetration could not be determined.

The second scour study in the spring of 2007 of the Mel Price Lock and Dam on the Mississippi River used a multibeam sonar system to image both the upstream and downstream portions of the structure. The system was able to image a large area of unanticipated scour that was 12 ft (3.7 m) wide and up to 10 ft (3.05 m) deep relative to the adjacent channel bottom located immediately upstream of one of the gate bays.

MASSACHUSETTS DOT (2008)

The Massachusetts DOT conducted a field study that compared the utility of 2D sector-scanning sonar and side-scan sonar for underwater bridge inspections. The study concluded that vertical surfaces were more readily imaged with sector-scanning sonar than with side-scan sonar. Additionally, the sector-scanning sonar was able to obtain image data near the water surface where the side-scan sonar could not.

UNIVERSITY OF DELAWARE (2008)

A study was conducted by the University of Delaware Center for Applied Coastal Research in which a sonar-based system was installed to monitor scour at the Highway 1 Bridge over Indian River Inlet in near real time. (24) The system consisted of two profiling sonar units mounted on bridge piers and two Acoustic Doppler Current Profilers that were set up to automatically survey the inlet on the ocean side of the bridge twice daily. Using this method the team was able to accurately map the extent of the scour over time and determine the probable controlling cause of the scour hole.

The study concluded that although the initial capital outlay for this custom system was costly, the repeatability over time made it a cost effective alternative compared to successive traditional multibeam or single-beam sonar surveys.

WISCONSIN DOT (2008, 2010)

The Wisconsin DOT conducted evaluations comparing sonar findings with diver observations. (25) Heavy deterioration of concrete substructures at a bridge in Wisconsin would have been difficult

and time consuming for a dive inspector to accurately report and quantify. Sector-scanning sonar was used to map the extents of heavy concrete scaling below water. The sector-scanning sonar clearly indicated areas with exposed reinforcing steel. Additionally, relative depth of scaling could be examined based on darkness of shading, but actual penetration depth could not be obtained from the sonar data. For this reason, the case study utilized a diver to document depth of penetrations at each portion of the pier faces.

QUEENS UNIVERSITY (2009, 2010)

A Queens University study focused on the use of ground penetrating radar (GPR), in conjunction with a hydrographic sonar survey, for the purpose of identifying scour and scour infill around the submerged substructures of a European bridge. (26) The study included a comprehensive listing of commercially available acoustic imaging devices.

The report concluded that GPR has several useful applications for underwater bridge inspection. It showed that the data gathered allows for the interpretation of depths of the river bed to form a contour map; the presence of rock versus sediment in the channel-bottom material composition; and the likely distribution of sediment depths in the waterway.

It showed that GPR was useful for creating a baseline survey of a bridge where areas of scour infill could be detected and then further monitored during subsequent inspections. Bridge owners could then determine if the extent and severity was increasing and whether remedial actions were required. The report did not address whether GPR was able to assist in any other aspects of underwater bridge inspection such as determining physical defects (cracks, corrosion, or the presence of voids) in the substructures.

IDAHO DOT (2011)

The Idaho DOT conducted a field study with the primary purpose of determining the usefulness of sector-scanning sonar to aid in underwater inspection of highway bridges. (27) The study included a limited literature review and three case studies. The case studies compared the quality of data gathered by sector-scanning sonar to the data gathered by a qualified inspection diver.

The conclusions of the report stated that cracks, horizontal penetration of voids, foundation undermining, extents of steel corrosion, presence of concrete scaling, and channel-bottom material composition could not be ascertained with the 2D sector-scanning sonar. However, the diver was able to give detailed descriptions of each of the above items. Additionally, the type of construction material present below the water surface was also difficult to verify with the sector-scanning sonar technology compared to tactile observations by a diver.

The primary benefits of the sector-scanning sonar included producing detailed images of the channel-bottom profile including scour depressions and imaging vertical components of submerged substructures in waters too swift and turbulent for a diver. Another benefit was that the sector-scanning sonar was very portable and could be deployed from a small boat or the bridge deck.

One of the three case studies included acoustic imaging of bridge piers with turbulent currents measured at 5 ft/s (1.5 m/s). Although a dive inspection was not able to be performed at this

bridge, the acoustic images were able to determine that three of the piers had no footing exposure and that one of the piers had footing exposure with 1 ft (0.3 m) vertical undermining. However, the penetration dimension of the undermining could not be determined.

APPENDIX B – SONAR APPLICATIONS

Acoustic imaging has been used for a variety of bridge inspection purposes. This appendix provides example applications grouped by the following purposes:

- Rapid condition assessment.
- Scour detection and documentation.
- Underwater construction inspection.
- Security threat assessment.
- Visual documentation of an underwater structure.
- Enhancement of diver safety and efficiency at challenging dive sites.

RAPID CONDITION ASSESSMENT

Both natural disaster and human caused events may require emergency structural assessment. Natural disasters include hurricanes, tornadoes, floods, earthquakes, and tsunamis. Human caused events can include vessel or vehicle impacts and dam breaks. Rapid condition assessment is often required immediately following an emergency event.

Emergency events can threaten the structural stability of a bridge. The immediate need for a bridge closure decision can result in overly conservative closures requiring unnecessary lengthy detours. With acoustic imaging technology bridge owners can collect important information about a structure during or soon after an event, whereas a dive inspection might have to wait weeks or months for conditions to become favorable for safe diving conditions.

In 2008, the Iowa DOT employed acoustic technology for vessel impact damage inspection. (28) The US-20 Bridge over the Mississippi River had three barge sections impact three different substructure units during flood conditions. One barge unit capsized and sank at the upstream nose of a pier. Local construction crews estimated that removal of the capsized barge section could take months. Sector-scanning sonar was used to quickly search for large scale impact damage and section loss of the concrete pier and to assess the channel-bottom configuration to ensure that water being deflected by the barge was not adversely contributing to scour of the foundation.

Also in 2008, the Texas DOT employed acoustic technology for hurricane damage inspection. (29) In the fall of 2008 Hurricane Ike struck Galveston Texas, an island in the Gulf of Mexico just off the Texas coast. As a result of the hurricane, the Rollover Pass Bridge was severely damaged. Water conditions consisted of low visibility and swift tidal currents that meant divers could only work for 15 minutes at a time during slack tide.

Because of the need to rapidly assess the condition of the bridge, the Texas DOT permitted the Center for Robot-Assisted Search and Rescue from Texas A&M University to deploy unmanned marine vehicles equipped with two types of sonar technologies (in addition to traditional video cameras and other sensors) to assess the bridge for scour and hazards to navigation.

One of the primary sensors was a lens-based multibeam sonar unit used as an acoustic camera for scour evaluation and a side-scan sonar unit for mapping the debris field. Because of these technologies the bridge owner was able to find that there was no sign of scour at the bridge or debris that could present a hazard to navigation. This study has obvious implications for other aspects of bridge assessment mentioned above such as diver safety and scour evaluation.

The Illinois DOT used sector-scanning sonar for the rapid assessment of a bridge incident in 2009 where an emergency inspection of a bridge was required due to a barge striking and overturning a steel sheet pile protection cell adjacent to a state route bridge over the Illinois River in Central Illinois. In this case, a sector-scanning sonar unit was used to create a highly detailed "big picture" of the barge impact, depicting the protection cell position and damage to scale, as well as how it related to the bridge substructure.

SCOUR DETECTION AND DOCUMENTATION

The number one cause of bridge failure in the United States is scour. This makes it paramount for bridge owners to be able to efficiently and safely be able to assess the presence of scour at a bridge site. The presence of scour can often be difficult for an inspection diver to detect for a variety of reasons and this makes underwater imaging technologies extremely useful. (31)

In addition to hydrographic surveys, fixed scour monitoring systems can be established for continuous scour monitoring at a specific site. A fixed scour monitoring system means that it is permanently or semi-permanently attached to a structure to repeatedly monitor a specific area. According to the Transportation Research Board, in 2009 over 30 states had fixed scour monitoring installations and over 60 of those installations utilized at least one sonar system. (31)

The Iowa DOT employed acoustic technology for scour assessment at a bridge embankment. During the summer months of 2011, the Missouri River water levels were sustained near record levels for several months. The sustained high water levels caused the main river channel to reroute itself and a new channel was established adjacent to the embankment leading up to the state highway 175 bridge abutment. Traditional hydrographic survey techniques were unable to produce depth data in shallow water near the large stones because of difficulties maneuvering a boat in the swift currents. While construction crews worked to place protective riprap along the embankment, sector-scanning sonar was used to document whether the slope was staying in position or continuing to wash away by the tremendous forces of the flood waters.

Nelson County Kentucky employed acoustic technology for bridge scour assessment. During the spring of 2011 bridge inspectors attempted to take depth soundings at the KY 84 bridge over the Rolling Fork River Slough in central Kentucky. Because of the extreme flood conditions and swift currents, it was nearly impossible to obtain accurate depth data at the piers. An inspection crew used sector-scanning sonar to create an image of the pier and measure the length of the exposed piles.

The lengths of the piles were compared with the as-built plans and the remaining embedment lengths of the piles were determined. The imaging assisted the engineers in determining that only 2 ft (0.6 m) of pile embedment was remaining at the downstream end of the pier and the bridge

was closed until repairs could be made. When flood waters receded, the river was dewatered to perform repairs.

Acoustic technology was used for a shallow water scour investigation in Japan. (34) This case study involved the use of a mechanical scanning multibeam sonar system to measure the scour of a bulkhead along the banks of the Susobanagawa River in Japan. The site conditions required the use of a system that could operate in approximately 3 ft (0.9 m) of water and be able to scan a vertical surface for undermining. The team was able to produce 3D point cloud data of the area that showed that more than half of the bulkhead was undermined with a maximum of almost 5.5 ft (1.7 m) of penetration beneath the structure. In this instance the mechanical scanning multibeam sonar unit was able to produce side-elevation data that traditional downward-looking swath multibeam sonar systems could not provide.

UNDERWATER CONSTRUCTION INSPECTION

Underwater imaging technologies can be used in all phases of construction from pre-construction planning, through the construction phase, to verifying as-built information.

Lens-based multibeam sonar systems have been successfully used in the offshore construction industry and have potential for application in bridge construction. Hull mounted and diver-held units have been used to locate and place underwater pipes as well as inspect North Sea drill platforms. Possible applications in bridge construction include inspection of formwork and placement of riprap. (35)

Another construction related activity that heavily uses sonar technology is the dredging industry. Everything from single-beam fathometer surveys to side-scan sonar and multibeam swath surveys have been used to quantify and classify river channels and the sea-bed. The primary uses for sonar in dredging is the charting of access channels for safe navigation of dredging vessels, the detection of obstacles that could damage the dredging head, to map the composition and distribution of the seabed sediments, and to calculate volumes. Many dredging operations are made more efficient by combining two or more sonar systems for simultaneous operation. For instance, a side-scan sonar system can be used because of its superior range to detect potential obstacles while a shorter range multibeam system creates detailed geo-located point cloud data at the same time. Careful consideration is required in the deployment and location of the systems to achieve the best results. (36)

A routine 2009 underwater bridge inspection by the Wisconsin DOT revealed undermining of a pier foundation. A contractor was hired to place riprap at the pier to prevent future undermining. The Wisconsin DOT utilized sector-scanning sonar to obtain visual confirmation that the riprap being placed by the contractor was as intended.

In 2009 at the Indian River Inlet in Delaware, sector-scanning sonar was used to verify contractor work for dock wall riprap placement for scour remediation. On a section of sheet pile bulkhead along the Indian River there was difficulty assessing the extent of scour with divers due to adverse conditions. A scanning sonar unit was deployed to check the specified placement limits of rock material. Using this method, deficiencies in the contractor work were found and the resulting images were used to direct placement of additional riprap.

SECURITY THREAT ASSESSMENT

The ability to image underwater structures has clear security implications for ports, harbors, and bridges in the United States. The potential applications are numerous and include scanning for explosives and detecting intruders. All types of commercially available imaging sonar have been used for this purpose and there are several cases showing that acoustic imaging technologies have proven to be an efficient and reliable way to accomplish this.

In 2007 a process was developed for ship hull scanning using a combination of a narrow-aperture upward-looking sonar system with multiple beam-formed imaging sonar scans to successfully image the underwater portions of ship hulls for possible explosive devices. (38) This proof of concept showed that it is possible to use sonar imaging technology to locate anomalies on underwater structures. This could be further developed for use in security applications of other structures such as the underwater portions of high-profile or at-risk bridges.

In late 2004 and early 2005, the University of South Florida Center for Ocean Technology working with various government agencies and manufacturers helped provide security for two large events: the 2004 Republican National Convention and Super BowlTM XXXIX. (39, 40, 41, 42) These case studies showed that acoustic imaging technologies can rapidly assess large structures in security applications. The U.S. Coast Guard used real-time multibeam sonar system to quickly and thoroughly scan over 20 mi (32 km) of dock walls, ship hulls, bridge piers, and bridge abutments for potential "targets" that could indicate terrorist activity. The underwater acoustic imaging technologies used included a real-time multibeam sonar system and a lens-based 2D multibeam sonar system.

Security officials conducted initial baseline scans in both New York and Florida in a fraction of the time that it would have taken for a traditional diving inspection. All of the data were accurately georeferenced using an internal navigation system. Over 1,000 "objects of interest" were identified in Florida alone and then narrowed down to seven when the images were sent to the control center. At this point police divers were used to investigate each object. After a handson inspection by divers they were found to be of no threat. Subsequent scans could then be conducted and compared to the baseline to identify new potential threats.

Sonar technologies have also seen extensive use for underwater intruder detection. (43, 44) There are many companies that manufacture such systems and they have been installed to monitor sensitive areas such as offshore oil platforms, coastal energy terminals, nuclear power facilities, naval bases, and VIP compounds. These systems could easily be adapted to monitor high-value bridges for divers or swimmers attempting to attach an explosive device or otherwise damage the structure.

VISUAL REPRESENTATION OF THE UNDERWATER STRUCTURE

One of the main advantages of underwater imaging technology is the ability to image a structure regardless of water clarity. Where other optical technologies or a diver might allow an inspector to visualize parts of a structure, several types of sonar allow an owner to see images of a structure in its entirety.

During the 2005 hurricane season, hurricanes Katrina and Rita destroyed many drilling platforms in the Gulf of Mexico. To safely and efficiently decommission them in little to no water visibility, several different types of sonar technology were used. For initial site reconnaissance, side-scan sonar was used because of its ability to scan large areas in a relatively short amount of time. Once the location of large features were found, a sector-scanning sonar system mounted on a tripod was used to further clarify the data and produce high resolution 2D images of the downed platforms. These first two steps were important for locating potential hazards for ships and diving operations. The final phase of the operation involved using a multibeam echosounder to produce detailed point cloud data of the downed platforms. The multibeam units were used in the traditional downward looking swath configuration, as well as mounted to an ROV in an innovative side-looking configuration. This was done in order to minimize shadows and help visualize the entire volume of the debris field. By taking advantage of the relative advantages of several sonar technologies and deployment techniques, the team was able to produce the data needed to safely decommission the wells.

Underwater inspection of a limestone dock wall in Freeport Bahamas revealed that large surface irregularities existed. (46) Accurate documentation of voids proved to be time consuming and cumbersome for dive inspectors. In order to provide an accurate depiction of underwater conditions, multibeam sonar was utilized to map the face of the wall. The resulting data provided for accurate volume calculations that were used to estimate repair quantities.

ENHANCING DIVER SAFETY AND EFFICIENCY

Underwater imaging technology can benefit diver safety and efficiency. Technologies such as lens-based multibeam sonar and sector-scanning sonar have the ability to generate data that can then be used to direct a diver to or away from a specific area.

A 2005 LNG terminal construction project in Qatar utilized real-time multibeam sonar technology to increase production efficiency and improve the health and safety of dive inspectors during the construction of a breakwall. The project required the precise placement of thousands of precast concrete tetrapods along the seabed. The traditional placement method involves the use of divers to visually guide the placement using cranes. This method is time consuming and dangerous. To help reduce the dangerous exposure to divers, a real-time multibeam sonar system and underwater video camera were installed on the excavator boom to allow the operator to view the orientation of the tetrapods in any water conditions. Fully georeferenced 3D survey data were superimposed onto the real-time sonar image to further aid the operators in the placement and orientation of the tetrapods. Dive inspectors were employed for the final verification of the work, however, use of the real-time multibeam sonar system resulted in an increased average daily production of over 300 percent.

REFERENCES

- 1. Federal Highway Administration (2012). "Tables of Frequently Requested NBI Information," available online: http://www.fhwa.dot.gov/bridge/britab.cfm, last accessed 2012.
- 2. Transportation Research Board (2009). *Underwater Bridge Maintenance and Repair*, NCHRP Synthesis 20-05/topic 22-04, Washington, D.C.
- 3. Federal Highway Administration (1998). *Technical Advisory-Revisions to the National Bridge Inspection Standards (NBIS)*, T5140.21, U.S. Dept. of Transportation, Washington, D.C., September.
- 4. Federal Highway Administration (1995). *Underwater Evaluation and Repair of Bridge Components*, FHWA report FHWA-DP-98-1, November.
- 5. ASCE (2001). *Underwater Investigations: Standard Practice Manual*, edited by Kenneth M. Childs Jr., MOP 101.
- 6. Federal Highway Administration (2010). *Underwater Bridge Inspection Manual*, FHWA-NHI-10-027, U.S. Dept. of Transportation, Washington, D.C.
- 7. Federal Highway Administration (undated). *Underwater Bridge Inspection*, National Highway Institute, Course Number 130091.
- 8. Federal Highway Administration (2009). Technical Resource Center Atlanta Memo by Cynthia Nurmi.
- 9. Browne, T. and Strock T. (2009). "Overview and Comparison of Nationwide Underwater Bridge Inspection Practices," *Transportation Research Record No. 2108 Maintenance and Management of the Infrastructure*, Journal of the Transportation Research Board.
- 10. U.S. Department of Labor (2011). *Directive Number CPL 02-00-151*, Occupational Safety and Health Administration, June 13.
- 11. Browne, T.M. and Stromberg, D.G. (2010). Advantages and Limitations of Underwater Acoustic Imaging Technology for Bridges and Transport Infrastructure.
- 12. L-3 Communications SeaBeam Instruments (2000). *Multibeam Sonar Theory of Operation*, East Walpole, MA.
- 13. Atherton, Mark (2011). *Echoes and Images, The Encyclopedia of Side-Scan and Scanning Sonar Operations*, OysterInk Publications, Vancouver, BC.
- 14. Browne, T. (2010). "Underwater Acoustic Imaging Devices for Portable Scour Monitoring" in *Scour and Erosion Proceedings of the Fifth International Conference on Scour and Erosion* (ICSE-5), ASCE.
- 15. U.S. Army Corps of Engineers (2002). *Engineering and Design Hydrographic Surveying*, Engineering Manual EM 1110-2-1003, Jan 1.
- 16. Waddington, Tom (2010). *High-Resolution Multibeam Surveys for Bridge Assessment*, Portsmouth, NH, available online:

 http://substructure.com/wpcontent/uploads/2011/05/Hydro_2011_bridge_assessment_trw_pdf, last accessed 2012.

- 17. Browne, T. (2010) "Improvement of Underwater Bridge Inspection Documentation with Innovative Sonar Technology," *FHWA Bridge Engineering Conference*, Orlando, FL.
- 18. Federal Highway Administration (2011). *Ground-Penetration Radar (GPR)*, Central Federal Lands Highway Division, July, available online: http://www.cflhd.gov/resources/agm/engApplications/BridgeSystemSubstructure/243GoundPenetratingRadar.cfm, last accessed Jan. 23, 2012.
- 19. Coda Octopus (undated). Fully Integrated Real Time 3D Inspection System for Maritime Security, Underwater Inspection and Search and Recovery, Edinburgh, UK, available online: http://www.codaoctopus.com/media/downloads/codaoctopus_echoscope-uis-brochure.pdf, last accessed 2012.
- Cunningham, Blair, et al. (2008). The Use of Advanced True 4D Sonar for Real Time Complex Mosaicing, Coda Octopus Products Ltd., August 26, available online: http://www.codaoctopus.com/echoscope-3d-sonar/documents/, last accessed Jan. 31, 2012.
- 21. Evans, James A. (2010). Acoustical Imaging Cameras for the Inspection and Condition Assessment of Hydraulic Structures, US Army Corps of Engineers ERDC/CHL CHETN-IX-23, Washington, D.C., August.
- 22. Hite, J.E. (2008). *Detection and Evaluation of Scour Protection for Navigation Dams*, US Army Corps of Engineers Navigation Systems Research Program ERDC/CHL TR-08-14, Washington, D.C., August.
- 23. Collins Engineers, Inc. (2008). *Boston Underwater Research Technology (BURT) Study*, Massachusetts DOT, MassHighway Report.
- 24. Hayden, Jesse T. and Puleo, Jack A. (2011). "Near Real-Time Scour Monitoring System: Application to Indian River Inlet, Delaware," *Journal of Hydraulic Engineering*, American Society of Civil Engineers, 137, 1037.
- 25. Collins Engineers, Inc. (undated). "B-49-92 inspection report, 2008-2010," prepared for the Wisconsin DOT.
- 26. Campbell, K., Ruffell, A., Hughes, D., Taylor, S., and Devlin, B. (2010). *Ground Penetrating Radar as an Innovative Tool for Identifying Areas of Scour and Scour Infill Around Bridges*, (Rep. Collins Engineers Ltd, Northern Ireland).
- 27. Collins Engineers, Inc. (2011). *Underwater Acoustic Imaging Comparative Study*, prepared for the Idaho DOT.
- 28. Collins Engineers, Inc. (2008). *Bridge No. 3120.1S020 Inspection Report*, prepared for the Iowa DOT.
- 29. Murphy, Robin R., et al. (2009). "Robot-Assisted Bridge Inspection after Hurricane Ike," *IEEE International Workshop on Safety, Security & Rescue Robotics (SSRR)*, The Center for Robot-Assisted Search and Rescue, Texas A&M University.
- 30. Stromberg, D. (2011). "New Advances in Underwater Inspection Technologies for Railway Bridges over Water," *Railway Track & Structures Magazine*, March, 35-38.

- 31. Transportation Research Board (2009). *NCHRP Synthesis 396: Monitoring Scour Critical Bridges A Synthesis of Highway Practice*, Washington, D.C.
- 32. Collins Engineers, Inc. (2011). *STH 175 Embankment Inspection Report*, prepared for the Iowa DOT.
- 33. Collins Engineers, Inc. (2011). *KY-84 over Rollins Fork River Slough Inspection Report*, prepared for Nelson County, Kentucky.
- 34. Blue View Technologies (undated). *OPT, Japan Measuring Scour in Shallow Water Environments*, available online: http://www.blueview.com/media/OPT_Japan_Case_Study_Measuring_Scour_v4.pdf, last accessed February 22, 2012.
- 35. Belcher, Edward O. (2007). "Vision in Turbid Water," *Underwater Intervention Conference*, MTS/ADCI, New Orleans, LA.
- 36. Lanckneus, J. and De Jonghe, E. (2006). *Side-Scan Sonar and Multibeam Surveys in Dredging Projects: Are Both Techniques Necessary?*" Rep. no. 113831, Flanders Marine Institute.
- 37. Collins Engineers, Inc. (2009). *B-56-110 Inspection Report*, prepared for the Wisconsin DOT.
- 38. Faulkner, L., *et al.* (2009). "Harbor Shield: A New Technique for Inspection of Vessels Below the Waterline," *IEEE International Conference on Technologies for Homeland Security*, HST '09, Waltham, MA, May 11-12, available online: http://ieeexplore.ieee.org/stamp/stamp.jsp?tp=&arnumber=5168038&isnumber=5168000 last accessed 2012.
- 39. Fillmore, Randolph (2005). *USF Centers Helped Protect Super Bowl from Terrorist Threats*, University of South Florida, available online: http://www.marine.usf.edu/news/archives-2005.shtml, last accessed 2012.
- 40. Davis, Anthony and Lugsdin, Angus (2005). "High Speed Underwater Inspection of Port and Harbor Security using Coda Echoscope 3D Sonar" *UDT 2005 Conference*, Session 8A.3, (Rep. Coda Octopus).
- 41. Homeland Security NewsWire (2007). "Coda Octopus Delivers First of Three Underwater Inspection Systems to U.S. Coast Guard," *Homeland Security NewsWire*, Nov. 19 2007, available online:

 http://www.homelandsecuritynewswire.com/codaoctopus-delivers-first-three-underwater-inspection-systems-us-coast-guard, last accessed 2012.
- 42. Trigaux, Robert (2004). "USF Sonar Guards GOP Convention," *Tampa Bay Times*, July 13, 2004, available online: http://www.sptimes.com/2004/07/13/Business/USF_sonar_guards_GOP_.shtml, last accessed 2012.
- 43. DSIT Solutions Ltd. (2011). "DSIT Receives a \$12.3 Million Order for Underwater Security Systems for Protection of Offshore Rigs and Coastal Energy Terminals," Dec. 12, available online: http://www.dsit.co.il/SiteFiles/1/112/12469.asp, last accessed January 27, 2012.

- 44. Sonardyne (2009). "Slovenian Navy Chooses Sonardyne Sentinel Intruder Detection Sonar," April 14, available online: http://www.sonardyne.com/news-a-events/all-news-articles/502--slovenian-navy-chooses-sonardyne-sentinel-intruder-detection-sonar.html, last accessed January 27, 2012.
- 45. Beck, Richard D., et al. (2008). "Imaging Downed Platforms, OTC-19650," Offshore Technology Conference, Houston, TX.
- 46. Jones, Jenny (2010). "Scanning Method Yields Fast, Accurate Underwater Surveys," *Civil Engineering Magazine*, P. 38-39, July.
- 47. Gelderen, Peter van, and Auld, Stephen (2005). *Innovative Technique for Single Layer Armour Unit Placement*, Codaoctapus Products Ltd. May 29, available online: http://www.codaoctopus.com/echoscope-3d-sonar/documents/, last accessed January 31, 2012.

ACKNOWLEDGMENTS

We would like to acknowledge the following State Departments of Transportation for providing funding, information, and the review of interim project documents:

- California Department of Transportation (Michael Johnson, Richard Hunt)
- Texas Department of Transportation (Alan Kowalik)
- Wisconsin Department of Transportation (David Babler)
- South Carolina Department of Transportation (Richard Lee Floyd)
- Missouri Department of Transportation (Scott Stotlemeyer)
- North Dakota Department of Transportation (Gary Doerr)

All images are owned by FHWA. The original maps in Figures 30, 32, 33, 43, 42, 60, and 91 are the copyright property of Google® EarthTM and can be accessed from https://www.google.com/earth. Each of these figures includes overlays showing key site features discussed in the text.